Balancing Ecological and Economic Objectives in Land Use and Management: Modeling to Identify Sustainable Spatial Patterns

by

Hui Xu

A dissertation submitted in partial fulfillment
of the requirement for the degree of
Doctor of Philosophy
(Natural Resources and Environment)
In the University of Michigan
2016

Doctoral Committee:

Professor Daniel G. Brown, Chair
Professor William S. Currie
Professor Michael R. Moore
Associate Professor Allison L Steiner

To my family

Acknowledgements

The past five years at University of Michigan was the most exciting adventure of my life so far. I am very grateful to my advisor, Dr. Daniel G. Brown, for his intellectual and financial support. He is talented, patient and supportive. It was an absolute pleasure working with him. He is also truly inspiring. He always encouraged me to take challenges, to explore the unknown, and to make contributions to sustainability of the world via rigorous scientific research.

I would like to appreciate my committee members, Dr. Michael Moore, Dr. Bill Currie and Dr. Allison Steiner for sharing their wisdom and insightful suggestions with me. I was fortunate to have a supportive committee to finish an interdisciplinary dissertation study. Their suggestions and comments improved the quality of my dissertation substantially. I also would like to thank Dr. Margaret Kalcic for her help with the SWAT model. She kindly shared her experience with hydrological modeling with me.

Part of my dissertation work at the University of Michigan was supported by the National Science Foundation Water Sustainability and Climate program under Grant No.1313897. In addition to financial support, I appreciate collaboration opportunities provided the project.

Finally, special appreciation to my family: my parents, who know little about my research but always believe that I am doing great things, and my wife, for her unconditional love and care.

Table of Content

List of Tables

List of Figures

Abstract

Human-driven land-use/cover (LULC) changes threatened the integrity of ecosystems in many ways, such as through biodiversity loss brought on by habitat destruction and eutrophication of freshwater and coastal ecosystems. To evaluate possible impacts of future LULC on ecosystem services and support more sustainable environmental management, it is essential to understand how land-use patterns affect both ecological and economic outcomes, and how alternative spatial land management strategies may effectively and efficiently improve sustainability in land-use systems.

I developed, tested, and applied a spatial simulation approach that improves our understanding of how human-driven landscape conditions at the watershed scale reshape both water quality and economic productivity in a Lake Erie watershed under a changing climate. The dissertation is organized into three chapters. The first chapter describes a study in which I evaluated the sensitivity of a stochastic land-change model (LCM) to the choice of pixels versus polygonal land units derived from parcel maps. To reflect the effects of geometrical changes in management boundaries, nine possible parcel subdivision scenarios were included and tested. By evaluating the effects of spatial land units while holding other model variables constant using the same model algorithm, this study provides an important sensitivity test of the performance of pixel- and polygon-based simulations. Results indicate that the model based on polygonal units generates more realistic spatial landscape patterns, but at the cost of accuracy in spatial locations. Performance of different parcel-change scenarios varied according to the type of land change being modeled, because different land changes proceed through different processes.

For the second chapter, I developed the first integrated assessment approach that compares the relative economic efficiency of alternative spatially optimal land-use and -management strategies for addressing non-point source (NPS) nutrient pollution from agricultural land. Using the Soil Water Assessment Tool (SWAT) and data on costs and profits associated with crop and forest production, I evaluated joint impacts on nutrient reduction and economic returns for optimized

patterns of land-use changes versus conservation practices (CPs) at the field scale. Optimal spatial patterns were identified using a mixed integer linear programming algorithm, given field level economic and nutrient loading trade-offs. Watershed level Phosphorous (P) reduction efficiency experiments indicate that relying on CPs alone is likely insufficient to meet policy goals for water quality restoration in Lake Erie. However, a combined strategy that also includes land-use change, including the conversion of cropland to other land uses, could achieve targeted reductions in NPS. I improved on previous land-use optimization studies in the following ways: (1) by integrating a process-based biophysical model (SWAT) with economic valuations, (2) bridged the gap between optimization studies aimed at CP targeting and land-use optimization by combining both options in the same modeling framework and (3) quantified achievable Pareto optimality via the combined strategy.

Finally, I examined sensitivity of optimized spatial patterns of land-use and –management approaches to climate change. I found that the efficiency of spatial patterns of land-use and -management actions optimized to reduce nutrient pollution in the most economically beneficial way, can be quite sensitive to changes in climatic conditions because changed temperature and precipitation patterns affect both plant/crop yields and nutrient discharges. Dissolved reactive phosphorus (DRP) load under future climate conditions and current land-use patterns was projected to be lower than the current level, which should make it easier to reduce DRP loading. For moderate DRP reductions, CP targeting was found to be more robust to climate change than land-use change, largely because costs and benefits of CPs are less sensitive to climate change than yields of alternative crops and plants. However, integration of CP and land-use change optimization was required to achieve policy goals for DRP reductions (~78%). This project was the first effort to quantify climate sensitivity of a strategy to NPS reduction that includes both land-use change and CP optimization. Also, results from this study highlight the need for future spatial optimization studies to consider adaptive capacity of conservation actions under a changing climate, rather than trying to identify a single ‘robust’ solution for the next decades.

Chapter 1

Sensitivity of a Stochastic Land-Cover Change Model to Pixel versus Polygonal Land Units

1 Introduction

Anthropogenic land-use and land-cover changes (LUCC) have been identified as among the most profound drivers of a wide variety of environmental problems, including water quality degradation, biodiversity loss, and climate change (Foley et al., 2005; Paeth et al., 2009; Tong and Chen, 2002). To evaluate possible impacts of future LUCC on ecosystem services and propose more sustainable environmental policies, it is essential to develop and advance land-change models (LCMs) to provide reliable future land-cover change projections (Houet et al., 2010).

Increasing need from both academic and policy communities to both project and explain LUCC has led to the development of a wide range of LCM approaches (Brown et al., 2013; Paegelow et al., 2013). In general, LCMs can be characterized along a continuum from pattern to process based models. We focus on the implications of spatial structure for the applicability of projections from a spatially explicit, pattern-based LCM, which models LUCC as transitions from one land-cover category to another (Mas et al., 2014). This type of model is based on an analysis of the spatial structure of land cover, rather than an explicit description of the decisions that lead to those changes (Verburg et al., 2004). The transition process is modeled empirically using past land-use/cover (LUC) maps to develop mathematical characterizations to guide allocation of future land-cover change.

While specific algorithms and/or model structures vary from model to model, spatially explicit LCMs are all based on some set of tessellated land units, which are used to map and simulate LUCC. Most LCMs are designed to use a fixed set of spatial units, either pixels or polygons, without evaluating the implications of this choice (Verburg and Overmars, 2007). Few studies to date have compared impacts of different types of land units on the performance of LUCC models. One reason is that very few models, and even fewer pattern-oriented or neutral models, support polygonal map units (Gaucherel et al. 2006). Pattern-oriented models tend to use pixels because they match very well with the format of land-cover data derived from remote sensing and allow for straightforward processing (NRC, 2013). However, pixels do not match well with spatial units over which land is changed (Verburg and Overmars, 2007), because the land area of anthropogenic landscapes (e.g. cites, farms, managed forests) is often divided into discrete units defined by management or property boundaries (Courbaud et al., 2001; Ellis et al., 2006). For anthropogenic landscapes, using spatial units that coincide with field or property boundaries can link LCMs with human decision making more directly (NRC, 2013).

Although pixels still dominate as the land unit implemented in LCMs, there has been an increasing interest in developing polygonal or patch-based models in both pattern and process-oriented LCMs. Several pattern-based LCMs have been developed that can handle polygonal or patch-based land units directly, such as the patchy landscape neutral models (PLNM) (Gaucherel et al., 2004) and L1model (Gaucherel et al. 2006). Polygon land units can be defined using “top-down” or “bottom-up” approaches. For pattern-based models, it is often more straightforward to adopt a “top-down” approach, in which patch size/shapes are pre-defined by existing polygons. Researchers interested in process-based models have also developed polygon-based CA models (Ballestores Jr. and Qiu, 2012; Stevens and Dragicevic, 2007) and agent-based models

(Alexandridis and Pijanowski, 2007; Crooks, 2010) using this top-down approach. The drawback of this approach is that it often requires a single land-use/cover type assigned to each land parcel (Ballestores Jr. and Qiu, 2012). Assigning single land-use/cover categories to polygons will inevitably affect the representation of land-cover composition and spatial patterns because any mixing of land-cover types within a unit will be simplified. In addition, geometrical shapes are typically fixed so that only the composition of land-cover types can be changed (Gaucherel et al. 2006, Le Ber et al. 2009). A more flexible approach is to build up patches from the bottom-up. Some studies have tried to include spatial or landscape pattern metrics in LCMs (Brown et al., 2002; Duh and Brown, 2007; Li et al., 2013; Sohl et al., 2007) to control interactions between pixels, so that patch structure emerges a posteriori (Gaucherel et al. 2006). Recently, Meentemeyer et al. (2013) and Chen et al. (2014) developed patch-based urban cellular automata (CA) models based on patch-growing algorithms. The problem with these "bottom up" approaches is that management boundaries were not directly utilized in these models. To take advantage of both "bottom-up" and "top-down" approaches, some studies have proposed a "hybrid" approach: the LCM starts with polygonal land units defined by management boundaries, but also allows geometrical modification during the simulation (Gaucherel et al. 2006, Moreno et al. 2008). However, dynamic modification is more complex to implement and is computationally expensive.

Previous studies focused on the polygonal approach have explained the advantage of using polygons, but few have demonstrated the trade-offs between pixels and polygons on a single LCM. Chen et al. (2014) compared CA models with and without a patch-growth algorithm, but they did not provide a direct comparison of models with pixels or polygons as the fundamental land unit. Rather, they assessed of the utility of patch-growth algorithm. Similarly,

Mas et al. (2012) evaluated impacts of pixel versus polygon/patch-based modeling by using different models, but algorithms and model structures are quite different among these models. A proper comparison would hold constant all variables aside from the spatial tessellation. Therefore, our study focusing on comparing the effects of pixels and polygons on the output from a given LCM provides an important contribution. Furthermore, current polygonal LCMs often focus on a single landscape context, such as urban (Chen et al., 2014; Crooks, 2010), agriculture (C Gaucherel et al., 2006) or forest (Mas et al., 2012). However, a more general discussion that includes multiple land-cover types is needed.

The objective of this study is to investigate the sensitivity of land-cover forecasts using a consistent modeling approach to alternative map units (i.e., pixels versus polygons). To simplify the temporal aspect of the study and focus on the effects of spatial units (pixels or polygons), the experiment uses data from two time points, 1992 and 2011. In order to test the effects of the spatial units on the spatial allocation of land covers and their effects on the simulated accuracy relative to observed landscape patterns, we simulated 2011 based on models fitted to data over the time period. We evaluate the match between model simulations and observations for pixel- and polygon-based implementations of a geostatistical LCM in the Medina County, northwestern Ohio, on two dimensions. The first is the degree of location agreement between the simulated and observed land-cover types; the second is the similarity in several spatial pattern statistics. The modeling approach we used is adapted from Brown et al. (2002) and involves a geostatistical simulation of future land-cover types by fitting the model according to three objectives: (1) an transition probability map, derived using generalized additive modeling, (2) semivariograms to control the spatial patterns, and (3) a transition matrix describing the amount of area in each future land-cover type. We conducted a sensitivity analysis to calibrate weights

for these objectives and the number of iterations for each simulation. To reflect changes in management boundaries, nine different parcel-splitting scenarios were included to reflect changes in field boundaries. The model was used to generate 100 realizations each for ten scenarios (i.e. pixels and nine parcel-splitting scenarios). Three different land-cover conversions were modeled: agriculture to developed land; forest to developed land; agriculture to forest.

2 Materials and Methods

2.1 Study Area and Data

The study area, Medina County, is located in north central Ohio. The landscape here is mostly a gently rolling plain with an average slope of 3.5%. As part of the Cleveland metropolitan area, Medina is about 40 miles from Lake Erie and Cleveland. In 2010, the county had a total area of 1,100 km2 and a population size of 172,332 (US Census Bureau, 2010).

In order to focus the analysis on how choice of spatial units affects model results, the National Land-Cover Dataset (NLCD) from 1992 (Fry et al., 2008) and 2011 (Homer et al., 2015) were used for both calibration and validation purposes. Original two-digit land-cover codes were reclassified to level-one codes by grouping similar land-cover types together. For example, low, medium and high intensity developed land-cover types were all classified as developed land. Inconsistencies observed between 1992 and 2011 datasets (e.g., urban to agriculture transition) were adjusted through manual editing, based on concurrent fine-resolution remote-sensing images available from Google Earth. According to NLCD, major land-use/cover types in the county were agriculture (~48%), forest (~29%) and developed (~18 %) in 1992. Between 1992 and 2011, three significant (>5% change) transitions were identified: (1) agriculture to developed (3064 ha); (2) forest to developed (2011 ha); and (3) agriculture to

forest land (1676 ha). The percentage increases for developed land and forest land were 16% and 5.5%, respectively.

Parcel maps were used to define polygonal land units. A parcel is an area of land circumscribed by ownership boundaries, i.e., an area of contiguous common ownership. Digital parcel maps for the study area were obtained from the local county tax assessment department.

Spatial data describing biophysical conditions (e.g., soil and terrain characteristics) and location relative to water features, major roads, urban areas, and natural amenities served as spatial predictors, which were used to create a transition probability (suitability) map (Table 1). All spatial predictors were created as raster files, with a spatial resolution of 30 meters, to correspond with the resolution of NLCD. Soil variables were converted from the vector SSURGO data (USDA NRCS, 2015a).

2.2 Simulation Framework

The LCM was designed to project future land-cover maps, given an initial land-cover map, transition probability maps, estimates of the quantities of land-cover changes, and geostatistical descriptions of land-cover patterns. The land allocation algorithm is based on a modified simulated annealing algorithm that seeks to honor three objectives simultaneously: (1) quantity of land-cover changes, (2) locations of future changes relative to transition probability maps, and (3) semi-variance describing spatial patterns of those changes. Overall simulation framework was illustrated in Figure 2.

The LCM was modified from Brown et al. (2002) with two key extensions. First, it was expand from a single transition type to multi-categorical land-cover changes, and second it is capable of handling of both pixel and polygonal land units. Unlike pixels, polygonal units have varying shapes and sizes. More important, perhaps, is that management boundaries are likely to

change over time. For instance, a parcel may be split into two or more parts for various reasons (e.g. re-selling, gifting to children) (Donnelly and Evans, 2008; Mehmood and Zhang, 2001). To reflect this sort of change, nine parcel-subdivision scenarios were included (Figure 3) to represent possible subdivision processes. For a given scenario, a common parcel subdivision strategy was implemented for all parcels. To avoid creating artificially small new parcels, we limited splitting scenarios to parcels larger than 10 ha.

The second extension was to represent more than one land-cover transition type. Brown et al. (2002) developed a model that represented only one transition type (not forest to forest). The modified model represents three observed transition types (i.e. agriculture to developed; forest to developed; agriculture to forest).

The model was calibrated to observed LUCC (1992-2011) derived from historical NLCD maps. Sensitivity tests were conducted to calibrate parameters of the land allocation algorithm. The calibrated model was then used to simulate 2011 maps using pixel and nine subdivision scenarios (Figure 3). We ran the model 100 times for each of the ten parcel subdivision scenarios (a total of 1000) to account for uncertainties in stochastic simulations. Simulations were completed using high-performance computers. Model performance was assessed using both spatial allocation and landscape pattern metrics.

One objective of our study design is to ensure comparability of results from pixel versus polygon-based simulations. Using polygons/parcels as discrete objects requires assigning a single land-cover type to each polygon, this removes spatial heterogeneity within parcels where multiple land-cover types exist. Land-cover maps produced using pixel and polygon-based simulations will be different for this reason alone, making it difficult to distinguish difference due to alternative land units from those due to discrepancies in aggregation level. To address this

problem, we combined polygonal boundaries with NLCD data to keep both management boundaries and fine-scale land-cover attributes, using the approach described in the following section.

2.2.1 Land-cover change allocation algorithm

We used a modified simulated annealing (SA) algorithm to generate alternative land-cover scenarios, chosen based on their difference from target objective function values, which are set so that simulated and observed transitions will have minimal differences. This algorithm has been reported as useful and effective in solving complex spatial problems in previous studies (Burnicki et al., 2007; Duh and Brown, 2007). The algorithm can be summarized as follows:

1) Perturb a portion (5%) of pixels in the initial land-cover map randomly to initiate process;

2) Compute the initial objective function values for all three objectives as the differences between current and target objective function values;

3) Visit all spatial locations (parcels or polygons), except for urban and water units, along a random path. At each location, consider the three possible land-cover transitions and compute objective function values corresponding with those changes.

3.1 Accept the change if it leads to a decrease in the difference from the target objective function value.

3.2 With a small probability, the model will accept a change that increases total difference in objective function values. The probability is termed as temperature, which will cool down (i.e., decrease) gradually over time.

4) Repeat step 3 for a specified number of iterations.

Figure 4 illustrates the method used to handle polygonal land units. We overlaid polygons with the initial land-cover map, so that pixels within each polygon received a membership identity. During the simulation process, one polygon, rather than one pixel, is visited at a time. Then a possible transitions are applied to eligible patches (based on the initial land-cover type) within that particular polygon. In this way, all simulations can use the same input land-cover maps.

2.3 Model Calibration and Sensitivity Analysis

2.3.1 Quantity of changes

The LCM requires information about the amounts of area undergoing each type of land-cover change (i.e., quantities). To calculate these quantities, we computed a Markov transition matrix by overlaying and comparing historical land-cover maps at two dates for Medina County (1992 and 2011).

2.3.2 Distribution on transition probability maps

Transition probability (i.e., suitability) maps express the relative suitability of a certain location for development or new forest land, based on where those cover types were located in 1992. Suitability for new urban or forest areas was modeled as a function of spatial predictors (Table 1). Weights of spatial predictors were determined using a generalized additive model (GAM) (Hastie and Tibshirani, 2005; Wood, 2006) because relationships between spatial predictors and land-cover patterns are not always linear (Brown et al., 2002). To reduce spatial autocorrelation in the data, NLCD data and spatial predictors were sampled systematically by taking every sixth 30-m by 30-m cell on every sixth line. Suitability maps were estimated using the mgcv package (Wood, 2001) in R (2.15.1) (R Development Core Team, 2014). The distributions of suitability

values at locations where land-cover changes were observed were summarize as frequency histograms. The Receiver operating characteristic (ROC) curve and Area under the Curve (AUC) associated with ROC were used to evaluate fit of GAM models.

2.3.3 Description of spatial pattern

We used semivariograms to describe the spatial patterns of simulated and observed land cover maps (Burnicki et al., 2007). Let S_α and $S_{\alpha+h}$ be land-cover categories at locations u_α and $u_{\alpha+h}$, respectively, which are separated by a distance vector **h** (ranges from one to four pixels). Occurrence of S_k at u_α or $u_{\alpha+h}$ can be coded using an indicator variable, as described in Equation 1.

$$\begin{cases} i(u_\alpha; S_\alpha, S_k) = 1 \text{ if } S_\alpha = S_k ; \\ \qquad\qquad\quad = 0 \text{ otherwise} \end{cases} \tag{1}$$

Indicator semivariance (Equation 2) measures the lack of spatial connectivity over **h**: the lower the value, the higher the connectivity (Brown et al., 2002). Cross-semivariance (Equation 3) describes frequency of having land-cover types S_m and S_n jointly occur at two locations separated by **h**. A lower value represents higher probability of joint occurrence.

$$\hat{\gamma}(h, t_0, S_k) = \frac{1}{2N(h)} \sum_{\alpha=1}^{N(h)} [i(u_\alpha; S_\alpha, S_k) - i(u_\alpha + h; S_{\alpha+h}, S_k)]^2 \tag{2}$$

$$\hat{\gamma}(h, S_m, S_n) \frac{1}{2N(h)} \sum_{\alpha=1}^{N(h)} [i(u_\alpha; S_\alpha, S_m) - i(u_{\alpha+h}; S_{\alpha+h}, S_m)] * [i(u_\alpha; S_\alpha, S_n) - i(u_{\alpha+h}; S_{\alpha+h}, S_n)] \tag{3}$$

where N(h) is pairs of pixels, which are separated by **h**, sampled from the 1992 land-cover map. Three indicator semivariances (i.e. developed, forest and agriculture land) and 12 cross-

semivariances were calculated, where at least one of the land-cover types in the cross-semivariance was forest, agriculture or developed land.

2.3.4 Sensitivity analysis

We developed detailed sensitivity tests to determine (1) the appropriate weights for each of the three objectives (i.e., quantity, distribution of suitability, and spatial pattern of changes), and (2) stopping criteria for the SA algorithm (i.e. number of iterations). Trial experiments showed that equal weights for the quantity of changes and histogram of the suitability map worked well for both pixels and polygons. Pixels and polygons had differential sensitivity to variogram weights because the size and shape of the units affected the average distance between them. We applied nine different weights ranging from 0.1 to 4.0 to both pixel and polygon-based simulations for the third objective (with the others set to 1.0). Suitability of any given weighting scheme was measured by calculating the total objective function (TOF) value, which reflects the difference between simulated and target objectives. A smaller TOF value indicates a better weighting scheme.

Once the weights were calibrated, a total of 2700 simulations was generated (30 simulations × nine weights × 10 land units). To identify stopping criteria for the SA algorithm, we ran the LCM for a number of different iterations for each land unit and traced out trajectories of total objective function values.

2.4 Model Validation and Assessment

The performance of the LCM was assessed by comparing simulated land-cover maps with the observed maps in 2011 using two separate criteria: (1) spatial allocation accuracy, and (2) landscape pattern similarity. Spatial allocation accuracy was evaluated using the “figure of

merit" (FoM), which is the ratio of the correctly predicted changes to the union of observed and predicted changes (Pontius et al., 2008). Compared to traditional two-map comparison metrics (e.g. Kappa), FoM allows users to distinguish spatial agreement obtained due to change versus persistence (Pontius et al., 2008). FoM ranges from 0 to 1, with a higher value signifying better agreement between simulated and observed changes. We employed a multiple-resolution analysis method recommended by Pontius et al. (2011). This method compares transitions at several coarser resolutions to distinguish minor allocation disagreement from major allocation disagreement. The lulcc package (Moulds et al., 2015) was used to calculate FoM scores.

To measure landscape patterns, we selected a total of six representative landscape pattern indices from the literature (Chen et al., 2014; Frate et al., 2014; García et al., 2012; Herold et al., 2002; Mas et al., 2012; Seto and Fragkias, 2005). Two of the most commonly used metrics, which are contagion index (CONTAG) and the fractal dimension index (FRAC_MN), were selected as the landscape level pattern metrics. Contagion index describes the intensity of aggregation of the landscape patches and the spatial connectivity between them and was selected to measure overall landscape fragmentation. Fractal dimension was designed to describe overall shape complexity across a range of spatial scales and was selected to quantify complexity of spatial patterns emerged in LUCC systems.

The remaining four class or landscape level metrics are: (1) number of patches (NP), (2) largest patch index (LPI), (3) mean perimeter-area ratio (PARA_MN), and (4) mean Euclidean nearest-neighbor distance (ENN_MN). NP and LPI are frequently used to describe patch size and distribution. PARA_MN is useful to compare patch shape complexity for observed and simulated patches. For forest or urban patch, connection or approximation between simulated and existing land-cover patches are important. ENN_MN was selected to measure proximity or

isolation of patches of same class. All indices were calculated using FRAGSTAT 4.2 (University of Massachusetts, Amherst) (McGarigal et al., 2012).

2 Results

3.1 Calibration and Sensitivity Analysis

3.1.1 Calibration

The GAM model for forest locations was slightly better fitted than the model for development (Table 2). However, the receiver operating characteristic (ROC) curves (Figure 5) show that the model for development produced a better suitability map. Area under the curve (AUC) for the models of new developed and forest land were 0.8 and 0.7, respectively. Fitted models were used to produce suitability maps for new developed (Figure 6a) and new forest land (Figure 6b).

The five variables with at least 1% explained deviance in the model for development were: (1) distance to small city center; (2) distance to forest; (3) distance to existing urban area; (4) distance to state highways; and (5) distance to national parks. For the model for forest, the four variables with at least 1% added explanation were: (1) distance to existing forest land; (2) distance to local roads; (3) distance to highways; and (4) distance to large city centres. Distance to existing forest land alone contributes to 40% of the deviance explained.

3.1.2 Sensitivity analysis

Results of the sensitivity analysis to different weights on semivariogram component of the objective function showed that 0.5 worked best for pixel land unit (Figure 7). For polygonal land units, normalized TOF values tended to decrease as weight for semivariogram increased, but TOF values were stabilized around 2.5 (Figure 8). Further increase in the weight on spatial

pattern makes it difficult for the model to match the quantity of changes objective. The reason for different optimal weights in the pixel versus polygon models is that initial random perturbations by pixels tend to change the spatial structure of the starting land-cover map more significantly than patches. For instance, the sum of differences between initial and target indicator semivariances for the Equal_2 scenario is 0.26, whereas the value for the pixel-based simulation was 1.20, approximately 5 times larger. For the same reason, the initial TOF value was higher for the pixel-based simulation (Figure 9). For all simulations, there was little change after 20 iterations; 25 iterations was sufficient for all simulation results to stabilize.

3.2 Model Validation and Assessment

Overall, the pixel-based simulation honored target objective function values better than polygon-based simulation. The average total objective function (TOF) value for pixel-based simulations was 0.23±0.03, compared to 0.68±0.04 for polygonal land units. Parcel subdivision scenarios Equal_2 and Equal_6 had the lowest TOF values, and therefore matched the three objective function values better than other scenarios. Both pixel and polygon-based simulations were able to meet the quantity of change target (average difference for all land units were within 5%).

Differences between the model results produced from the different polygon-based scenarios were smaller than the difference between and polygonal land units. Using the Equal_2 scenario as illustrative of the differences between pixel and polygonal land units, visual inspection of observed and simulated development changes (i.e. agriculture/forest to developed) reveals that spatial patterns of transitions are different among three group maps (Figure 10). Observed forest to developed transitions presented an “infill” growth pattern, where new patches are found close to the existing developed area. On the other hand, the agriculture-to-forest transition tended to exhibit “spontaneous” or new growth in rural areas. Most changes produced

for the pixel-based model (Figure 10d and Figure 10e) were placed on edges of initial developed or forest patches, whereas patches generated by polygon-based simulations (Figure 10g and Figure 10h) were scattered over large regions. When zoomed in to agriculture-to-forest transitions in the northeastern part of the study area, it can be observed that sizes and shape of patches based on polygons (Figure 10i) are more similar to observed new patches (Figure 10c).

3.2.1 Spatial allocation accuracy

Mean FoM values for pixel-based simulation increased from 0.1 to 0.69 as the cell-size increased, whereas FoM ranged from 0.07 to 0.46 for the Equal_2 polygon scenario (Figure 11). It is clear that pixel units obtained higher location accuracy across scales, which is a finding consistent with visual inspection results (Figure 10). Nonetheless, polygon-based simulations were better than neutral changes (allocating desired quantity of three transitions randomly across the map).

To understand the effect of difference parcel subdivision processes on the fit of the polygon-based simulations to observed patterns, we calculated relative FoM values at different resolutions. The relative transition-specific FoM scores for the nine parcel-subdivision scenarios demonstrated different patterns for agriculture-to-developed change versus forest-to-developed change at different resolutions (Figures 12). At native resolution, analysis of variance (ANOVA) indicated significant differences among subdivision scenarios for the agriculture-to-developed transition ($F=3.91$, $p<0.01$), but not for forest-to-developed transition; at coarser resolutions, ANOVA tests show significant differences among subdivision scenarios for both transition categories. At coarser resolutions, relative FoM scores for the forest-to-developed transition were more consistent. Additionally, Equal_2 scenario tended to produce higher FoM scores than other scenarios.

For agriculture-to-forest FoM values, Tukey's honest significant difference (HSD) test indicated that Equal_2 and Equal_6 perform significantly ($p<0.01$) better than other scenarios at native resolution (Figure 12); at the resolution of 64 pixels, parcelization configurations with more splits (e.g. Equal_6) worked better than simpler scenarios (e.g. Equal_2). However, at coarser resolutions, there were no significant differences among parcel subdivision scenarios.

3.2.2 Landscape pattern similarity

Overall, polygonal land units outperformed pixels ($p<0.01$) on all landscape pattern metrics, with the only exception of LPI for forest land. Both pixel and polygon simulations generated lower CONTAG and FRAC values than observed, but polygon-based simulations obtained a spatial structure that was more similar to the observed (Table 3). We observed a decreasing trend in metrics values from simpler split scenarios (e.g. Equal_2) to multiple split scenarios (e.g. Equal_6) (Figure 13), which resulted in simpler split scenarios reproducing CONTAG and FRAC metrics better than multiple splits.

The largest mismatches in spatial pattern metric values were observed for NP and PARA_MN values (Tables 4 and 5). For developed land, pixel- and polygon-based simulations generated 60 and 10 times more patches than observed, respectively. However, differences for forest land were much smaller for both types of land units. PARA_MN from the pixel-based simulations was almost doubled, when compared to observed maps, whereas polygon-based simulations generated only about 35% larger than observed on average.

NP and PARA values shared a similar pattern of differences in class-level metric values among subdivision scenarios for forest and developed land (Figure 14). NP increased from Equal_2 to Equal_6 scenario, whereas PARA_MN decreased from Equal_2 to Equal_6 scenario. Simpler split scenarios outperformed multiple splits on the patch-size metric (NP), but the

multiple splits scenarios matched the shape metric (PARA_MN) better. Configurations had similar performance on LPI index for forest land (Figure 14d), but there was a clearly decreasing trend for developed land (Figure 14c). ENN decreased from Equal_2 to Equal_6 for forest land (Figure 14h), but the trend was reversed for developed land (Figure 14g). Because ENN_MN values were lower than observed, multiple splits were helpful to meet observed values for developed land, but not for forest land (insignificant differences among groups with $p>0.05$ for all pairs).

4 Discussion

Our comparative experiment explored the behavior of a stochastic land-change model (LCM) using as the spatial foundation of both pixels and polygonal land units derived from parcel maps. Simulation results for Medina County in Ohio indicated that model performance is sensitive to the choice of land units and how they change. There is a clear trade-off between pixels and polygons: for each of three different land-cover transitions, polygon-based simulations generated more realistic landscape patterns, but pixel-based simulations achieved higher spatial allocation accuracy. Though the difference among scenarios that used different approaches to parcel subdivision is much smaller than that compared to the difference between pixels versus polygons, statistical tests indicated there are significant variations among parcel subdivision scenarios. Unlike the pixel-polygon comparison, the relative model performance among parcel subdivision scenarios was sensitive to not only which land-cover transition we examined, but also the resolutions at which analysis was performed.

Because pixels are often much smaller than management boundaries, pixel-based simulations are more flexible in placing changes in the right locations. In contrast, polygon-based simulations force a group of pixels to change simultaneously. Finding and changing a suitable patch in a way

that improves all three objectives is harder because there are fewer patches than pixels. In addition, the semivariogram component controls interactions between pixels at short distances, which encourages changes near edges of existing patches. This strategy distributes change to likely locations more effectively, and thus increases the possibility of coincidence with observed changes. In contrast, fewer polygon units limits possible changes to fewer locations, therefore these simulated changes are less likely to match with observed changes. Also, in polygon-based simulations there tend to be more transitions in remote areas because new growth by patches is less likely to affect spatial structures measured by semivariograms.

Depending on the objective of a certain project, different aspects of LCM performance can be critical. When location accuracy is important for a given study, it makes sense to use pixels because they can match with observed changes better than polygonal land units. On the other hand, generating realistic spatial landscape patterns is central to a range of environmental studies (Gaucherel et al. 2006, White 2006, Mas et al. 2012, Meentemeyer et al. 2013). In these cases, accuracy of spatial allocation is less critical than generating realistic patch sizes/shapes. Our study indicates that using polygonal units may match spatial landscape patterns of land-cover projections better with observed maps than using pixels. This is because the distributions of sizes of land-units and changes in land covers is more like the pattern of actual change. Pixel-based simulations generated significantly more patches compared with observed transitions, and therefore the simulations produced an over fragmented landscape. Confining changes to management boundaries reduced the number of new patches significantly. However, both pixel and polygon-based projections obtained lower CONTAG and FRAC values than observed 2011 land-cover map, suggesting that actual land-change processes tend to form larger and more complex cluster/patches. LUCC decisions are usually decentralized and autonomous, but

complex spatial patterns can emerge in real-world LUCC systems (Parker et al., 2003; White et al., 1997). Different from process-oriented models, pattern-oriented models often lack the mechanisms to model complex interactions between units. Using polygonal land units can mitigate the problem somewhat, but not eliminate it.

When the polygonal approach is preferred for a certain modeling exercise, choices must be made about how best to implement it. Using pre-defined polygon boundaries is one of the most popular strategy for pattern-oriented LCMs. The problem with this approach is that it would eliminate spatial heterogeneity within polygonal spatial units because only a single land-cover type is assigned to each polygon land unit. Compared to this 'top down' approach, our model utilized both pixel-land land-cover maps and parcel maps. Parcels were selected randomly for the simulated annealing algorithm, but only groups of pixels within the parcel that had the initial land-cover type of interest were set to transition, preserving some of the sub-polygon heterogeneity. This implementation enhanced comparability between pixel and polygon land units. An alternative approach is to build up patches from pixels. Several urban CA models (Chen et al., 2014; Meentemeyer et al., 2013) have employed this strategy. CA models using this "bottom up" strategy is more flexible at reproducing emergent complex dynamics, but patch shapes and forms, other than size distribution, are often not controlled in previous studies. In our study we found that orientation and shape of newly generated patches was an important factor affecting model performance. For instance, Equal_2 and Equal_2_S scenarios both split a parcel into halves, but along different directions. In this case, splitting along the long edge performed better than the short edge. This may be partly because splitting along the long edge allowed all new parcels to have road access, and therefore represented the actually subdivision process better. A third option is 'hybrid' CA models, which use a dynamic modification algorithm to

update management boundaries during the simulation process. Compared to this 'hybrid' approach, our model is simpler and faster to implement, and more computationally efficient.

We also looked at the benefit to model performance from incorporation of multiple parcel subdivision scenarios. One previous study (Alexandridis and Pijanowski, 2007) assessed performance of a parcelization algorithm using an agent-based model and found that including parcelization is helpful to better represent LUCC based on land ownership. In their model, parcels could only be split into halves in their model. However, our study found that split parcels in half may not be the best option for all land-cover transitions. We were able to show that the performance of different subdivision schemes varied significantly, both within and across land-cover transition types. Although some previous studies have developed different parcel subdivision algorithms (Dahal and Chow, 2014; Vanegas et al., 2012), these algorithms were designed for urban areas only. However, as our study has demonstrated, lessons learned from one land-cover transition (e.g. development) may not apply to another transition (e.g. reforestation). Thus modelers should consider the suitability of a particular parcelization configuration based on the type of land-cover transition they are modeling.

Examining the scale dependence of validation results provided additional information about model performance. A multi-resolution assessment technique has been recommended for model validation in recent studies (Pontius et al., 2011) because it can distinguish minor disagreements from major disagreements. However, it is often not clear which scale is most appropriate for judging model performance. This is especially true when ranking of alternative units becomes erratic cross resolutions. Comparing the agriculture-to-forest and urbanization transitions showed that differences between parcel subdivision scenarios become smaller at coarser resolutions in

the former case, and larger in the latter. This kind of variability requires the modeler to consider the scale of the process (e.g., does it tend to occur on small or large parcels, in clusters or scattered) and to interpret what the results at different scales imply about the suitability of the different model schemes for representing the process. For example, we found Equal_2 scenario worked better than Equal_6 scenario for simulating new development, but Equal_6 worked better for simulating agriculture to forest transition. This difference is probably caused by sizes and distributions of parcels involved in different transition processes: development changes often occur in the units of parcels or land lots, and sizes of parcels involved in urbanization transition tend to be smaller than other transitions. In this case, the Equal_6 scenario may over-split the initial parcel and generate artificial small patches. In contrast, the agriculture to forest process observed in this study suggested that reforestation only takes a small part, which is less than 10% on average, of the area of an agricultural parcel. Therefore, a multiple split scenario would reflect the actual reforestation process better. Furthermore, the scale of analysis should reflect patch sizes and distributions of interested land-cover types. For instance, average patch size for forest patches is only about one-tenth of that for urban patches. Also, distribution of observed new forest patches, when compared to new development, presented a more scattered pattern. When measured at a coarser scale, a more evenly distributed transitions pattern would lead to a higher chance of resolving minor locational disagreements through swapping cells, regardless of parcel subdivision scenarios. This explains why differences of FoM scores among parcel subdivision scenarios become insignificant at resolutions higher than 64 pixels for agriculture to forest transition. The result suggests that, for the reforestation process, it is more reasonable to focus on finer resolutions.

Our simple parcel subdivision process kept the model efficient, but may have limited model

performance. For example, the model could have been improved by replacing the uniform parcel subdivision scenario with a mixing of multiple parcelization configurations and allow the LCM to select suitable configurations for each parcel, depending on local geographic characteristics and the type of land-cover changes to be modeled. The actual parcel-splitting process would be affected by parcel size, location, orientation and local conditions. For instance, realistic parcel splits should provide road access for new parcels, which is not explicitly modeled in this study. Additional useful information to be considered includes, but not limited to, proximity to natural resources such as rivers and parks. In addition to parcel subdivision, in the future it would probably be helpful to consider parcel aggregation trajectories as well in the future. All of these modifications would likely come at the cost of more computational effort.

It is well known that some LCMs may be sensitive to the size of cells. We did not aggregate cells to coarser scales in this study to keep spatial heterogeneity at native resolution, but it would be interesting to evaluate how trade-offs between pixel and polygonal land units might be changed when pixel-based simulations were run at multiple coarser resolutions. Finally, results obtained in this study might be limited to our study area only. While the broader lessons about model sensitivity and trade-offs between pixel and polygon-based simulations are generalizable, application to other regions with different landscape characteristics and LUCC patterns is needed to validate generality of lessons learned in this study.

5 Conclusion

We examined the effect of alternative land units on the performance of a stochastic land-change model (LCM) to evaluate the sensitivity of a LCM to pixel versus polygon land units. Performance was measured according criteria that included spatial coincidence with observed changes and similarities in landscape patterns. To reflect geometrical changes in management

boundaries, nine possible subdivision scenarios were included and tested. Performance of pixel- and polygon-based simulations was considerably different, even though all aspects of the model were consistent aside from the tessellation scheme. Selection of the most appropriate tessellation scheme depends heavily on the objective and context of individual applications. If spatial allocation accuracy is a more important objective, then the pixel-based model is the best option. Polygon-based land units derived from management boundaries were found to perform better in terms of generating realistic spatial pattern. Enabling both options in any given LCM can give users a more complete understanding of how simulated land dynamics are affected by selection of land units for a LCM, although polygon-based land units much more rarely implemented. If allowing both options is not feasible for a particular project, our results indicate that it is helpful to at least consider the benefits of a polygon-based tessellation scheme. Also, we were able to show that the performance of various subdivision approaches was sensitive to not only the type of land-cover transition being modeled, but also the resolution at which the validation is performed. The comparative experiments presented in this study provide input to researchers interested in choosing among alternative tessellation schemes that can affect model performance from different perspectives.

Funding

This research is supported by the National Science Foundation Water Sustainability and Climate program under Grant No.1313897. Partial funding provided through a Rackham Graduate Student Research Grant.

Table 1.1 List of spatial predictors

Variable	Description	Source
DEM	Elevation	National Elevation Dataset from USGS
Pslope	Slope	Calculated from DEM
Dmjrrd	Distance to major roads	Calculated from Census 2000/2010 TIGER
Dlcity	Distance to large cities	Calculated from Census 2000/2010 TIGER
Dmcity	Distance to median cities	Calculated from Census 2000/2010 TIGER
Dhway	Distance to highway	Calculated from Census 2000/2010 TIGER
Dresrd	Distance to residential roads	Calculated from Census 2000/2010 TIGER
Dshore	Distance to shore	Calculated from National Hydrography Dataset
Dlakes	Distance to lakes	Calculated from National Hydrography Dataset
Drivers	Distance to rivers	Calculated from National Hydrography Dataset
Dnalparks	Distance to national parks	Calculated based on park data from Ohio DNR
Dlocparks	Distance to local parks	Calculated based on park data from Ohio DNR
AWC	Available water capacity	SSURGO data (NRCS)
Pclay	% of clay in soil	SSURGO data (NRCS)
pH	pH of soil	SSURGO data (NRCS)
Porgam	Soil organic content	SSURGO data (NRCS)
Psand	% sand in soil	SSURGO data (NRCS)
nccpi	Crop productivity index	SSURGO data (NRCS)

Table 1.2 GAM model summaries.

New Land-Cover Type	R^2 (adjusted)	Deviance Explained	Restricted Maximum Likelihood (REML)
Developed	0.42	36.6%	6316.9
Forest	0.45	38.4%	4060.8

Table 1.3 Summary of landscape level indices values for pixel and parcel subdivision scenarios.

Groups	CONTAG	FRAC
Observed 2011	1.117	52.44
2011 based on pixel unit	1.04 ± 0.001	48.24 ± 0.177
2011 based on polygons	1.09 ± 0.001	50.40 ± 0.103

Table 1.4 Summary of class level (developed) indices for pixel and parcel subdivision scenarios.

Groups	NP	LPI	PARA_MN	ENN_MN
Observed 2011	262	21.79	697.7	101.2
2011 based on pixel unit	17532 ± 1138	19.38 ± 0.16	1269.87 ± 3.94	89.3 ± 1.2
2011 based on polygons	2282 ± 63.94	20.09 ± 0.36	970.99 ± 10.15	91.2 ± 0.94

Table 1.5 Summary of class level (forest) indices for pixel and parcel subdivision scenarios.

Groups	NP	LPI	PARA_MN	ENN_MN
Observed 2011	2359	1.19	559.6	100.5
2011 based on pixel unit	8113 ± 157.1	1.05 ± 0.08	1065.5 ± 4.77	81.3 ± 0.55
2011 based on polygons	4110 ± 63.94	0.96 ± 0.09	743.3 ± 17.44	87.7 ± 0.71

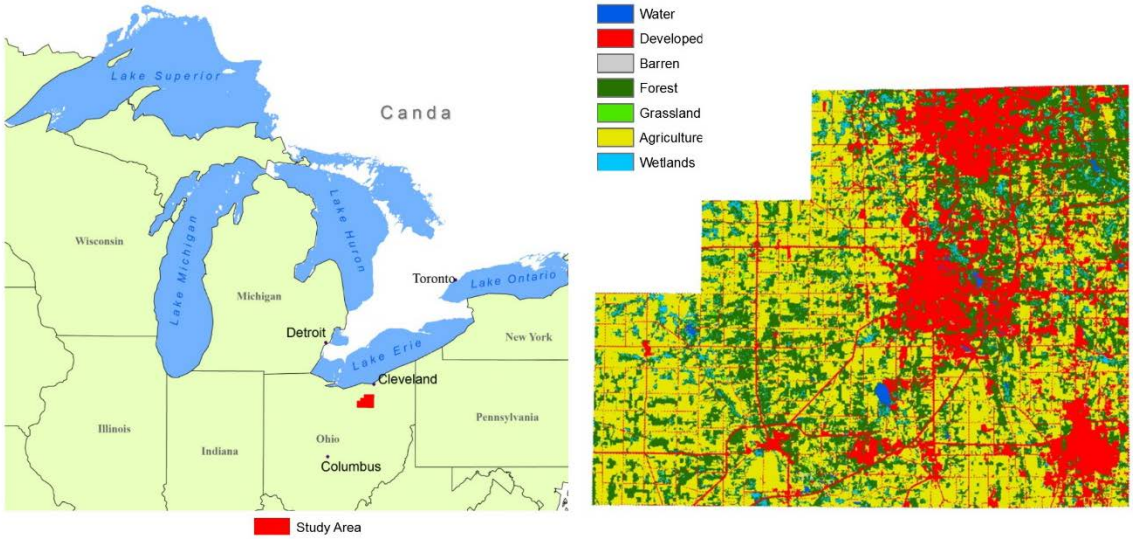

(a) Medina County is located on north central Ohio, part of the Great Lakes basin.

(b) Land-cover map (1992) for Medina County.

Figure 1.1 Study area location and land-cover map

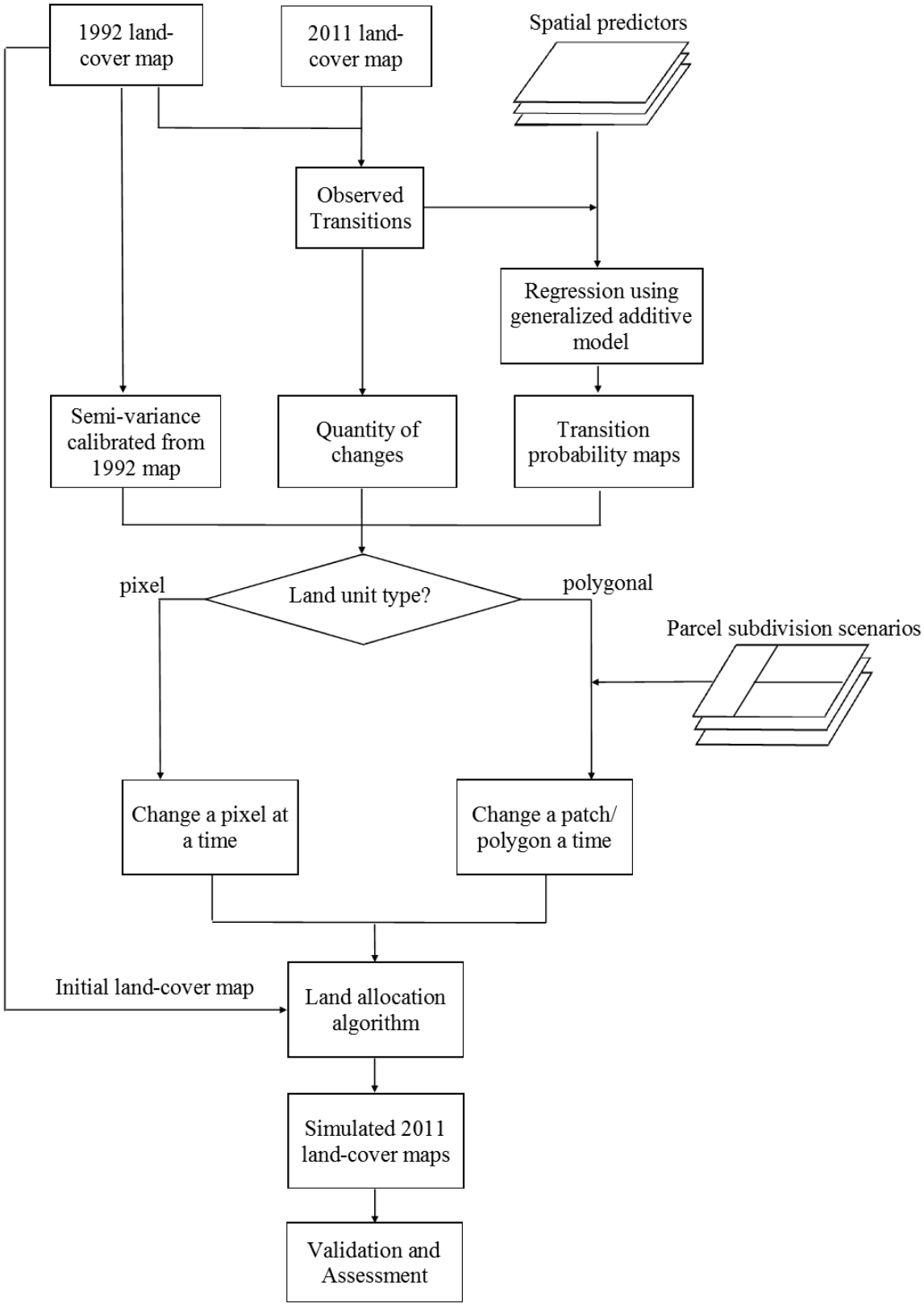

Figure 1.2 Simulation framework

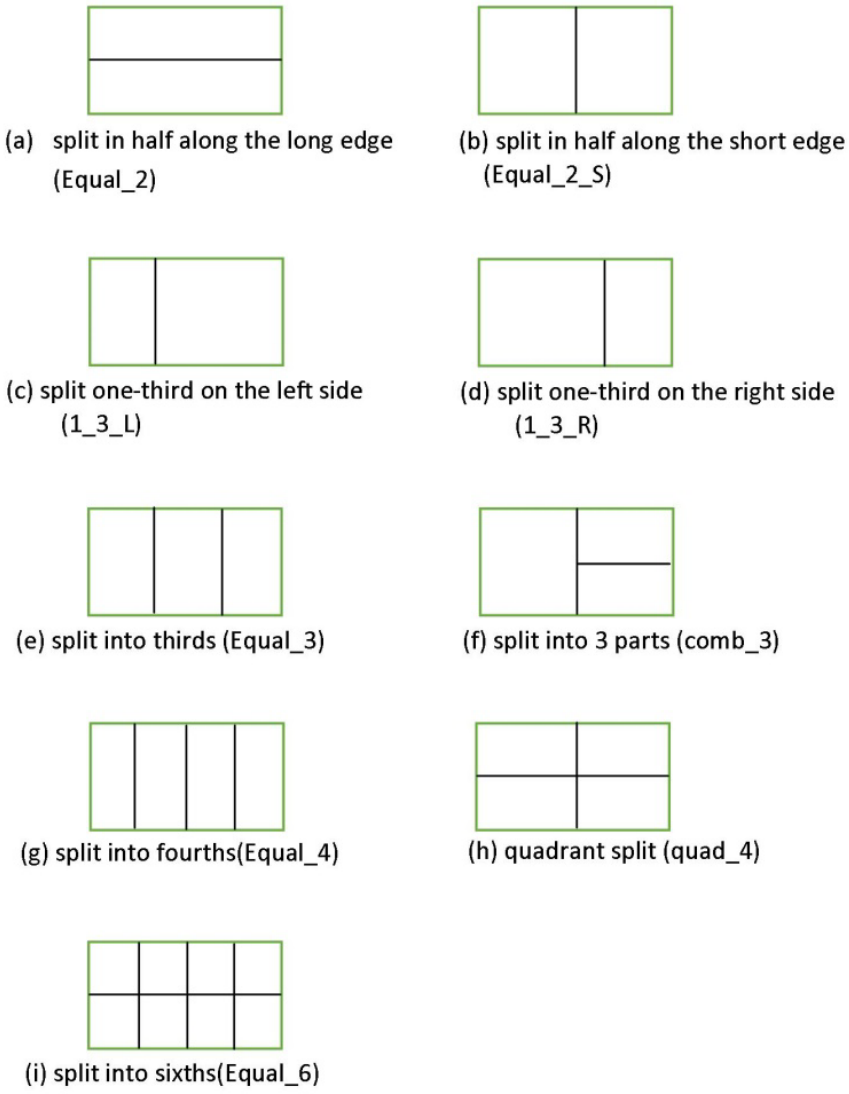

Figure 1.3 Parcel subdivision scenarios.

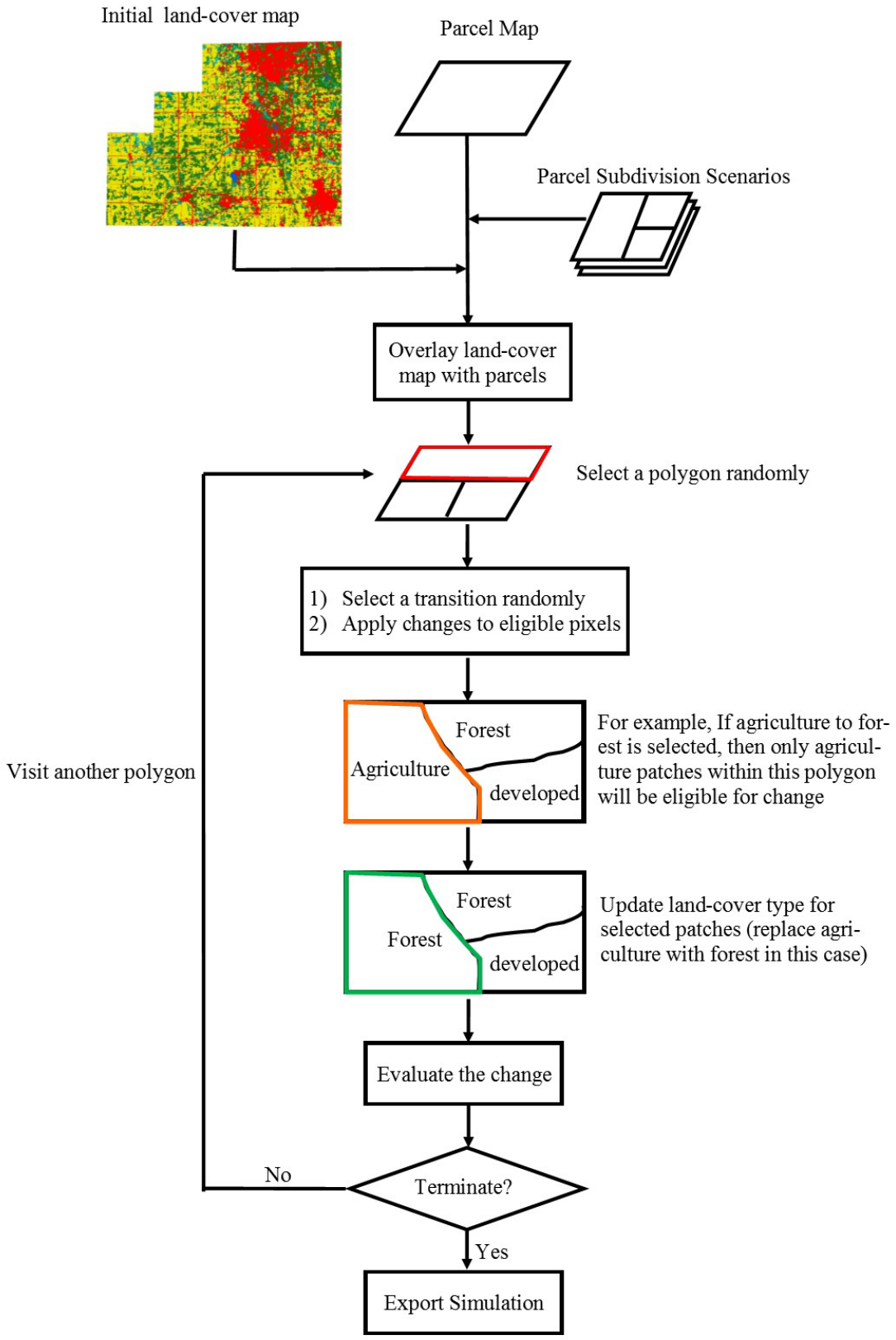

Figure 1.4 Manipulation of polygonal land units.

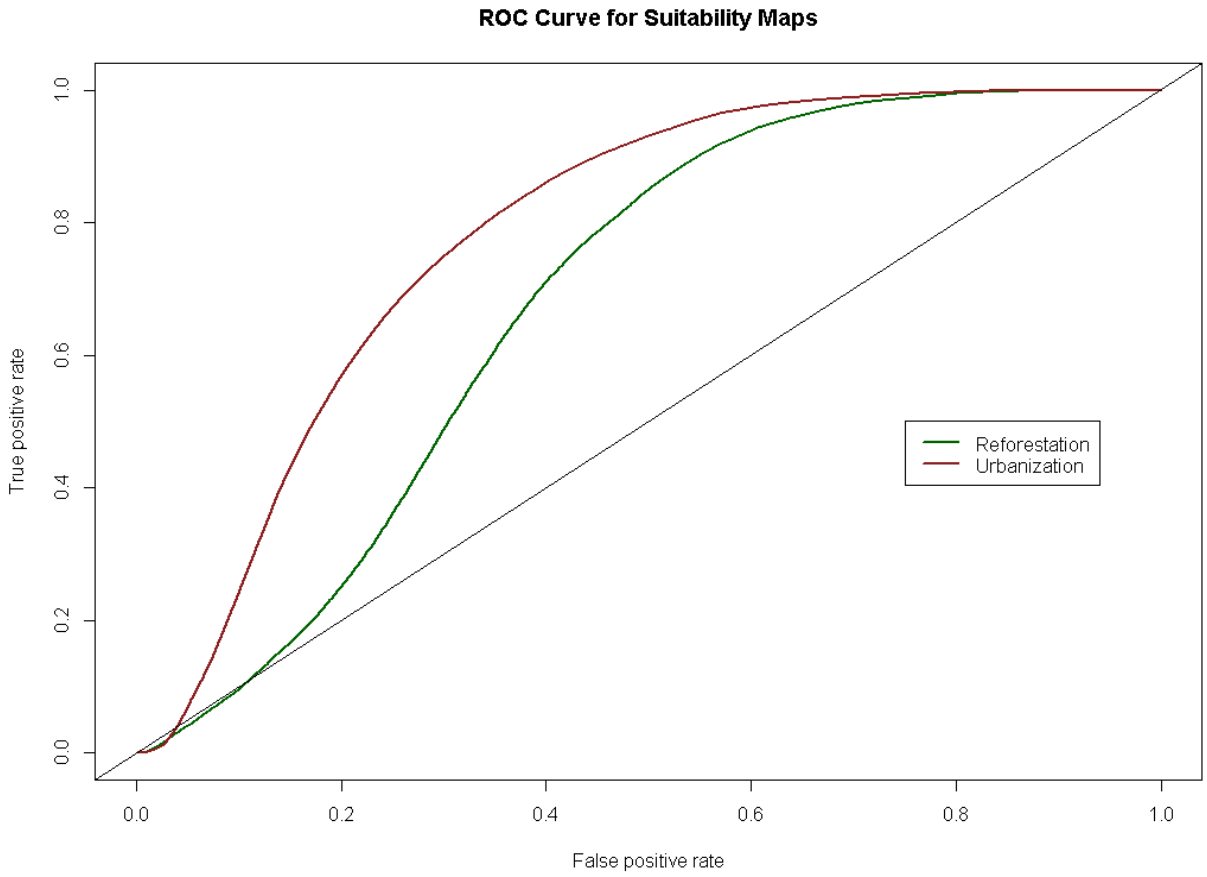

Figure 1.5 ROC curve for suitability maps.

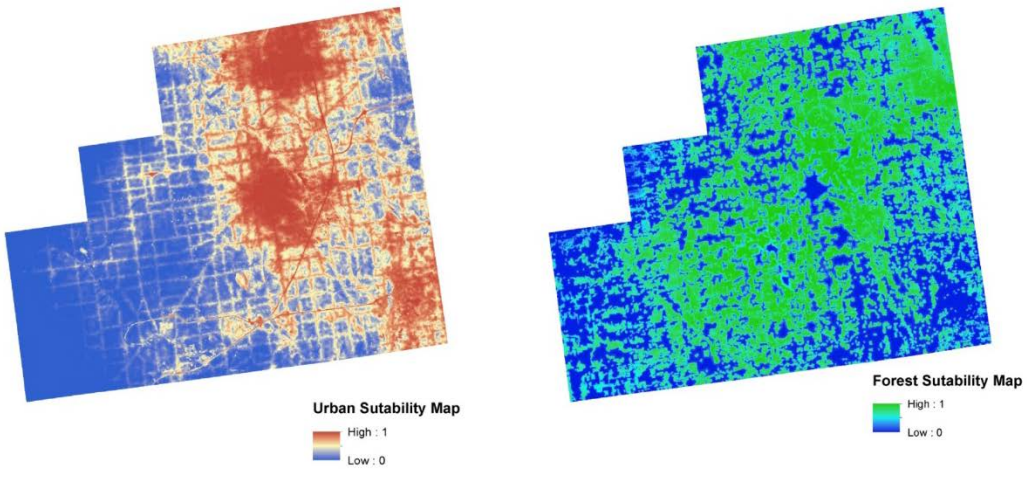

(a) (b)

Figure 1.6 Suitability maps for new urban (a) and new forest (b) land.

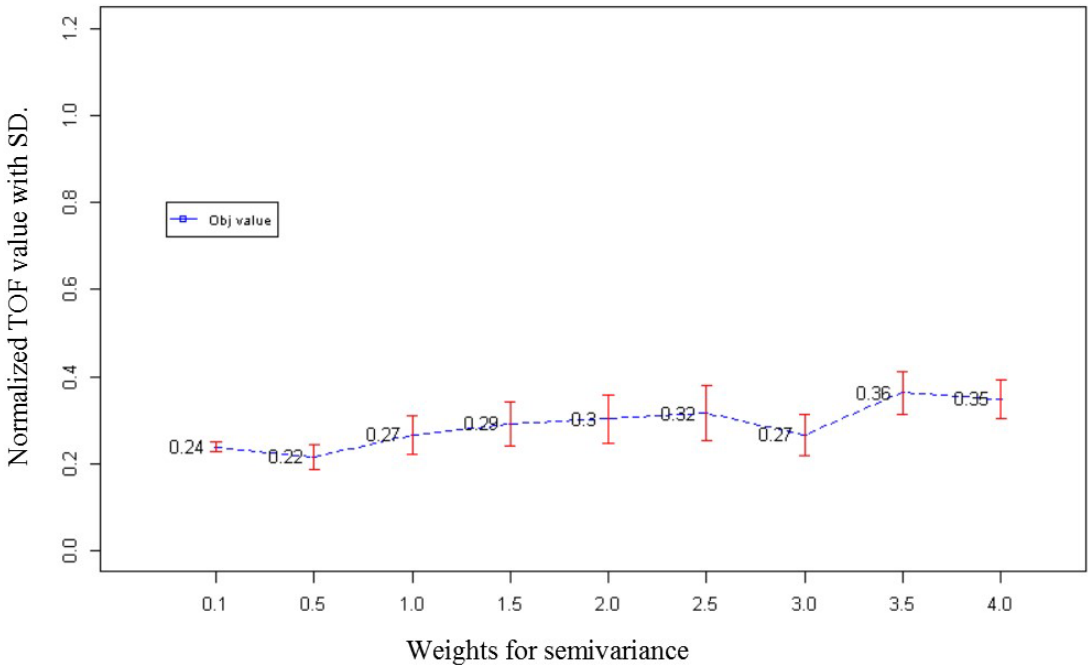

Figure 1.7 Sensitivity of total objective function (TOF) values (means and standard deviations) to weight of semi-variance component for pixel land units. TOF value. measures the difference between simulated and target objectives; therefore a smaller TOF value is desired.

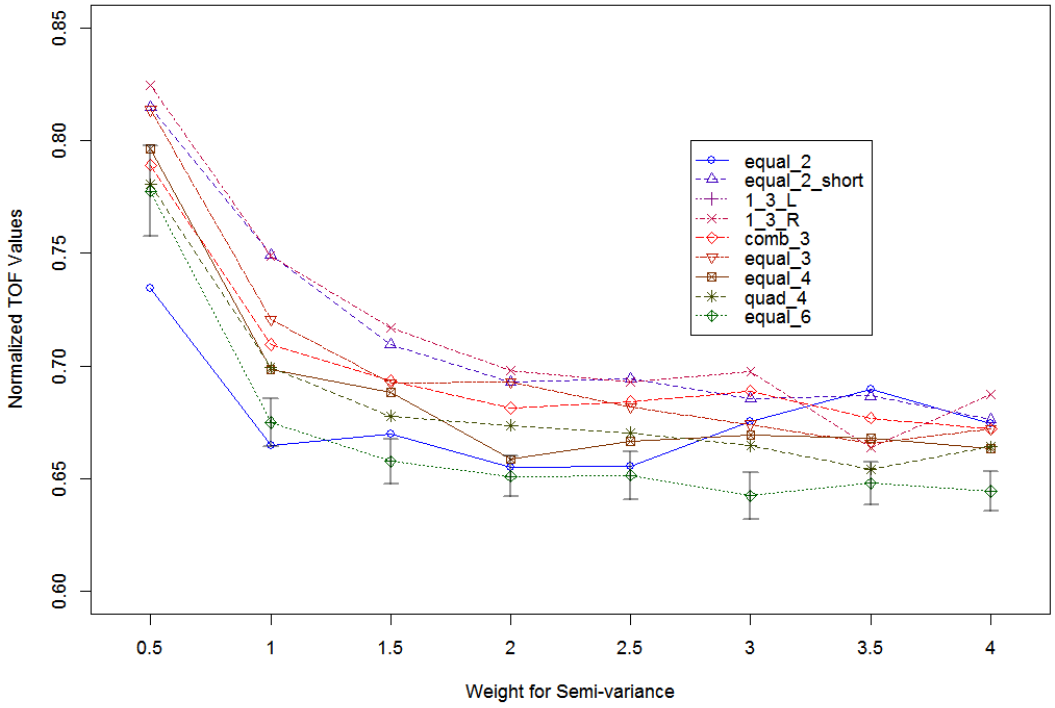

Figure 1.8 Sensitivity of TOF values (means and standard deviations) to weight of semi-variance component for polygonal land units.

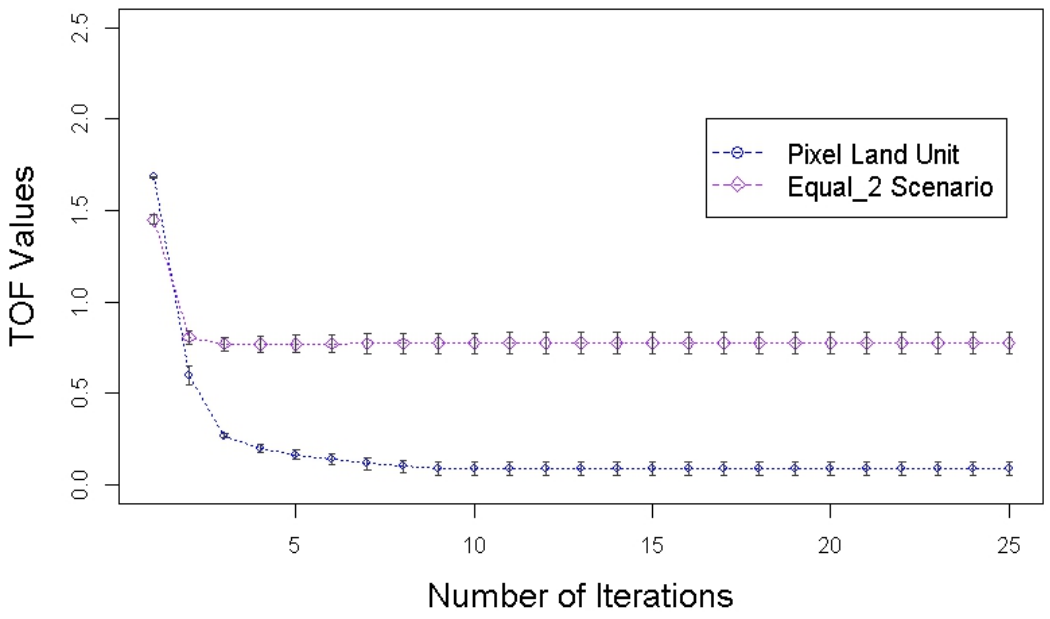

Figure 1.9 Sensitivity of TOF values (mean and standard deviations) to number of iterations for pixel and equal_2 scenarios. Since polygonal simulations have similar patterns, Equal_2 scenario was included as a representative.

Figure 1.10 Observed and simulated transition from agriculture/forest to developed land, and from agriculture to forest land (Zoom on the North-eastern part of the study area) using pixel and polygonal (Equal_2 scenario) units.

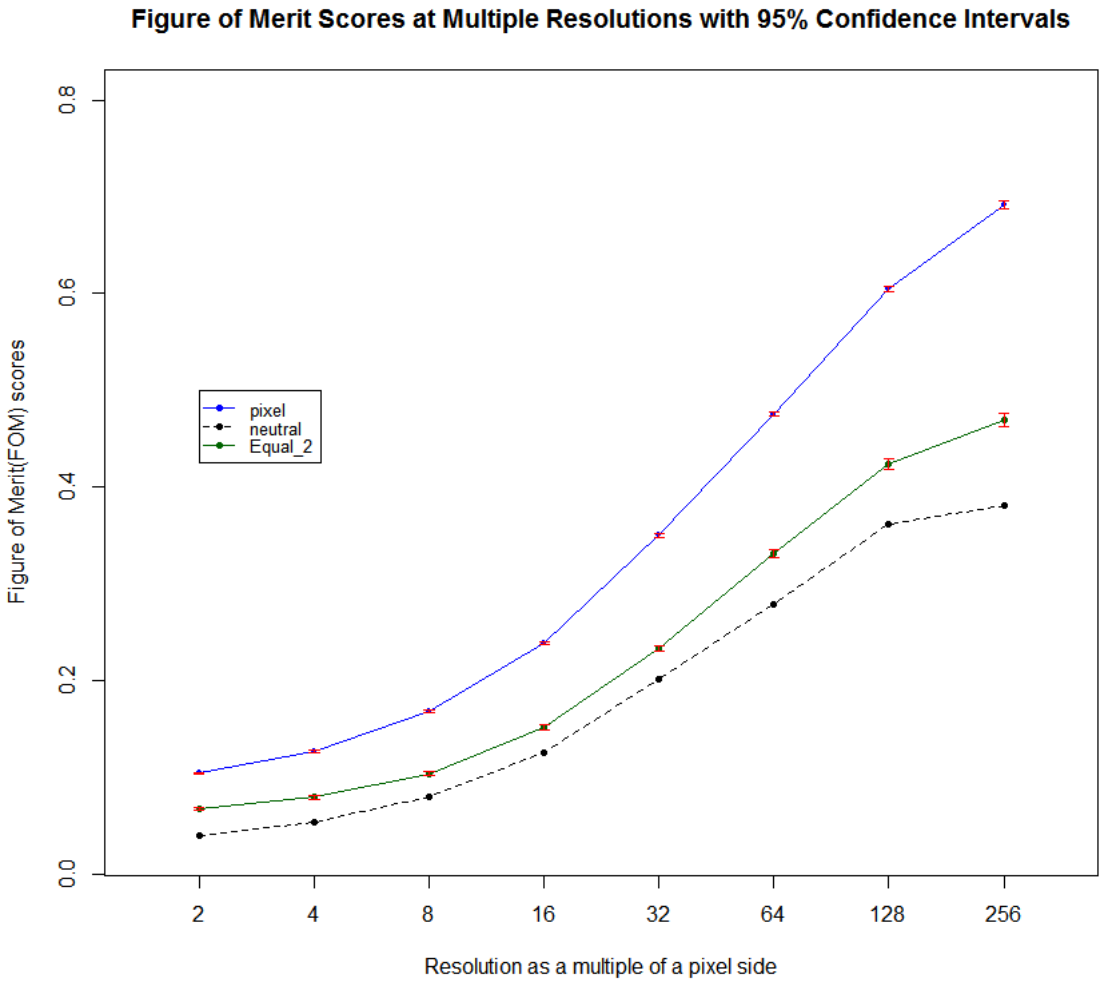

Figure 1.11 Figure of merit scores (means with 95% CIs) for forest to developed transition simulated using pixel versus polygon (only Equal_2 scenario is presented) land units at multiple resolutions.

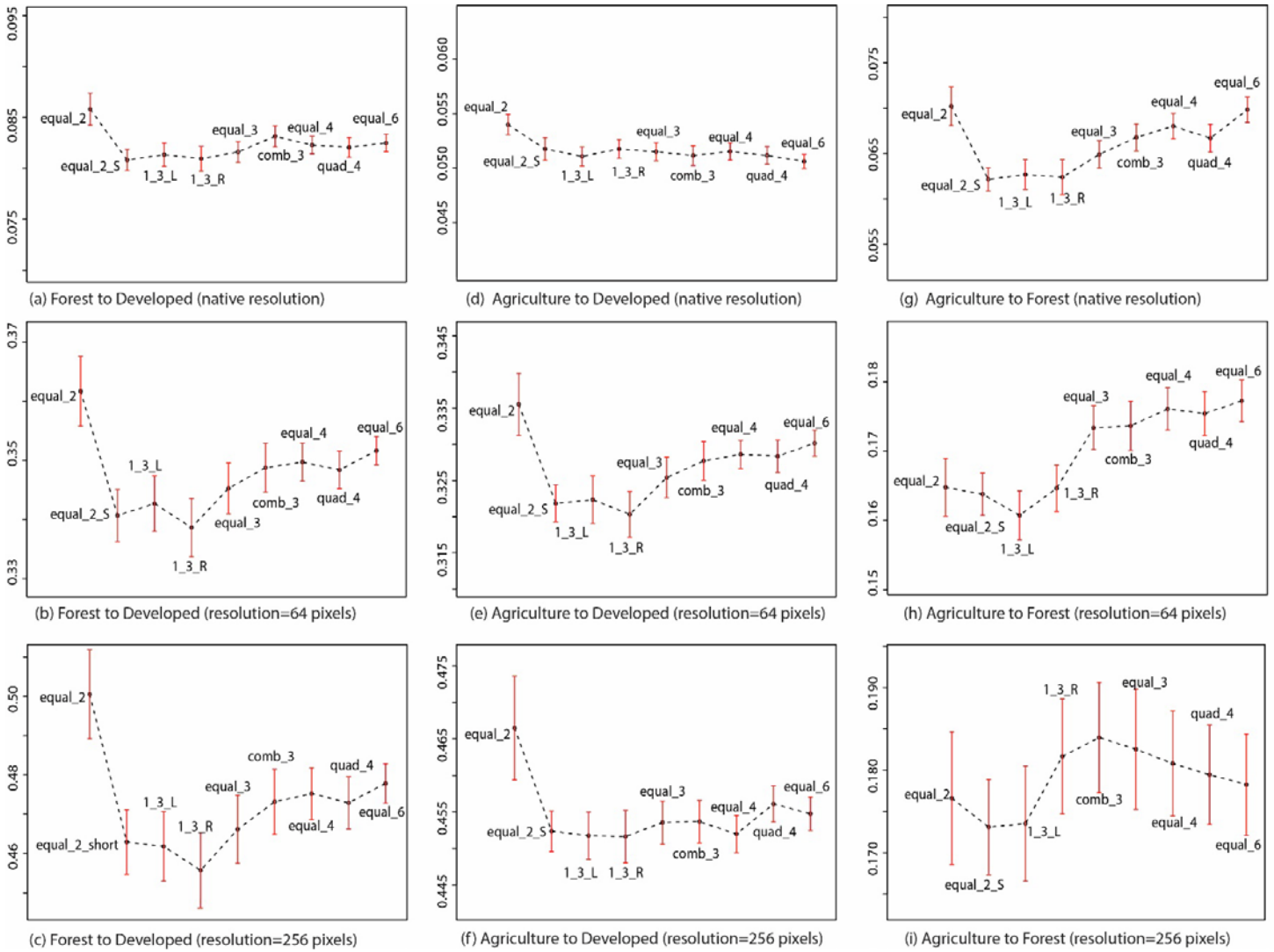

Figure 1.12 Figure of merit scores (means with 95% CIs) for forest to developed (a,b,c), agriculture to developed (d,e,f) and agriculture to forest (g,h,i) transitions at multiple resolutions.

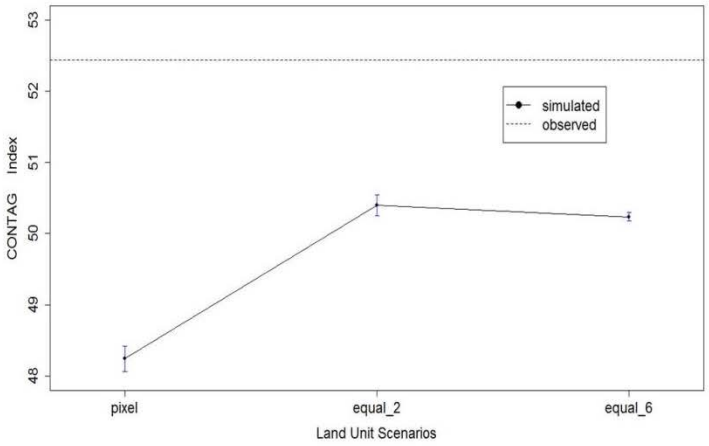

(a) CONTAG values for pixel and polygonal land units

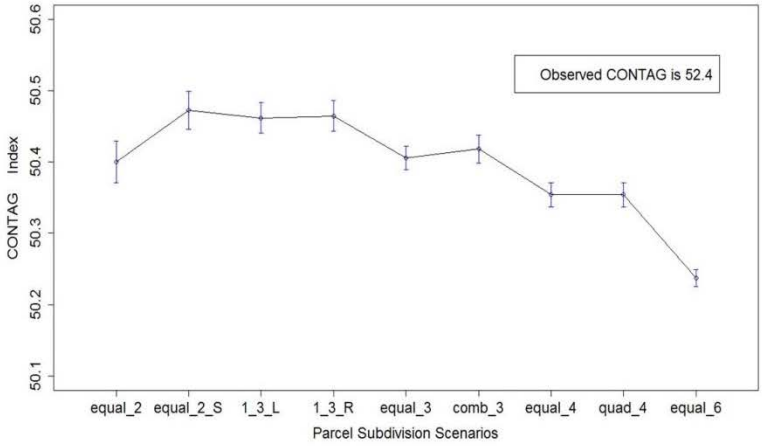

(b) CONTAG values for nine parcel subdivision scenarios

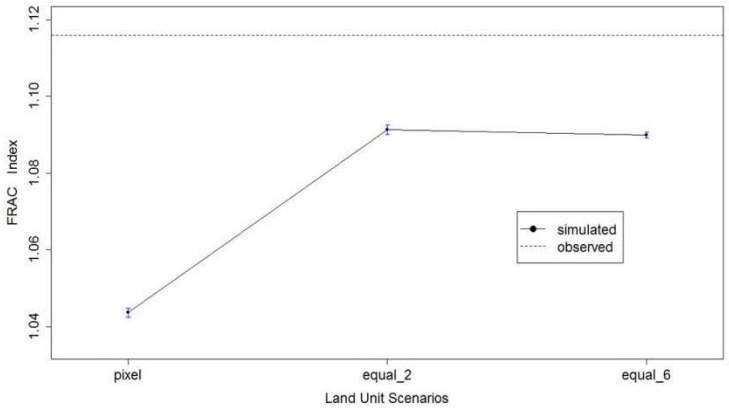

(c) FRAC values for pixel and polygonal land units

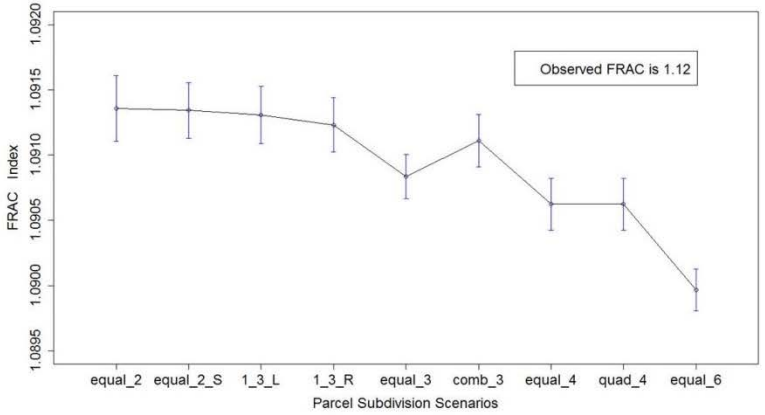

(d) FRAC values for nine parcel subdivision scenarios

Figure 1.13 Comparison of landscape level index (CONTAG and FRAC) values (means with 95% confidence intervals) for pixel and parcel subdivision scenarios (polygons).

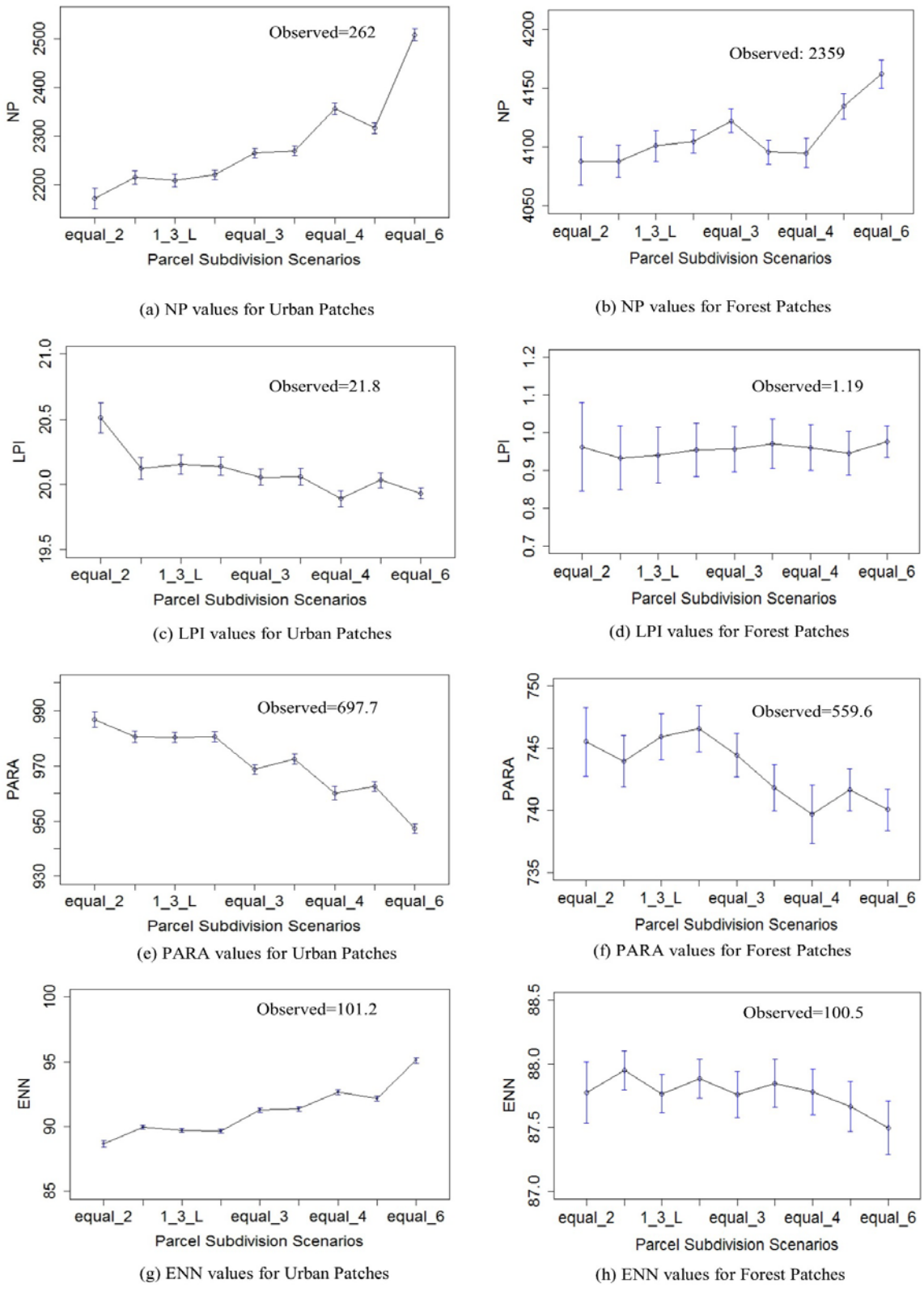

Figure 1.14 Comparison of class level landscape pattern index values (means with 95% confidence intervals) for urban (a,c,e,g) and forest (b,d,f,h) patches among nine parcel subdivision scenarios.

Chapter 2

Optimizing Spatial Land Management to Balance Water Quality and Economic Returns in a Lake Erie Watershed

1 Introduction

Human-driven land-use/cover (LULC) changes have threatened the integrity of ecosystems in many ways, such as through biodiversity loss, contributions to emissions that drive climate change, and eutrophication of freshwater and coastal ecosystems (Foley et al., 2005; Rockström et al., 2009; Smith et al., 2006). These problems result, partly, from the fact that land-use decisions are made without consideration of the wide range of valuable ecosystem services provided by natural landscapes (Bateman et al., 2013). Nutrient loading resulting from extensive agricultural land development, for example, has been repeatedly linked with water quality and related health problems (Michalak et al., 2013; Schilling et al., 2010; Turner and Rabalais, 2003). To improve sustainability in land-use systems, recent studies have highlighted the importance of incorporating ecosystem services into decisions about land use and management (Goldstein et al., 2012; Guerry et al., 2015). Some regulatory programs have been put into place in the United States (e.g. Clean Water Act and Total Maximum Daily Loads (TMDL) (Houck, 2002)), but these efforts are far from sufficient (Hoornbeek et al., 2013; NRC (National Research Council), 2009), largely because they do not address non-point source (NPS) pollution from agricultural land, which is a key contributor to water quality problems.

Among the multiple possible strategies to mitigate NPS pollution, implementation of agricultural conservation practices (CPs) is the focus of many current studies (Duriancik et al., 2008; McCarty et al., 2008; Scavia et al., 2014; Tomer and Locke, 2011; USDA NRCS, 2010).

Agricultural CPs are management tools aimed at controlling soil erosion and reducing nitrogen (N) and phosphorus (P) discharge to surface waters (Lowrance et al., 1997; Santhi et al., 2006). Previous studies have recommended spatial targeting of CPs as a cost-effective approach to solve the NPS pollution problem (Arabi et al., 2006; Maringanti et al., 2009; Rabotyagov et al., 2010), but the effectiveness of these approaches is limited (Bhattarai et al., 2009; Merriman et al., 2009; Tiessen et al., 2010; Verbree et al., 2010). In general, it is much more difficult for agricultural CPs to reduce soluble nutrient loads like dissolved reactive phosphorous (DRP) than soil erosion (Kleinman et al., 2011; Osmond et al., 2012). Several watershed level experiments led by USDA (Osmond et al., 2012) show that current conservation practices have little impact on improving water quality. Aggressive implementation of CPs at watershed scales would be needed to achieve even moderate (~25%) reductions in nutrient discharges (Bosch et al., 2013; Rabotyagov et al., 2014; Scavia et al., 2014). Relying on CPs alone to achieve water quality objectives may not be sufficient, nor is it likely the most economically efficient strategy. Before making large investments in new conservation actions, it is necessary to compare the efficiency of alternative strategies, including CPs. “Landscape approaches” have been recommended as a promising strategy to reconcile conservation and production trade-offs (Sayer et al., 2013). By re-allocating land uses to suitable locations based on the comparative advantages of each land unit (Goldstein et al., 2012; Polasky et al., 2014; Ruijs et al., 2015), previous studies have demonstrated that optimizing land-use patterns can be an effective approach to improving land-use efficiency by jointly improving economic and ecosystem services outcomes (Nelson et al., 2008; Polasky et al., 2008; Seppelt and Voinov, 2002). Given the same financial resources, providing incentives for land-use modification (e.g., converting corn-soybean rotations to other land-use types, like alfalfa hay, grasslands, or forests) might be relatively more efficient than implementing CPs.

To make land-use and -management more effective, it is essential to understand the comparative advantages of possible strategies in a spatially explicit manner (Balmford et al., 2011). However, previous studies have not considered the relative efficiency for reducing NPS pollution of changes in the spatial patterns of land use versus land management, in the form of CPs. Whether one strategy would be relatively more efficient than the other, given the same nutrient reduction objective, remains an open question. Because resources are limited, prioritization of new conservation investments is needed. Therefore, an understanding of the tradeoffs and complementarities in efficacy and economic efficiency of land-use versus land-management approaches to reducing nutrient pollution is essential to guiding future planning. Because previous studies have not compared these two approaches in an integrated model framework, it is not clear how a hybrid approach might take advantage of both approaches to achieve better ecological and economic performance.

We developed an integrated modeling framework that (i) evaluates the efficiency of CPs, conversions of cropland to other land use/cover (LUC) types, and combinations of both strategies for reducing NPS pollution, and (ii) compares optimal spatial land-use and -management patterns based on different strategies. The joint ecological and economic performance of alternative land-use and CP options was estimated using an ecohydrological model combined with an economic valuation component. The ecohydrological model is the Soil and Water Assessment Tool (SWAT)(Arnold et al., 2010, 1998), which has been widely used to evaluate the effects of alternative management decisions on nonpoint-source pollution in large river basins (Arnold et al., 2010). We used the SWAT model to estimate the effects of conservation practices and alternative land uses (e.g., alfalfa hay, grassland and forestry) on nutrient discharges from each field. We set up the SWAT model based on field boundaries (SI Text: The Field Boundary Map)

in order to represent conservation efforts implemented at farm scale, i.e., the scale of landowner's decisions. Market price, simulated plant yield, and costs of management options were integrated in the economic valuation to calculate net profit that can be obtained under each CP or land-use option for all farm fields.

Field level options were integrated into a spatial optimization model based on mixed-integer linear programming. Using this approach, we identify efficient spatial patterns of land-use and -management changes, given estimated field level tradeoffs in performance on economic and nutrient-reduction goals. A solution is efficient if it maximizes economic returns for a given nutrient loading reduction target, and vice versa. Instead of providing a single optimal solution, we developed a full efficiency frontier that represents a range of nutrient-reduction objectives and their associated maximum profit.

Using data from the Sandusky watershed in northern Ohio, we demonstrate the opportunities for a more integrated approach to reducing non-point source pollution [see supplemental information (SI) Fig. 4a]. The dominant land use in the watershed is agricultural land (>80%) with some areas of urban development (SI Fig. 4b). The landscape is generally flat, with some gently rolling plains in the central and southern portions (Grunwald and Qi, 2006). The Sandusky watershed is part of the Lake Erie basin, which has received increased public attention due to massive microcystis blooms. In 2011, Lake Erie experienced its largest recorded bloom. To restore impaired water quality, the International Joint Commission (IJC) has established the Lake Erie Ecosystem Priority, and recommended that the United States and Canadian governments to take actions to significantly reduce phosphorus (P) loading to Lake Erie (International Joint Commission, 2014).

To decrease the hypoxic area in the central Lake Erie Basin by 50% and limit the number of hypoxic days to 10 days per year, the IJC recommended 46% and 78% reductions in the total phosphorous (TP) and DRP loads for the western and central basin, respectively, relative to the 2003 to 2011 and the 2005 to 2011average. Various studies have highlighted the need to differentiate DRP from TP reductions, and focusing on TP vs. DRP could mean different management strategies and different optimal solutions (International Joint Commission, 2014; Michalak et al., 2013; Scavia et al., 2014).

By comparing the economic efficiency of three approaches to P reductions with each scenario resulting in an efficiency frontier, our analysis will help policymakers to understand the tradeoffs between land-use and -management approaches, and between agricultural production and P reduction under each scenario. To establish a baseline, we assume farmers will keep current cropland as a corn-soybean rotation. The three P reduction scenarios are:

(1) Optimizing CPs placement: selected corn-soybean fields will receive one of the five frequently adopted CPs (Tomer and Locke, 2011), including reduced tillage, no tillage, vegetative filter strips, grassed waterway and winter cover crops. We added to this list a nutrient management option, assuming farmers will reduce fertilizer applications by 20%.

(2) Optimizing land-use patterns: selected cropland can be converted from corn-soybean rotation to one of the following alternative land-use types: switchgrass, alfalfa hay, managed forestry, conservation reserve program (CRP) modeled as grassland, and rural-residential land.

(3) Combined optimization of CP and land use: each targeted farm field can either implement a CP, or be converted to another land-use option.

2 Results

2.1 Phosphorus reduction efficiency

For TP and DRP reductions, efficiency frontiers (Fig. 1) generated based on 10-y (2001 to 2010) average performance show that there is a clear tradeoff between P reduction targets and economic returns. Patterns of these frontiers are also quite different across scenarios. An efficiency frontier shows the maximum gains in profit over baseline conditions, which could be negative (reflecting a reduction in profits), that can be obtained from the landscape given a range of fixed P reduction objectives. For each frontier, the original point (0, 0) represents the status quo point. Each point on the frontier corresponds to an optimized spatial allocation of land-use and/or -management changes. If the efficiency frontier associated with a P reduction strategy is above another one for the same set of P reduction targets, we considered this strategy as relatively more efficient than the other strategy. Starting from any point on each frontier, a negative slope indicates that further reductions in P loading require a loss of profits from the sale of agricultural products. However, when compared to baseline conditions, we found that optimization of changes in either land use and CP could, in fact, increase watershed-level economic returns for low to medium (<40%) P-reduction objectives. For land-use optimization, positive changes in economic gains are achieved by replacing corn-soybean rotations with more competitive options at suitable fields. Reduced fertilizer cost is the major contributor to increasing profits in the CP scenario, but CPs may also increase profits by improving crop yields.

Overall, land-use optimization tended to be relatively more efficient than relying on CPs under goals for either DRP or TP reductions, because it can achieve higher economic returns given the same P reduction target. Differences in efficiencies between land-use and CP scenarios tended to

narrow as the P reduction target increased. Perhaps more importantly while CPs can achieve the targeted 46% reduction in TP, CPs are limited to around a 60% reduction on DRP (Fig. 1). Further reductions would require more aggressive fertilizer control and/or implementation of multiple CPs at the same field (SI Fig. 2a). However, even when we included these options in the optimization model, results indicated that it is still difficult for CPs to reduce DRP more than 68% (SI Fig. 2a). On the other land, land-use optimization could easily achieve 80% or higher DRP reductions, although such levels of reduction come at the cost of reduced economic returns.

Over most of the range in P reduction, the gradient of the frontiers generated based on land-use optimization were generally steeper than those from the CP optimization. Between any two points on the frontier, differences in profits can be considered as marginal P reduction cost under optimal conditions. As we increase P-reduction targets, marginal costs associated with land-use optimization increased faster than those for CP optimization, which indicates that economic performance of the land-use optimization scenarios is more sensitive than CP placement to P-reduction objectives.

When we include both CPs and alternative land uses as optimization options at each field, substantial improvements in efficiency were attained. Improvements in efficiency in this combined scenario were not simply additive. Unlike the differences between the frontiers generated by the optimizations that used only land-use and CP options, additional gains achieved via a combined strategy increase with P-reduction targets, and the difference peaks around 70% or 85% for DRP or TP reductions. The advantage of the combined scenario over land-use optimization alone diminishes for higher P-reduction targets, because nearly all CPs are replaced by land-use options to achieve the greatest nutrient reductions (Fig.2). The results reveal the importance of adopting multiple strategies for conservation planning, especially when significant

nutrient reductions are needed to restore impaired water bodies. For instance, CPs are not sufficient to meet the 78% DRP reduction target; land-use optimization could achieve the reduction, but would result in large losses (~$7M) in annual profit. The combination scenario, on the other hand, can achieve the target level of P reduction while actually increasing annual profit (~$1M).

An additional important finding is that the optimal solutions to achieve targets for TP reduction do not satisfy the targeted level of DRP reduction. Under the plan generated using the combination scenario based on a targeted TP reduction of 46%, DRP would be reduced by 29.3%, which is far from the 78% target for DRP reduction. On the other hand, optimal land-use patterns generated based on DRP reduction objective could achieve a 82% reduction in TP (and 62% in TN). This result confirmed the need to adjust conservation practices to reflect the fact that DRP is the primary concern.

2.2 Biofuel Scenarios

Switchgrass has been considered a potential bioenergy for cellulosic ethanol production (Chung et al., 2014; Schmer et al., 2008). Based on current market prices, switchgrass (marketed as grass hay) is not an economically competitive land-use option, even on marginal land. However, to achieve an 80% reduction or more in DRP, switchgrass becomes a competitive option. Switchgrass is a type of cellulosic or second-generation ethanol feedstock. Although industrial-scale cellulosic production technology is not mature at this time, advances in technologies (Chung et al., 2014) indicate that it could be an economically competitive option in the future. We included two price scenarios for switchgrass as a bioenergy feedstock. Previous studies found that the energy content of switchgrass is about 80% to 90% that of corn grain/stover

(Gelfand et al., 2010; Mani et al., 2004; Patzek, 2004; Pordesimo et al., 2005). If the price of per unit dry matter of switchgrass could reach 65% or 70% of the corn grain price, a great improvement in land-use efficiency could be achieved. For instance, with assuming a switchgrass price that is 70% that of corn, the watershed could achieve a substantial improvement in annual profits (~$15M) and reduce DRP by 60% at the same time (Fig. 1b).

2.3 Compositional Change and Spatial Pattern

Fractions of the land area of the watershed in various CP and land-use options varied significantly and non-linearly across both DRP and TP reduction objectives (Fig.2). For moderate P-reduction objectives (<50%), alfalfa hay, vegetative filter strips, nutrient management (20% fertilizer reduction), and replacing agriculture with forest were the top four options for both TP and DRP reductions. For greater TP and DRP reductions, broader forest coverage is necessary to reduce P loss from agricultural land. About half of the fields need either a CP or a land use alternative to achieve 46% TP reduction. To achieve the 78% DRP reduction target, nearly all fields need some treatment. The top four options selected to achieve this target were vegetative filter strips (39.9%), forest (23.3%), alfalfa hay (16.8%) and 20% fertilizer reduction (12.8%). Switchgrass also became a competitive option (5.8%), and played a vital role for DRP reductions of 80% or more (Fig. 2), because filter strips have limited effects for high DRP reductions, and alfalfa hay requires more fertilizer input than switchgrass. Unlike field crops, switchgrass does not require tillage and it can grow with little fertilizer application (Wright and Turhollow, 2010). Residential land has a small fraction because area of new residential land was limited to be less than 10% of current urban land area. This limitation is necessary because of the low rate of historical (2001-2010) growth in urban land area (3%),

signaling weak demand. However, new residential land would be a more significant option if there were more demand.

The spatial distributions of changes in CPs and land use for both TP and DRP reductions indicated that options were not randomly or evenly distributed across the landscape. Instead, it is clear that fields receiving a given option tended to form spatial clusters, largely determined by similar soil and terrain characteristics. Areas receiving alfalfa hay, forest, switchgrass or nutrient reduction options are mostly fields with poor soil drainage capacity (SI Fig. 1d) or relatively steep slope (>5%) (SI Fig. 1c). For instance, alfalfa hay and nutrient management were concentrated in the southern part of the watershed, and conversion to forest tended to occur in the northwest, because these areas need tile drainage (SI Fig. 1d) and CPs are not quite effective on reducing P loss via tile flow. The center of the watershed remained in crop production to reduce TP by 46% (Fig. 3a), but most fields would need vegetative filter strips to reduce DRP by 78% (Fig. 3b). Under the assumption that price for switchgrass is 70% of corn price, switchgrass tended to replace forest and alfalfa hay in much of the western part of the watershed (Fig. 4b) because this makes switchgrass more profitable than timber production.

Efficiency improvements achieved by land-use optimization relied heavily on alfalfa hay and forest to replace corn-soybean rotations. We tested the sensitivity of the land-use optimizations to price changes in these two land-use types. If price for alfalfa hay or timber decreases by 20%, land-use optimization could still be more efficient than CP optimization, but CP placement would be more efficient for medium DRP reductions when prices for alfalfa hay and forest decrease more than 10% simultaneously. However, since CP alone cannot meet desired DRP target, mixing of both scenarios is still needed. In fact, the combined strategy still improves on land-use efficiency considerably, especially for high DRP reductions (SI Fig.2b).

2.4 TP and DRP Abatement Costs

Effects of changes suggested by the spatial optimizations on individual economic benefits may vary substantially, and certain landowners may lose more profit as result of the suggested changes. To make sure no one would be worse off, financial support may be required to compensate for economic costs associated with CP implementation or change in land use. We calculated this compensation as the minimal - abatement cost. For the CP options, implementation cost is calculated as reduction in revenues as a result of yield decrease, if any, and CP implementation and maintenance costs. For alternative land-use options, P-abatement cost is calculated as any reductions in net profit due to conversion from agricultural land with corn-soybean rotations to other options. On average, it seems that implementation of CPs does not affect profit of corn-soybean production that much, but converting corn-soybean to other uses like timber production may lead to considerable revenue loss (SI Fig. 3). Based on the combined scenario, we found that total abatement costs for 46% TP and 78% DRP reductions would be $1.17M and $5.82M annually, respectively. To reduce TP by 46% based on CPs alone would cost $1.98M. Since CPs cannot reduce DRP by 78%, we calculated abatement costs for a 61% DRP reduction. Abatement costs for 61% reductions under the CP and combined scenarios would be $3.13M and $2.32M, respectively. Even if prices for alfalfa hay and timber drop by 20%, the combined strategy saves on abatement costs (SI Table 3). Under the biofuel price scenario, if government payments would make up the difference between grass hay price ($95/Mt) and 65% of corn grain price ($115/Mt), then an additional $2.3M would be required. Under the 70% price scenario for switchgrass ($124/Mt), an additional $14.3M would be required. SI Appendix, SI Tables 1 and 2 provide a summary abatement costs associated with individual options for DRP and TP reductions.

3 Discussion and Future Research

We developed the first integrated modeling approach that compares the relative efficiency of alternative spatial land use and management strategies for addressing NPS pollution. By coupling a process-based biophysical model with economic valuations and a spatial optimization approach, we developed a scientific approach to evaluate strategies for nutrient reduction that, for the first time, include both conservation practices and land-use change. More importantly, we identified strategies for NPS pollution control that are economically efficient via a combination of both strategies.

Using the Sandusky watershed as an example, our results indicated that relying on traditional agricultural CPs alone is neither sufficient, nor the most efficient strategy to meet P reduction targets. Results based on a 10-year (2001 to 2010) simulation indicate that integrating land-use optimization into conservation planning can help not only overcome limitations of CPs on improving water quality, but also improve economic returns. Also, we find that the optimal solutions to meet targets for TP reduction are far from sufficient to meet the goal for DRP reduction. While exact nutrient reduction objectives vary spatially, results from this study reinforced the need for conservation planning to differentiate mineral or soluble nutrient from particulate nutrient pollution, especially in the Lake Erie basin where DRP is the primary concern (International Joint Commission, 2014; Scavia et al., 2014).

Our analyses illustrate the trade-offs between using CPs versus land-use strategies. Although land-use change appears to be more efficient than CPs, it is important to point out that both strategies have their limitations and performance of each option is subject to changes in local

conditions. CPs modeled in this study do not require changes in the cropping system, which could be an advantage of CPs because it can maintain current crop production and, unlike land-use conversion, the marginal cost of applying CPs does not change significantly. However, leaving the current cropping system unchanged has several limitations. First, our results show that it is generally much more difficult to achieve significant reductions in mineral nutrients with CPs. This finding is consistent with lessons learned from several watershed level experiments conducted in the U.S. (Rabotyagov et al., 2014; Tomer and Locke, 2011). In the U.S. Midwest, subsurface (tile) drainage system is widely adopted to support agricultural production. A recent field study in the region (Smith et al., 2015) found that more than 40% of P losses happen via tile drainage. This poses another challenge for CPs, because traditional CPs were primarily designed to address nutrient loading to surface water and may have little or even negative impacts on reducing soluble nutrients when tile drainage is presented (Bhattarai et al., 2009; Lemke et al., 2011). On the other hand, converting corn-soybean fields to perennial vegetation and/or less fertilizer-intensive land uses, is generally more effective at reducing nutrient discharge due to significant reduction in fertilizer application and improved soil cover. One key concern with land-use conversion is the cost. We found that, when government crop subsidies are not included, the corn-soybean rotation is not necessarily the most profitable option at all fields. Instead, replacing some of current corn-soybean fields with alfalfa hay and forest would jointly improve economic and nutrient-reduction objectives.

It is important to keep in mind that efficiency obtained via an optimization algorithm does not guarantee equity. While optimization can improve regional economic returns, revenue losses may hit some land owners harder, therefore financial incentives or compensation may be required to engage land owners in conservation efforts. But, implementation and maintenance of

CPs is not free either. We find integrating land-use optimization with CPs targeting can save on the financial costs of improved P abatement.

Another potential limitation with land-use optimization is that costs of land-use conversion are subject to changes in profitability of alternative land-use options, which may increase or decrease required abatement costs significantly. According to USDA projections, corn prices will remain stable and soybean prices may increase up to 5% from 2015 to 2025 (USDA ERS, 2016). Alfalfa hay and timber are the two major alternative land uses suggested by the optimization model. Prices for alfalfa hay may increase marginally, since it is correlated to grain prices, and demand for alfalfa has increased significantly over the last decade (Sumner and Rosen-Molina, 2011; Tejeda et al., 2015). Predictions for timber products can be challenge, partly because it usually take decades for forest to mature. We assumed a constant annualized return for timber production (SI Text: Economic Valuation in the Model), but actual returns can be lower since land owners may discount future profits. Both long-term and temporal changes in prices may induce shocks to farm incomes. Holding corn-soybean prices constant, if alfalfa and timber prices drop by 20%, then total economic costs required to achieve a 78% DRP in the study area would increase from $5.82M to $8.35M per year. If land-use changes are going to be implemented, a safety net program may be needed to protect farmers from price volatility. A similar program exists for major crops (e.g., corn, soybean, and rice). The 2014 U.S. Farm Bill introduced the new Agriculture Risk Coverage (ARC) and Price Loss Coverage (PLC) programs. Average payment rates under the ARC program for corn and soybean production in the study area in 2014 are $89.79 and $3.04 per base acre (USDA FSA, 2016). If half of corn-soybean fields in the watershed receive these rates, then total payments would be around $25M. This generous payment would mask the inefficiency of current land-use decisions and discourage

farmers from converting current cropland to otherwise more efficient land-use options. Since the main purpose of the ARC/PLC programs is to maintain farmers' income levels, rather than a certain crop price, it is possible to get 'win-win' results by revising the ARC/PLC programs to include more environmental sensitive options so that nutrient loadings can be reduced without harming individual farmers' benefits.

The land-use optimizations in this study focused on reducing P discharges from farm fields so that water quality can be improved in an economically efficient way, but converting cropland to more natural conditions can also enhance many other ecosystem services. For instance, the optimal spatial configurations obtained in this study indicate that conversion from corn-soybean to forest and switchgrass tends to form clusters rather than random patches. This pattern indicates that there are opportunities to coordinate timber and hay production with carbon sequestration, provision of wildlife habit, and recreational activities(Löf et al., 2015; Olschewski and Benítez, 2010). However, substantial uncertainties in the valuation of these non-marketable ecosystem services remains a challenge in integrating ecosystem services in landscape planning (de Groot et al., 2010; Johnson et al., 2012).

Another limitation is the fact that not all potentially cost-effective CPs and land-use options were modeled in this study. For instance, drainage water management might be a potential CP to address nutrient losses via subsurface tiles (Williams et al., 2015). In addition to alfalfa hay and forestry, it is certainly possible that other options might be more competitive in other regions. Also, changes in land use may affect local market equilibria since supply of crops would be different. We did not include a price feedback in this study, given the relatively small size of the watershed. For large areas like the Mississippi river basin, structural changes in crop supply would need special attention. Additionally, although we simulated crop yield and nutrient

discharge over 10 years to account for weather variability, long-term changes in regional climate may affect both efficacy and efficiency of alternative spatial management strategies. In this study, the nutrient discharges estimated are edge-of-field nutrient loss, which is different from P delivered to Lake Erie. For instance, nutrients reduction achieved by CPs are expected to be lower at the outlet of watershed than sum of edge-of-field discharges, because in-stream processing may dampen the response (Bosch et al., 2014). Given these processes, our results provide a conservative estimate of the measures needed to reduce nutrient loads, and additional actions might be needed to achieve the same level of nutrient reduction at the watershed scale. We did not model in-stream processing and interactions between subwatersheds because the SWAT model has only a limited capacity to model in-stream water quality dynamics (Gassman et al., 2007; White et al., 2014), and because it requires a dynamic link between the SWAT model and the optimization model. Even if a genetic algorithm is used, dynamic linking would require tens of thousands of simulations to trace out efficiency frontiers (Maringanti et al., 2009), but a single simulation took about three hours in this study. Insufficient computing power given the current model configuration prohibits currently employing the dynamic linking strategy. We also did not consider long nutrient residence times. Lessons learned from previous studies suggest lag times in nutrient transport mean that it may take years or even decades before water quality improvement can be observed (Tomer and Locke, 2011).

Success in improving water quality requires long-term commitment and coordinated effort (Osmond et al., 2012). Findings from this study highlight the need for policy makers and scientists to work together, and demonstrate the potential gains from innovating on current conservation planning strategies. Efficiency frontiers developed in this study provide insight into the efficacy and efficiency of alternative spatial land use and management strategies for

addressing NPS. Maps associated with spatial configurations of optimal solutions provide not only detailed trade-off information, but also a spatial distribution pattern for each scenario. This information generated by the integrated assessment model can serve as a useful tool for promoting more scientifically informed discussions among interested parties and stakeholders.

4 Materials and Methods

The Field Boundary Map. We used the Common Land Unit (CLU) data layer, originally developed by USDA to delineate agricultural field boundaries, together with parcel maps obtained from local governments, to form the spatial unit of analysis. Land use and management were represented over these spatial units defined in the rural and urban areas by CLU and parcel boundaries, respectively (see SI Text: The Field Boundary Map). The resulting map divided the Sandusky watershed into 41,233 distinct spatial units. A 2006 land-use/cover map (Jin et al., 2013a) was overlaid with field boundaries to identify an initial land-use pattern. We apply alternative land-use and -management options to current agricultural fields only. Other uses, like urban and forest, were kept constant in our simulations.

Effects of CPs and Alternative Land Uses. We modified the SWAT model to calculate crop productivity and nutrient runoff for agricultural fields, so that spatially explicit trade-offs of alternative options can be assessed at the level of individual fields. The modified model was calibrated against observed hydrology from USGS, nutrient discharges from Heidelberg University, and crop/plant yields from USDA NASS. Assuming the baseline scenario of corn-soybean rotation for all agricultural fields, we simulated the effects of CPs by adding selected

CPs to each field. For land-use optimization, we replaced the corn-soybean rotation with alternative crop or land-use options to evaluate changes in nutrient discharges leaving the fields. See SI Text: SWAT Model Setup, Calibration and Validation for more details about representation of individual CP and land-use options in the model.

Profit and Cost Estimation. For field crops and forest land, observed 14-y average (2001-2014) market prices and simulated yields from SWAT were used to calculate revenues. Data from USDA ERS and Ohio State University Extension were used to estimate costs so that net profit can be calculated for each option. We did not include government subsidies like direct payments in this study. Conservation Reserve Program (CRP) enrollment and rural residential land were two special cases. Profits of land in CRP were calculated as the county average of CRP payments (USDA FSA, 2015) minus maintenance costs. We modeled the present value per acre of rural-residential land as a function of geographic (e.g., distance to urban centers and parks) and site conditions (e.g., parcel size, elevation, and slope). Using real estate appraisal and sales data from local tax departments, we estimated a hedonic property price function to estimate the value of rural-residential land use at each farm (see SI Text: Economic Valuation in the Model). Estimated net returns for residential land use were converted to a constant annualized equivalent, which was used in profits calculation for residential land use.

Optimization Algorithm. Given estimates of nutrient discharge and economic return for each alternative option at each field, the goal of optimization is to find the efficient spatial configuration of changes to land use and land management, which we define as the configuration that would maximize economic returns given a certain nutrient load target. Since choices made at each field are discrete, this problem can be formulated as a mixed integer program involving a large number of fields. By varying nutrient (TP and DRP in this study) load constraint, we were

able to trace out efficiency frontiers for each of the three scenarios. We solved the optimal problem using the A Mathematical Programming Language (AMPL) (Fourer et al., 1990) software and the CPLEX solver (see SI text: Spatial Optimization).

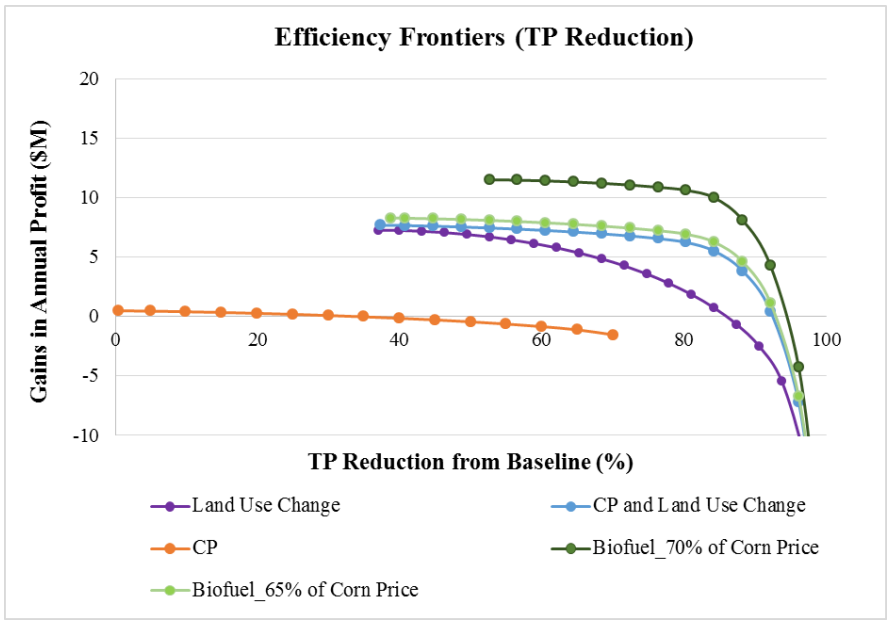

(a)

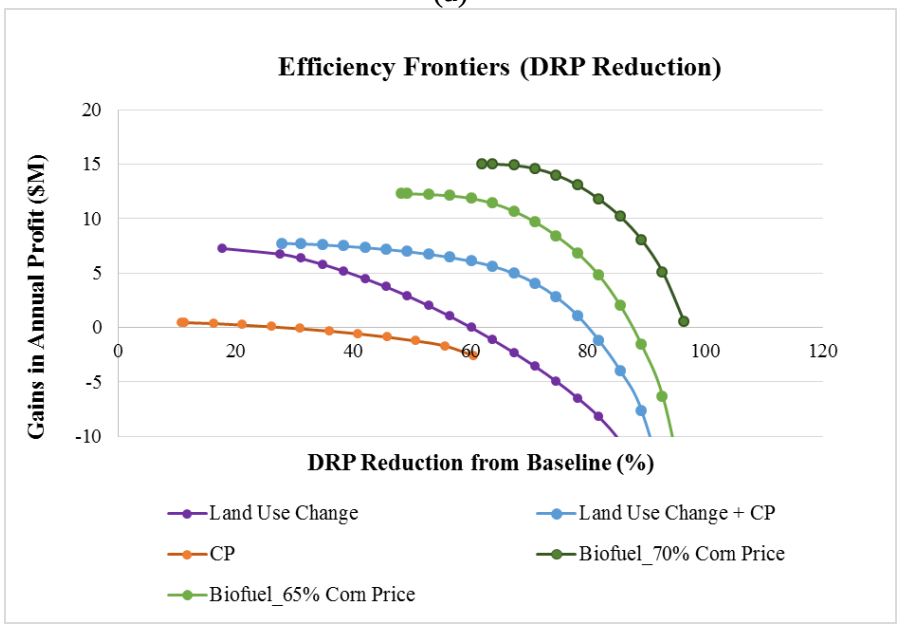

(b)

Figure 2.1 Efficiency frontiers for (a) TP and (b) DRP reductions based on the CP targeting, the land-use change and a combination of both strategies. The original point (0, 0) stands for baseline annual profit ($122 M) and P load levels for the 2001-2010 period. Biofuel scenarios assume switchgrass price per metric ton dry matter could reach 65% and 70% of that for corn grain price, respectively.

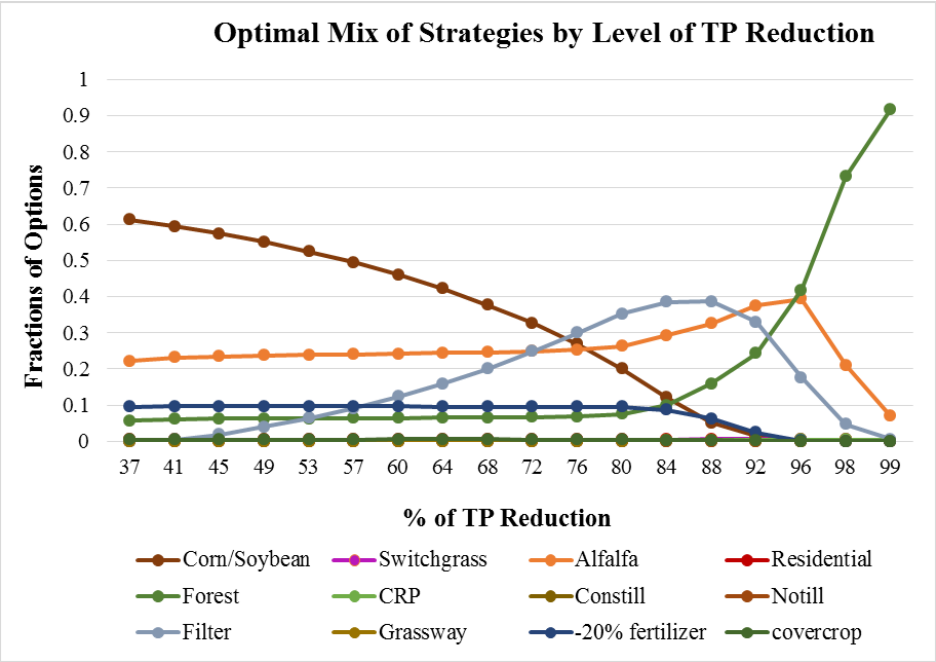

(a)

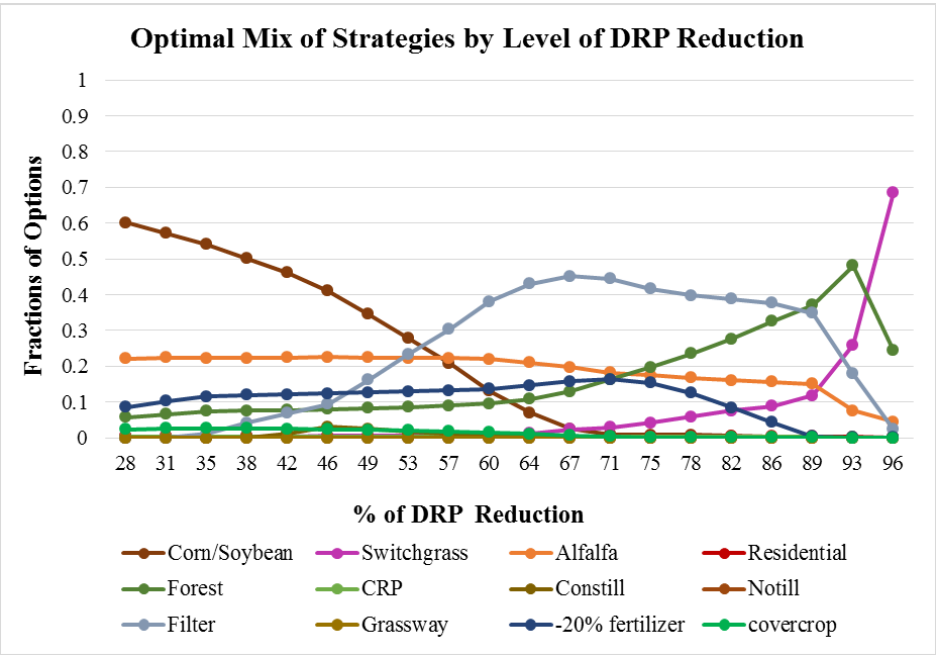

(b)

Figure 2.2 Optimal mix of strategies by level of (a) TP and (b) DRP reduction based on combined optimization of CP and land-use strategies.

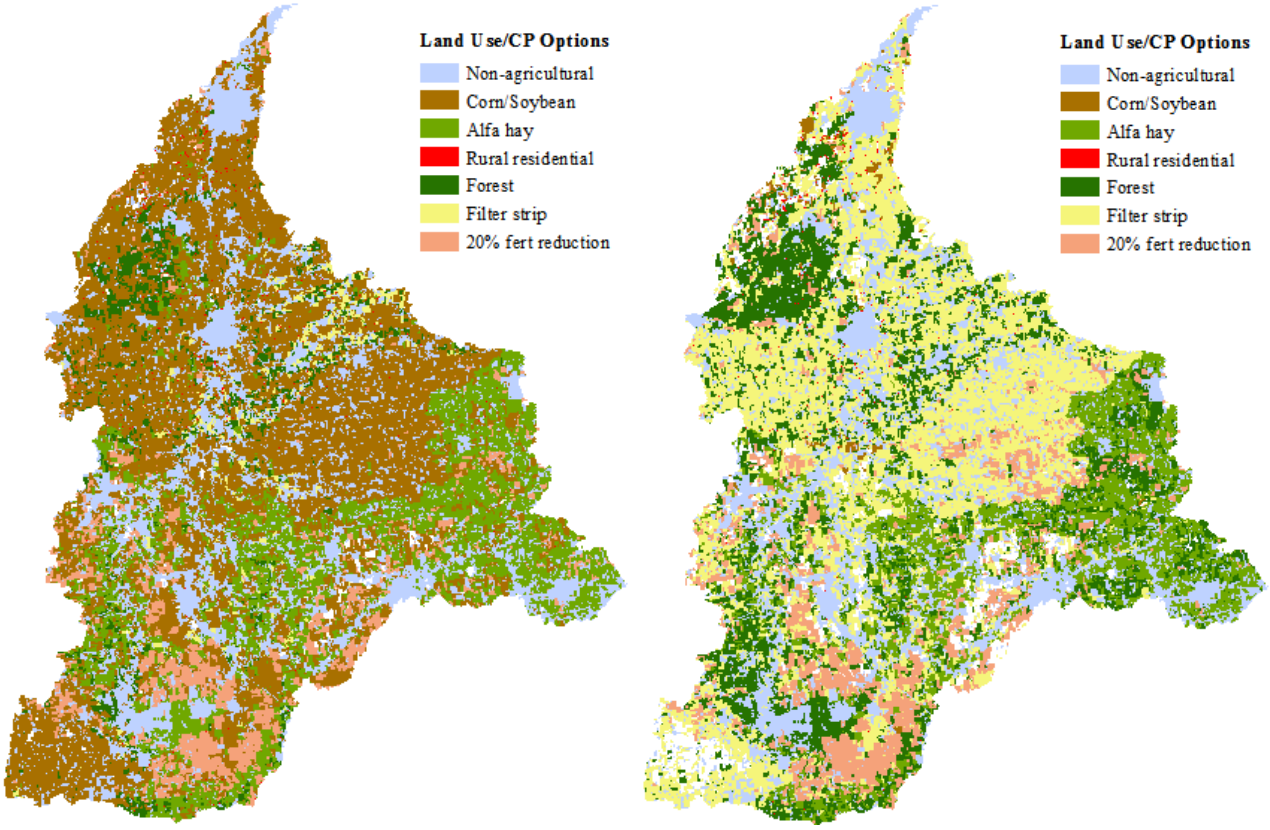

(a) (b)

Figure 2.3 Distribution of CP and land-use options based on combined optimization of CP and land-use change with (a) the 46% TP reduction and (b) the 78% DRP reduction from baseline targets, respectively.

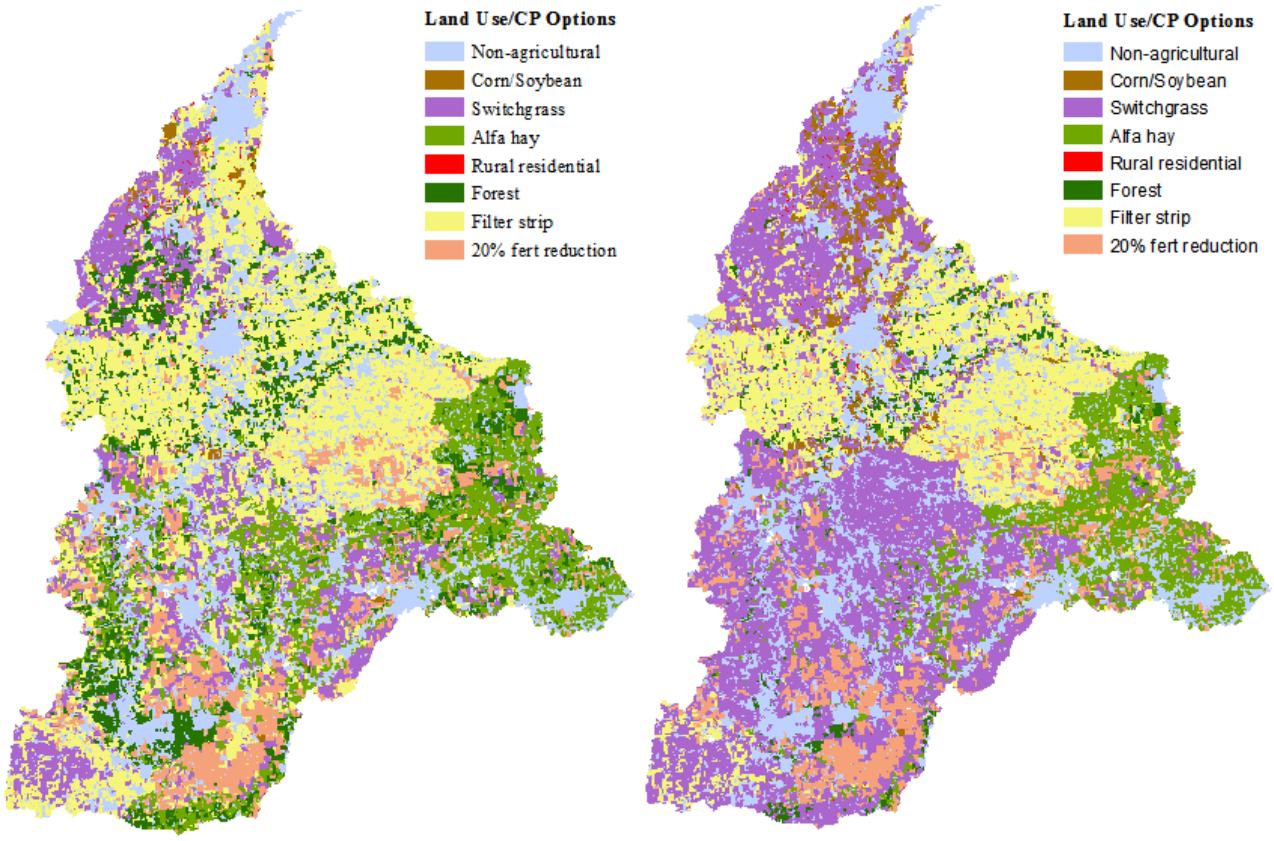

(a) (b)

Figure 2.4 Distribution of CP and land-use options based on combined optimization of CP and land use change and 78% DRP reduction, assuming switchgrass price ($/dry metric ton) is (a) 65% of corn grain price and (b) 70% of corn grain price, respectively.

6 Supplementary Information (SI)

6.1 The Field Boundary Map

The Sandusky River watershed covers about 3,926 km^2 in Northwestern Ohio in the United States (SI Fig. 1). The watershed was divided into 41,233 distinct fields. Field boundaries were identified by overlaying the Common Land Unit (CLU) layer with parcel maps obtained from local county tax assessment departments in the study area. A CLU is "the smallest unit of land that has a permanent, contiguous boundary, a common land-cover and land management, a common owner and a common producer in agricultural land associated with USDA farm programs" (USDA, 2013). Parcel maps outline property boundaries in both rural and urban areas. Since the CLU layer does not include non-agricultural land, we filled in those areas with parcel maps. The CLU layer contains not only field boundaries, but also ground features like fences and ditches, which is not practical to model in SWAT, so the CLU layer was simplified by merging those small features into the fields containing them. Sizes of all spatial units range from 0.08 to 197.8 ha, with an average of 8.4 ha for the watershed.

The SWAT model requires a complete coverage of the study area, thus all fields were included in the modeling simulation. However, for optimization purposes, we selected only those fields whose major land use/cover type was cultivated crops. A 2006 land use/cover map, derived from the National Land Cover Dataset (NLCD) (Jin et al., 2013b), was employed to identify land use/cover type for each field. Based on these criteria, a total of 27,905 agricultural fields, which cover about 82% of the study area, were selected to participate in the optimization problem.

6.2 Spatial Optimization

Optimized spatial patterns of land-use change and CP implementation are formed by assigning a unique land-use type or CP option to each of the 27,905 fields. Since agricultural production in the watershed is dominated by corn/soybean rotation (USDA NASS, 2016), we assume all fields with cultivated crops are maintained as corn/soybean rotations for the baseline scenario. In addition to corn/soybean rotation, our model includes five alternative land-use categories and six common agricultural conservation practices (CPs). The five alternative land-use options are switchgrass, alfalfa hay, managed forestry, Conservation Reserve Program (CRP) modeled as grassland, and rural-residential land. The six CPs modeled are reduced-tillage, no-tillage, vegetative filter strips, grassed waterway, winter cover crops and a nutrient management option (assumed a 20% reduction in fertilizer application rate).

The objective of spatial optimization is to identify efficient placement of either alternative land uses or CPs, or both, that can maximize net economic benefits of the watershed given a certain water quality or nutrient loading target. By varying the nutrient reduction target, we trace out the efficiency frontier. A point on the model's efficiency frontier is found by identifying an efficient pattern of land-use changes and/or CPs by solving the following:

$$NR = Max \sum_{j=1}^{N} \sum_{k=1}^{P} R_j^k A_j(k_j) \qquad (1)$$

$$Subject\ To:$$

$$\sum_{j=1}^{N} \sum_{k=1}^{P} NP_j^k k_j \leq RT \qquad (2)$$

$$\sum_{k=1}^{P} k_j = 1 \qquad j = 1, \ldots, N \qquad (3)$$

$$k_j = \{0,1\} \qquad j = 1, \ldots, N \qquad (4)$$

Where j indexes fields (j=1,…,N where N=27905), k indexes land-use or CP option (k=1,…,P where P=6 for the land-use-only scenario, P=7 for the CP-only scenario, and P=12 for the combined scenario), k_j indicates the land-use or CP option assigned to field j, R_j^k is the annual per-hectare net economic returns of choosing option k at field j, A_j is field j's area in hectares, NP_j^k is edge-of-field DRP discharges at field j with option k, NR is profit (net return) and RT is a given nutrient loading limit. Assuming a corn-soybean rotation for all baseline agricultural fields, average TP and DRP loads for the 2001-2010 period were 379,440 Mt/year and 34,508 Mt/year, respectively, estimated using the SWAT model. Based on simulated yields and reported market price and production costs, baseline profit was estimated to be about $122 M/year.

The problem defined above can be considered as a mix-integer linear optimization problem, and sovled using the Mathematical Programming Language (AMPL) software (Fourer, 2007; Fourer et al., 1990) and the CPLEX solver(IBM ILOG, 2012).

6.3 SWAT Model Setup, Calibration and Validation

6.3.1 SWAT Model Input and Setup.

The SWAT model requires various input files, including elevation, stream network, soil type, land use, weather and land management characteristics. Observed daily precipitation and maximum/minimum temperature data for the study area were retrieved from the NOAA Global Historical Climatology Network-Daily (GHCN-DAILY) data (Matthew J Menne et al., 2012; Matthew J. Menne et al., 2012). National Land Cover Database 2006 (NLCD 2006) (Jin et al., 2013b) was downloaded from the Multi-Resolution Land Characteristics Consortium (MRLC) to

use as the land use map. Digital elevation model (DEM) (Gesch et al., 2002) data downloaded from USGS served as the source for calculating slope, and watershed delineation used by the SWAT model. The SSURGO soil database (USDA NRCS, 2015a) provided detailed soil attributes.

Since corn and soybean rotation dominates the study area, for the baseline scenario, we assume all agricultural land was maintained as a corn-soybean rotation. Exact crop management information varies spatially based on field condition and famer's preference. Without field-scale information, we assumed a uniform management scheme for all agricultural fields. Nitrogen and phosphate fertilizer prices and application rates were downloaded from USDA (USDA-ERS, 2013). Other management information for corn and soybean rotation (e.g. tillage, plant and harvest time) was adapted from published literature (Bosch et al., 2011; Margaret M Kalcic et al., 2015). For the two year corn-soybean rotation, 213 kg/ha nitrogen and 45 kg/ha phosphorus were used. Phosphate fertilizer was assumed to be applied broadcast and incorporated into the soil once every two years in the fall after soybean harvest. Spring regular tillage and no-tillage practices were assumed for corn and soybean year, respectively.

For land-use change scenarios, we replaced corn-soybean rotation with alternative crops or plants. Farm management information for alternative field crops (i.e. alfalfa hay and grass hay) was derived from farm management enterprise budgets published by Ohio State University Extension (Ohio State University(OSU)-Extension, 2015). Switchgrass was assumed to be planted on a 5-year rotation, based on a USDA NRCS technical report (USDA NRCS, 2009). We applied nitrogen fertilizer (78 kg/ha/year) only to switchgrass, similar to values reported in (Perrin et al., 2008). Switchgrass can grow with little fertilizer (Wright and Turhollow, 2010), but P input may be necessary to compensate P removed by biomass harvest for long-term

production. For timber production, we use the default SWAT management schemes. Conservation practices specifics were retrieved from NRCS Ohio Field office Technical Guide (FOTG) (USDA NRCS, 2015b). For the winter cover option, cereal rye was planted after corn harvest and killed before soybean production.

6.3.2 Defining the HRU by Field Boundaries.

The SWAT model divided the watershed into subbasins. In each subbasin, SWAT lumps areas sharing the same soil and land-use attributes together to form a basic hydrologic response unit (HRU), regardless of their spatial location. The problem with this approach is that it is impractical to get a one-to-one match between farm fields and HRUs (Teshager et al., 2016) because HRUs contains parts of multiple spatial disconnected fields. This would cause a disconnection between model units and human decisions. To avoid this problem, HRUs were defined by field boundaries in this study, based on the field boundary map mentioned above, using a method similar to Kalcic (2015).

6.3.3 Calibration and Validation.

The SWAT model was run for 1993 to 2010, including three years for model warm-up (1993-1995), 11 years for calibration (1996-2006), and four years for validation (2007-2010), using the historical observed climate data mentioned above. Monthly calibration and validation were performed for streamflow, sediment, total nitrogen (TN), total phosphorous (TP), and dissolved reactive phosphorous (DRP). Streamflow data were obtained from the U.S. Geological Survey 04198000 gage station near Fremont, OH (SI Fig.1a). Sediment and nutrient concentration data were generated based on records provided by the National Center for Water Quality Research at Heidelberg University (Heidelberg University, 2015).

Evaluation of model performance was completed using the Nash-Sutcliffe Efficiency (NSE), correlation efficient (R^2), and percent bias (PBIAS), as recommended in (2015). NSE values range from -∞ to 1, which 1 indicates a perfect fit between observed and model predicted output. PBIAS measures average tendency in model bias, where 0 is the optimal condition; a positive value means over prediction and a negative value means underestimation.

Overall, the calibrated SWAT model is able to simulate surface runoff and nutrient transport with reasonable accuracy. According to model performance ratings for R^2, NSE and PBIAS defined by streamflow, TP and TN can be rated as very good, and Sediment and DRP can be considered as good (SI Tables 4). Comparison of observed and simulated stream flow (SI Fig. 4) shows that the model is generally capable of capturing stream flow patterns, but tends to underestimate some peak flows. The PBIAS metric shows that there was about 3% discrepancy between observed and simulated stream flow over a 15-year period, which is consistent with well calibrated SWAT model applications (Moriasi, 2015).

Calibration/validation results for TP and DRP (SI Fig. 5) show that the model is able to reproduce observed TP loads well, though both underestimation and overestimation can be observed throughout the simulation periods. Reproducing the DRP pattern is more difficult than flow and TP, as reflected by lower NSE and R^2 metrics. The calibrated model performs well on low-to-medium loads months, but tends to underestimate high loads between 2005 and 2008. Difficulties in reproducing the observed phosphorous runs may be caused by a number of factors. While flow data are available on a daily basis, the number of days with nutrient discharge measurement is less than 30% of the days during the simulation period. We limited comparison to dates with observational data only to make it comparable, but that means performance on dates with missing data is not evaluated. Also, DRP loads are more sensitive to

fertilizer application rate and timing. For modelling purpose, these parameters were fixed overtime and uniformly distributed, which is not true in reality. Other uncertainties include parameter selection and hydrological calibration.

6.3.4 Yield Analysis.

A further validation analysis was conducted for crop/plant yields (SI Table 5). Observed 10-year average (2001-2010) yields for corn, soybean, cereal rye and alfalfa hay for the study area were retrieved from U.S. Department of Agricultural National Agricultural Statistics Service (USDA NASS) (USDA NASS, 2015). Reported yields of switchgrass can range from 5 Mt/ha to 13 Mt/ha (Baskaran et al., 2010; Jager et al., 2010; Schmer et al., 2008). Expected yield for large-scale switchgrass production is estimated to be about 7-8 Mt/ha for the region (Miller, 2016, pers. comm). Simulated switchgrass yield is calibrated to about 7.5 Mt/ha. As suggested in previous studies (Nair et al., 2011), default values for the radiation use efficiency parameter (BIO_E) for crops mentioned above were lowered so that simulated field crop yields better matched reported yields in the study area. Although cereal rye is modeled as a conservation practice (winter cover) in this study, we also calibrated its yield against observed data.

We assumed managed forestry, based on a mix of red maples and white oaks, would be harvested on a 30-year rotation. Average total biomass and marketable portions for these two species in northern Ohio were retrieved from Forest Inventory and Analysis (FIA) databases using the Forest Inventory Data Online (FIDO) tool (USDA Forest Serive, 2015). We adjusted the BIO_E and the BIO_leaf parameter as suggested in (Khanal and Parajuli, 2014) so that simulated biomass matches with observed values well (SI Table 6). BIO_leaf parameter controls the fraction of forest biomass that is converted to residue during annual dormancy (Neitsch et al.,

2011). Average total biomass and marketable portions for these two species in northern Ohio were retrieved from the Forest Inventory and Analysis (FIA) databases using the Forest Inventory Data Online (FIDO) tool (USDA Forest Serive, 2015).

6.4 Representation of Conservation Practices and Alternative Land Uses in SWAT

Conservation practices were implemented in the SWAT model according to existing parameterization guidance (Arabi et al., 2008; Margaret M Kalcic et al., 2015). Winter cover crop is modeled as cereal rye. Fields enrolled in the CRP program is modeled as grassland. For land use scenario, parameters for each HRU were reset to the updated land use option using default SWAT database values. After that, parameter values were adjusted according to model calibration results.

6.5 Economic Valuation in the Model

Field Crops: Annual per-hectare profit for field crops (i.e. corn/soybean, alfalfa hay and switchgrass) was calculated as follows:

$$Profit\left(\frac{\$}{year}\right) = yield_j^k * price - management\ costs \quad (5)$$

where $yield_j$ is simulated 10-year (2001-2010) average yield for crop k at field j. Management costs (e.g. seed, fertilizer, machinery and labor) for corn and soybean production were adapted from USDA Economic Research Service (USDA ERS)(USDA ERS, 2015). Costs for other crops was adapted from farm budgets generated by Ohio State University Extension(OSU -Extension, 2015). Since biofuel production for switchgrass is not currently in practice, we assumed switchgrass was planted as grass hay. Detailed management and budget information collected for

individual crop is available from the author upon request. We excluded government payments and land rental costs from the calculation to make profitability of alternative options comparable.

Conservation Practices. When conservation practices are included, per-hectare profit was calculated as follows:

$$Profit\left(\frac{\$}{year}\right) = yield_j^k * price - management\ costs - CP\ costs - forgone\ income \quad (6)$$

where $yield_j^k$ is simulated 10-year average corn/soybean yields at field j when CP option (including the -20% fertilizer reduction option) k is applied at field j. Management costs are the same for corn/soybean production. CP costs include the annualized one-time CP installation cost and annual maintenance costs. Also, since structural CPs would take a small portion of field out of production, we calculated yield loss due to CP implementation as forgone income. CP costs were retrieved from Ohio Field Office Technical Guide (FOTG) prepared by USDA Natural Resources Conservation Service (USDA-NRCS) (2015b)

CRP. Fields enrolled in CRP program do not provide marketable commodities, therefore revenues of CRP fields were determined by county-level average CRP program payment rates (USDA FSA, 2015), while costs were calculated as grassland maintenance (USDA NRCS, 2015b).

Managed Forestry. We simulate managed forestry as maple and oak trees, modeled as a 30-year rotation, assuming each year a parcel can get 1/30 of simulated biomass product, we calculated annual profits for timber production as follows:

$$Profit\left(\frac{\$}{year}\right) = \frac{Biomass_j^{30} * P_{30} * r * \theta * \gamma - Site\ Cost - managment\ cost * 30}{30} \quad (7)$$

where $Biomass_j^{30}$ is SWAT simulated total biomass for maple or oak with a 30-year stand age at field j, P_{30} is stumpage price of white oak and red maple per 1,000 board feet (mbf), r converts price from mbf to metric ton dry matter, θ is portion of aboveground biomass and γ is proportion of marketable bole. Site cost includes site preparation costs needed to convert from cropland to forest land, and management cost is annual maintenance cost.

Stumpage prices for timber production are reported by Ohio State University Extension (Ohio State University(OSU)-Extension, 2016). Marketable portions for these two species in northern Ohio were retrieved from FIA using the FIDO tool (USDA Forest Serive, 2015) with the help of Charles J. Barnett from USDA Forest Inventory & Analysis Program. Site preparation and management costs were adapted from NRCS (USDA NRCS, 2015b). Site preparation is needed to convert corn-soybean fields to forestland. Since maple and oak were modeled, we assumed new forest were established as hardwood planting using bare-root seedling, which is main method used in the region (Pijut, 2003).

We assume there would be an even-aged forestry management and 1/30 of each forestry parcel is harvested each year, but this may not be true in reality. We did not calculate net present values for managed forestry because it is difficult for the SWAT model to get reliable biomass estimate for each year over 30 years. It is more reliable to use average biomass for a forest with a stand age of 30 years.

Low Density Rural Residential Land. Returns to residential land uses were calculated as the net present values of a perpetual stream of urban returns over 100 years, then converted to a constant annualized equivalent with a 5% discount rate (Lubowski et al., 2008). Net present

value of rural residential land use on field j was determined using an hedonic property price model (Polasky et al., 2008) as follows:

$$\begin{aligned}\log LV_x &= \alpha_0 + \alpha_1 Hardin_x + \alpha_2 Marion_x + \alpha_3 Sandusky_x + \alpha_4 Seneca_x + \alpha_5 Wyandot_x \\ &+ \alpha_6 \log Acres_x + \alpha_7 \log PARA_x + \alpha_8 dmcity_x + \alpha_9 \log dlakes_x \\ &+ \alpha_{10} dresd_x + \alpha_{11} \log drivers_x + \alpha_{12} \log dshore + \alpha_{13} \log dpark + \varepsilon_x\end{aligned} \quad (8)$$

where LV_x is the per-acre appraised value of residential lot x; $Hardin_x$ is equal to 1 if x is in Hardin County; $Marion_x$ is equal to 1 if x is in Marion County; $Sandusky_x$ is equal to 1 if x is in Sandusky County; $Seneca_x$ is equal to 1 if x is in Seneca County; $Wyandot_x$ is equal to 1 if x is in Wyandot County; $Acres_x$ size of x in acres; $PARA_x$ is perimeter to area ratio for lot x; $dmcity_x$ is distance from x to medium size cities (population size between 40,000 and 8,000); $dlakes_x$ is distance from x to the nearest lake; $dresd_x$ is distance from x to nearest residential road; $drivers_x$ is distance from x to the nearest river; $dshore_x$ is distance from x to the shoreline of Lake Erie; $dpark_x$ is distance from x to the nearest park. SI Table 7 summarized regression results for the model.

Appraised land values were obtained from local county assessment departments. Although appraised value is estimated based on market value, they are not sale prices. We collected sale prices of residential lots with buildings from local county tax assessment departments. We ran parallel regressions using appraised and sale values as the dependent variable to validate the appraisal data, and results indicate that appraised value generally underestimates market value by about 10%, but deviations change across fields. The reason to use appraised value is that sale data does not differentiate land value from building value.

The per-hectare net present value for a field converted to rural-residential land use was calculated as:

$$\mathrm{NV_x} = (\widehat{\mathrm{LV}}_\mathrm{x} * 0.91 * \mathit{Acres}_x)/\mathrm{A_x} \quad (9)$$

Where $\widehat{\mathrm{LV}}_\mathrm{x}$ is predicted per-acre sale price for field x; 0.91 represents the deflator used to convert 2014 to 2008 dollars; $\mathrm{A_x}$ is field x's area in hectares.

Using a 5% discount rate as mentioned above, the equivalent annual per-hectare net return was calculated as:

$$\mathrm{R_x} = \mathrm{NV_x} * \frac{0.05}{(1-1.05^{-100})} \quad (10)$$

SI Table 2.1 DRP Abatement Costs by CP and Land Use Option (78% DRP Reduction)

Option	**Total Cost ($Million)**	**Unit Cost ($/acre)**	**Area of Fields with Profit Loss(km2)**	**Area of Fields Adopted (km2)**
Filter strips	1.40	5.23	1083.85	1083.85
Forest	2.68	31.87	340.05	631.35
Alfalfa hay	0.04	3.53	50.51	455.63
-20% fertilizer	0.18	5.74	123.86	347.59
Switchgrass	1.43	39.88	145.51	157.07
CRP	0.08	44.37	7.51	7.51

Note: abatement costs for each option vary spatially. Reported unit cost is average cost.

SI Table 2.2 TP Abatement Costs by CP and Land Use Option (46% TP Reduction)

Option	**Total Cost ($)**	**Unit Cost ($/acre)**	**Area of Fields with Profit Loss(km2)**	**Area of Fields Adopted (km2)**
Filter strips	72,204	4.32	67.58	67.58
Cover crop	991,499	90.82	44.18	64.02
Alfalfa hay	17,276	1.76	39.67	641.56
Forest	6,632	2.31	11.61	168.11
CRP	79,382	44.16	7.27	7.27
-20% fertilizer	25	0.04	2.41	234.67
Switchgrass	535	1.34	1.61	11.40

Note: abatement costs for each option vary spatially. Reported unit cost is average cost.

SI Table 2.3 Watershed Level P Abatement Cost

Scenarios	**Costs for 46% TP Reduction ($ Million)**	**Costs for 61% DRP Reduction ($ Million)**	**Costs for 78% DRP Reduction ($ Million)**
CPs only	1.98	3.13	NA
Mixing CPs and land uses	1.17	2.32	5.82
Optimizing based on mix strategy and reduced alfalfa & timber prices (-20%)	1.89	3.17	8.35

SI Table 2.4 Monthly Statistical Performance of the SWAT model

	R^2	**NSE**	**PBIAS**	**Performance Rating**
	Calibration (Validation)	Calibration (Validation)	Calibration (Validation)	Calibration (Validation)
Stream flow	0.83 (0.89)	0.82 (0.87)	-1.66 (-2.76)	Very good (Very good)
Sediment	0.90 (0.77)	0.83 (0.73)	-1.02 (9.8)	Good (Good)
TP	0.73 (0.77)	0.66 (0.76)	-4.83 (-2.13)	Very good (Very good)
DRP	0.59 (0.69)	0.56 (0.62)	-4.84 (-11.35)	Good (Good)
TN	0.84 (0.75)	0.83 (0.75)	2.29 (-0.27)	Very good (Very good)

SI Table 2.5 Comparison of SWAT Simulated versus Observed 10-year (2001-2010) Average Yields for Field Crops

Crop/Plant	Simulated Yield (Mt/ha/yr)	Observed Yield (Mt/ha/yr)
Corn	7.86	7.78
Soybean	2.50	2.49
Switchgrass	7.43	~6 to 12
Grass hay	5.19	5.25
Alfalfa hay	7.44	7.37
Cereal Rye	1.33	1.32

SI Table 2.6 Comparison of SWAT Simulated versus Observed Average Total Biomass for a Forest with a 30-year stand age.

Forest Group	Type	Observed Mean Biomass(Mt/ha)	SWAT Tree Model	Simulated Biomass (Mt/ha)
Oak/hickory	Forest	110	Oak	110.2
	Timber	111		
Maple/Beech/Birch	Forest	115	Maple	115.9
	Timber	126		

SI Table 2.7 Summary of the Hedonic Pricing Model.

	Coefficient Estimates	**Robust Standard Errors**	**P-value**	**Significant level**
(Intercept)	7.86	0.142	< 2.2e-16	***
log(Acres)	0.41	0.013	< 2.2e-16	***
log(PARA)	-0.111	0.02	4.36E-08	***
dmcity10	2.07E-05	2.82E-06	1.96E-13	***
dpark	3.87E-06	1.14E-06	0.000708	***
log(dshore)	0.039	0.012	0.001269	**
dresrd	-8.16E-05	2.41E-05	7.18E-04	***
log(drivers)	0.013	3.65E-03	0.000282	***
log(dlakes)	0.011	4.77E-03	0.024745	*
Hardin	-0.121	0.018	1.58E-11	***
Marion	0.381	0.024	< 2.2e-16	***
Sandusky	0.782	0.019	< 2.2e-16	***
Seneca	0.483	0.013	< 2.2e-16	***
Wyandot	-0.024	0.014	0.076149	.
R^2	0.612			

Notes: N = 7,466 observations. OLS estimator. Heteroscedasticity-constant standard errors were reported as the robust standard errors.

*** Significant at the 1 percent level.

** Significant at the 5 percent level.

* Significant at the 10 percent level.

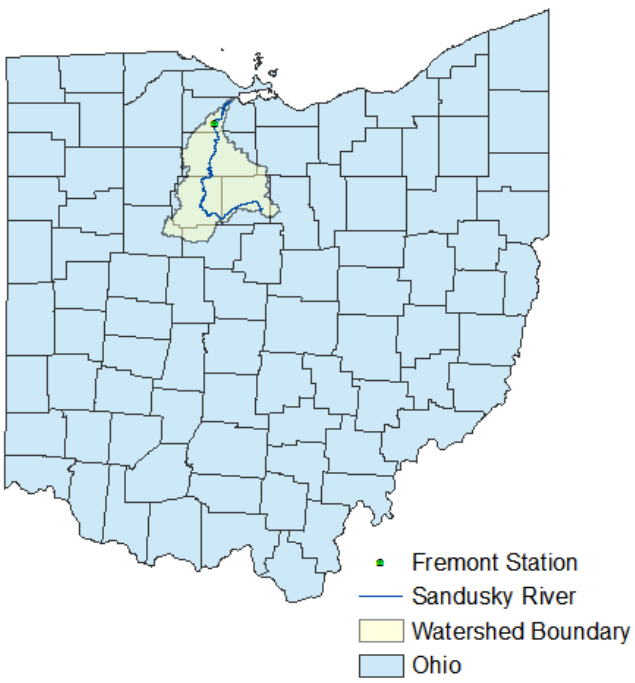

(a)

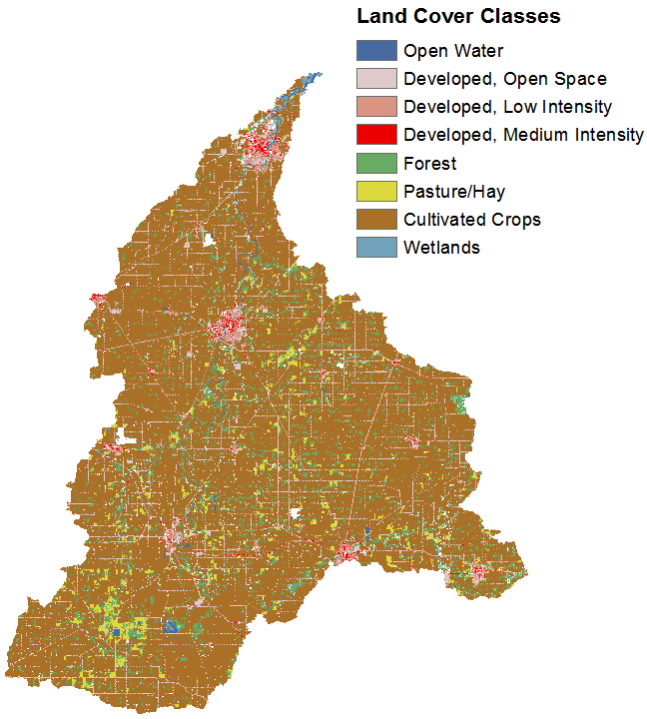

(b)

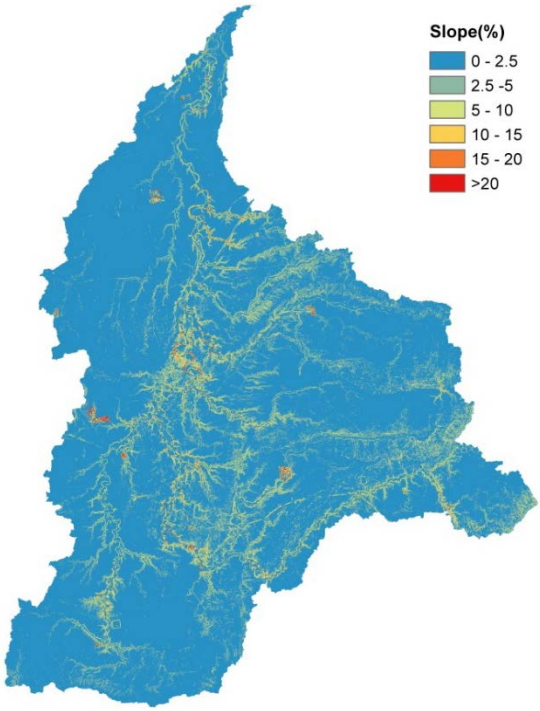

(c)

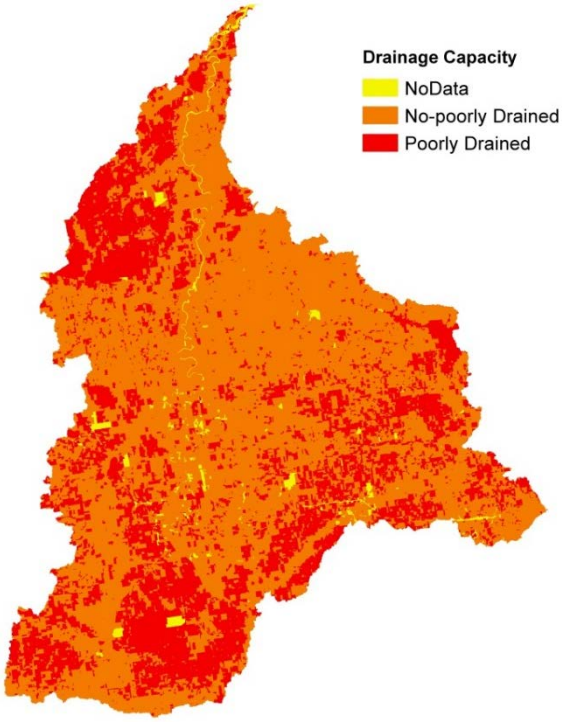

(d)

Figure 2.5 The Sandusky River Watershed, Ohio. Location of the watershed (a), land-use/cover map in 2006 (b), terrain slope (c) and soil drainage capacity (d).

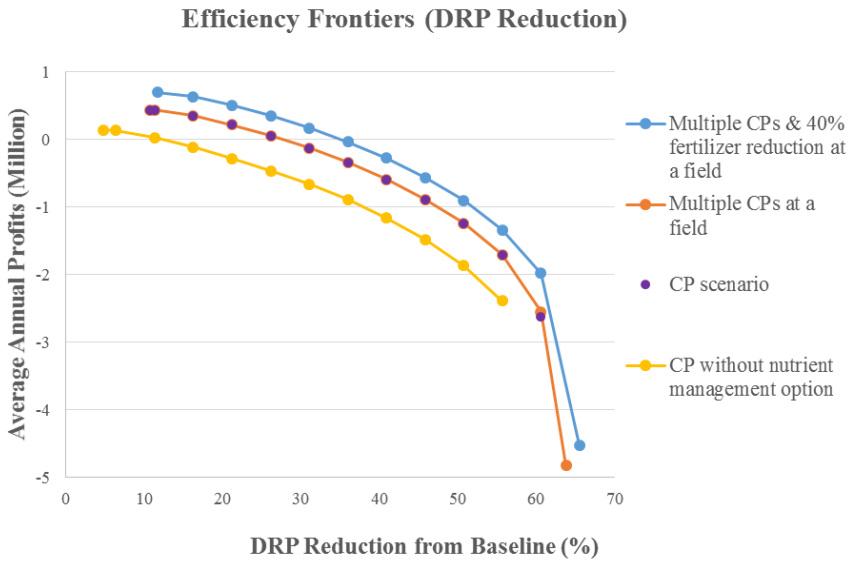

(a)

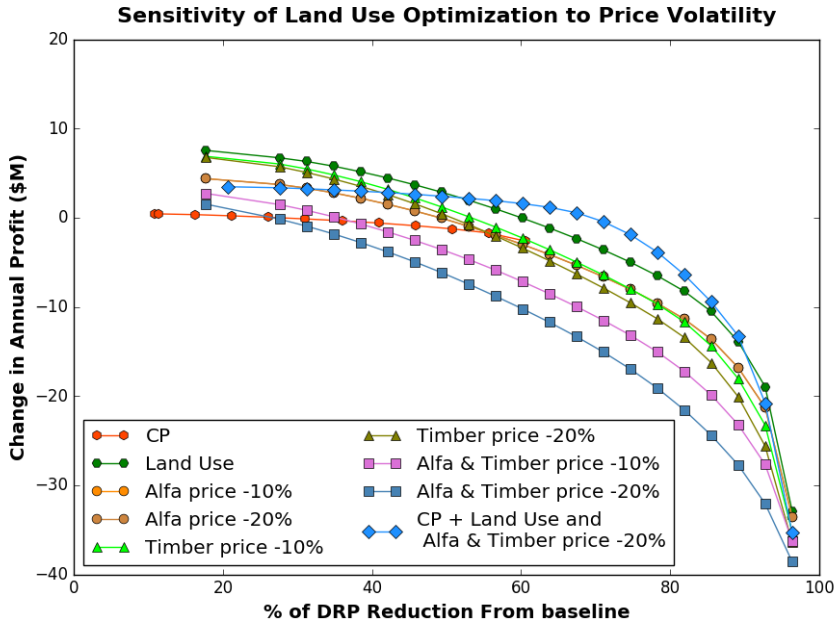

Figure 2.6 Sensitivity of Spatial Optimization**.** Efficiency frontiers for the CP targeting scenario with multiple CPs and the aggressive fertilizer reduction (-40%) option enabled (a), and impacts of forest and alfalfa hay price reductions on land use optimization efficiency (b).

(b)

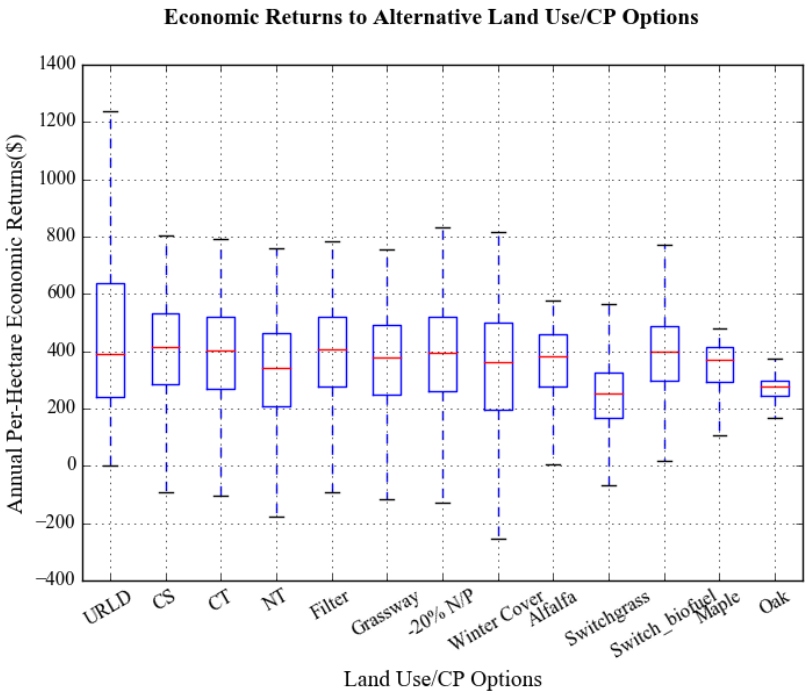

Figure 2.7 Comparison of Profitability of Alternative Land Use and Management Options. URLD, CS, CT and NT stand for rural residential land, corn/soybean rotation, conservation tillage and continuous no-till practices. Boxplots show median annual profits ($/ha) with first and the third quartiles. The whiskers stand for values past 1.5 interqurtile range (IQR) of the first and third quartiles.

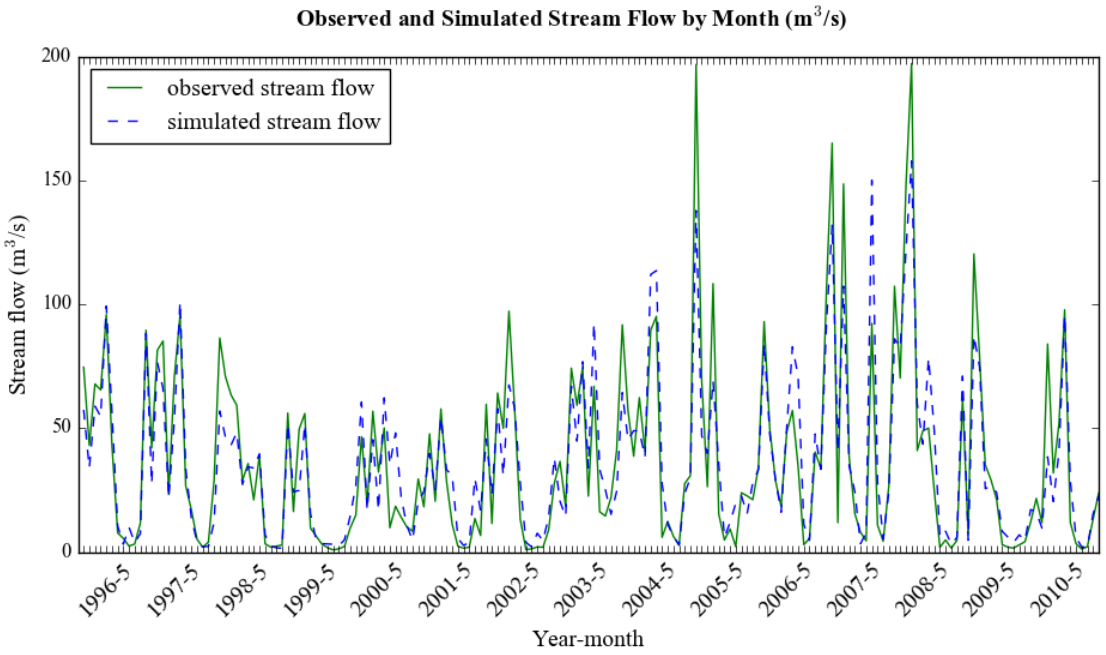

Figure 2.8 Hydrology Calibration and Validation. Comparison of average monthly observed and modeled stream flow for calibration (1996-2006) and validation (2007-2010) period.

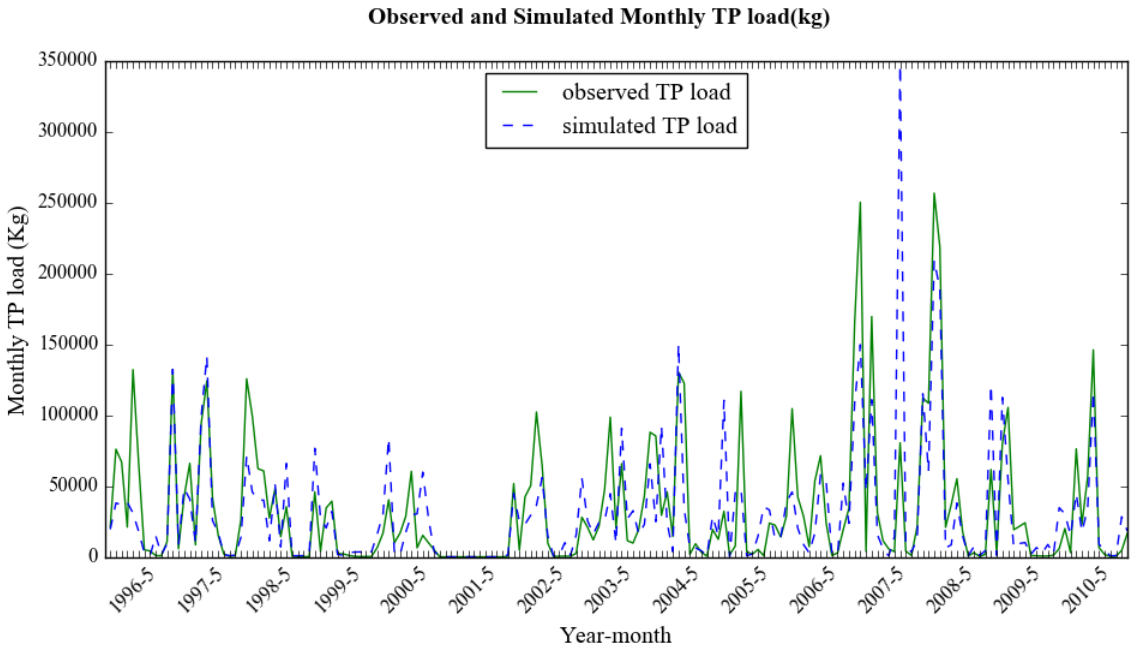

(a)

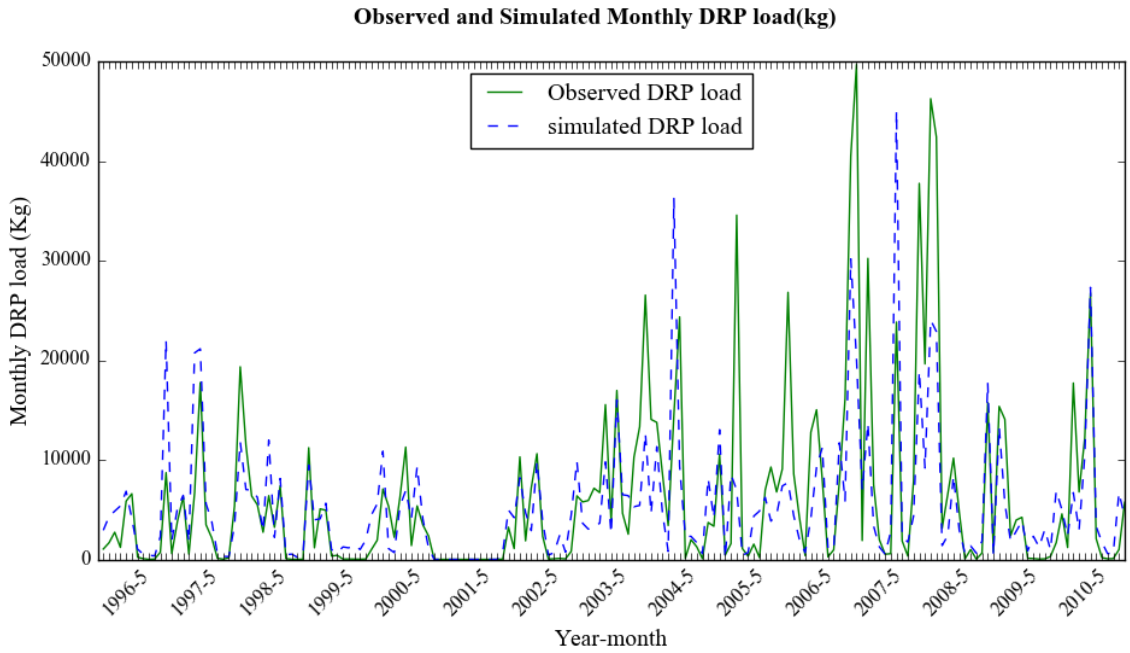

(b)

Figure 2.9 Phosphorous Load Calibration and Validation**.** Comparison of observed and modeled phosphorus loads (limited to dates with observational data) for: (a) average monthly total phosphorous (TP) for calibration (1996-2006) and validation (2007-2010) periods, (b) average monthly dissolved reactive phosphorous (DRP) for calibration (1996-2006) and calibration (2007-2010) period.

Chapter 3

Sensitivity of Optimized Spatial Patterns of Land Use and Management to Climate Change

1. Introduction

Degradation of freshwater and marine ecosystems has become a significant problem both in the United States and globally (Carpenter et al., 2011). Nutrient loading from anthropogenic landscapes has been identified as the main driver of water quality problems (NRC, 2009). While several programs have been developed in the U.S., current efforts are far from adequate to address water quality problems. An important reason is that non-point source (NPS) nutrient loading from agricultural land is not regulated. Studies have suggested that substantial reduction in nitrogen (N) and phosphorous (P) load is needed to protect freshwater and coastal resources. However, control of NPS pollution remains a formidable challenge because nutrient reduction often needs to be achieved at continental scales (Tomer et al., 2013), while agriculture production is being intensified to meet increasing demand for food (Lobell et al., 2009) and biofuel feedstock (Mehaffey et al., 2012). Given that intensification of agricultural production is likely to continue, effective land management strategies are critical to balance the need for agriculture production and environmental protection of aquatic resources.

Multiple strategies have been developed to address NPS pollution from agricultural land. Conservation practices (CPs), such as conservation tillage, riparian buffers and nutrient management, are frequently used to reduce soil erosion and nutrient run-off from farm fields. When targeted at appropriate fields, CPs can be a cost-effective approach to reduce surface

runoff (Arabi et al., 2006; Maringanti et al., 2009). However, effects of CPs can be limited when the objective of watershed management is to reduce mineral or soluble nutrients. While field- or plot-scale studies have reported encouraging results, lessons learned from watershed-level experiments indicate that it is generally much harder to reduce nutrient load than sediment. Using eco-hydrological models, studies in the Midwestern US found that even a 100% coverage of CPs on agricultural land cannot reduce mineral nutrient load by more than 30% (Bosch et al., 2013; Kalcic et al., 2015). An alternative approach is to convert certain row crops to less-intensive land uses, such as grassland and forest, to reduce nutrient losses (Wilson et al., 2014). While land-use conversion may lead to a loss of revenue for owners of certain fields, watershed-level performance can be improved by allocating alternative land-use activities at suitable locations (Ruijs et al., 2015). This 'landscape approach' has emerged as a promising solution to trading off production and environmental protection (Sayer, 2009; Sayer et al., 2013). Previous studies have demonstrated that land-use optimization can be a useful tool to identify land-use and land-management patterns that jointly improve economic output and ecosystem services (Nelson et al., 2008; Polasky et al., 2008).

Lessons learned from previous studies have indicated that restoration of impaired water bodies requires sustained effort (Osmond et al., 2012). Improvements in water quality through conservation practices tend to occur on the scale of years to decades (Scavia et al., 2014). Similarly, land-use optimization studies often target land-use decisions implemented over several decades (Nelson et al., 2008; Polasky et al., 2008), for example to account for the natural and economic life cycle of managed forests. Because of the long time frame associated with land-use and -management changes and their effects, it is important to consider potential impacts of a changing climate on their effectiveness (Scavia et al., 2014). Potential changes in climate are

likely to alter hydrologic and nutrient fluxes considerably (Paerl and Paul, 2012), with nutrient loads and surface runoff likely to increase under increased CO_2 emissions (Jeppesen et al., 2009; Shrestha et al., 2012). These impacts could potentially offset nutrient reductions achieved from CP targeting or land-use change. Sensitivity analyses have shown that the performance of CPs is sensitive to climate change (Woznicki and Nejadhashemi, 2012) and climate variability may compromise the effectiveness of CPs (Chaubey et al., 2010). Simulation results have suggested that CPs tend to be less effective under future climates, and more aggressive implementation of CPs is required to obtain the same nutrient-reduction results (Bosch et al., 2014). The sensitivity to climate change of optimized patterns of land use is unclear because few studies have investigated their robustness. Unlike CP targeting, efficiency of spatial land-use optimization, which addresses the joint objectives of economic productivity and nutrient reduction, depends on profitability of alternative land uses. Johnson et al. (2012) found that changes in the profitability of competing land uses significantly affects the economic performance, and therefore the overall performance, of alternative land-use arrangements. Climate change is expected to affect yields of crops and trees and, therefore, the economic efficiency of optimized land-use patterns. When extreme weather, like drought, is not considered, elevated CO_2 is generally expected to have positive impacts on plant growth and yields (Kirilenko and Sedjo, 2007; Tubiello et al., 2007). Because these impacts vary by plant species, previous studies have shown that diversifying row crops with more natural land-use types, like forest, can improve the resilience of agricultural watersheds (Garrity et al., 2010; Mbow et al., 2014). Still, some studies reported negative impacts of climate change on forest growth (Briner et al., 2012).

Considerable uncertainties associated with the performance of conservation actions highlight that, for long-term conservation planning, watershed management strategies should consider not only near-term cost-effectiveness, but also the capacity to adapt to future climate change. However, previous studies focused on either spatial targeting of CPs (Arabi et al., 2006; Kalcic et al., 2015; Maringanti et al., 2009; Rabotyagov et al., 2014) or land-use optimization (Nelson et al., 2008; Polasky et al., 2008; Sadeghi et al., 2009) were mostly conducted based on current or historical climate conditions. It is unclear how optimized placement of CPs or land-use changes affects nutrient reduction under future potential climate scenarios, and more importantly, which strategies are more robust under a changing climate. Understanding robustness of alternative management strategies to climate change is important for managers, policy makers, and stakeholders as they seek to prioritize allocation of limited conservation funding for more effective and robust actions, which can be critical to ensure success of water quality improvement.

The objective of this study was to develop and apply an integrated modeling framework to compare the efficiency and robustness of optimized spatial patterns, developed for targeting CPs and land-use changes to control nutrient loss from agricultural watersheds under a changing climate. The integrated framework includes three components: (1) an ecohydrogical model – the Soil and Water Asesseent Tool (SWAT; Arnold et al., 1998) – to evaluate the effects of CPs and alternative land uses on crop/plant yields and nutrient discharges at field scale, (2) an economic valuation component that estimates economic costs and income losses associated with each CP or land-use change, and (3) a linear optimization algorithm to identify optimal spatial land-use and management plans that can maximize economic returns at watershed scale, given a certain nutrient reduction target. Three land scenarios were assessed: (1) relying on CPs only, (2) relying

on land-use changes only, and (3) allowing a combination of CP and land-use-change strategies. Using the Sandusky river watershed in Ohio as an example, we evaluated the efficiency of optimized patterns of CPs versus land uses on P reduction based on current climate (2001 and 2010), and compared the robustness of optimized plans under mid-century future climatic conditions (2046 to 2065) using a suite of global and regional climate change projections.

2 Materials and methods

2.1 Study Area

The Sandusky river watershed is located in northwestern Ohio, USA (Fig.1a). The watershed covers about 3,458 km^2 and is dominated by agricultural land use (~80% of the area), followed by urban (~9%) and forest area (~8%; Jin et al., 2013; Fig.1b). About 85% of agricultural land is maintained in corn and soybean row crops (USDA NASS, 2016). Given the temperate climate, adequate rainfall, and flat or gently rolling topography (Fig 1c; average slope is 1.7%), artificial subsurface (tile) drainage is used to lower the water table below the crop rooting zone in order to support agricultural production (Smith et al., 2015). According to the Soil Survey Geographic (SSURGO) Data Base (USDA NRCS, 2015a), about 32% of soils in the watershed are in the poorly or very poorly drained category (Fig.1d).

The Sandusky River is 210 km in length and drains into Lake Erie (Gillenwater et al., 2006). Lake Erie is the shallowest and most productive of the five Laurentian Great Lakes, which collectively have the largest surface area of freshwater in the world (Michalak et al., 2013). The

water quality of Lake Erie's western basin deteriorated dramatically during the 1950s and 1960s as nutrient pollution from both point and non-point sources increased (Boegman et al., 2008). Algal blooms disappeared in Lake Erie in the 1980s after a series of abatements, but reemerged in the 1990s (Millie et al., 2009). To address the harmful algal bloom and hypoxia problems in Lake Erie, the International Joint Commission (IJC) has established the Lake Erie Ecosystem Priority (IJC, 2014), and recommended significant reductions in phosphorous (P), particularly dissolved reactive phosphorous (DRP), to restore water quality in Lake Erie.

2.2 Spatial Optimization of Conservation Practices and Land-Use Patterns

The objective of our spatial optimization approach is to identify patterns of land use or CP placement that can maximize net economic benefits of the watershed given a targeted level of reduction in nutrient loading. The effects of alternative land uses and CP implementations on economic profits and nutrient discharges were estimated using an integrated modeling framework (Fig. 2) that links the SWAT model, estimates of costs and returns to different land uses and management approaches, and a spatial optimization algorithm similar to Polasky et al. (2008). In this study, we focus on DRP reduction for water quality improvement because DRP is the primary concern in the Lake Erie basin (IJC, 2014; Scavia et al., 2014).

The effects of converting a corn-soybean rotation to a different land use, or of installing a CP on a current corn-soybean field, were simulated using the SWAT model. Default spatial units in the SWAT model, the so called hydrological response unit (HRU), are discrete land areas with common land use, soil, and slope within a subwatershed. In order to link SWAT units with land management practices, we set up the SWAT model based on field boundaries using a method similar to Kalcic et al. (2015). Field boundaries were identified by overlaying the Common Land

Unit (CLU) layer with parcel maps obtained from local county tax assessment apartments in the study area. A CLU is “the smallest unit of land that has a permanent, contiguous boundary, a common land-cover and land management, a common owner and a common producer in agricultural land associated with USDA farm programs” (USDA, 2013). Since CLUs do not cover non-agricultural land, we filled in those areas with parcel maps, which outline property boundaries. The watershed was divided into 41,233 distinct fields. For optimization purposes, we selected only those fields whose major land use/cover type is cultivated crops; all other types remained unchanged in the optimizations. A 2006 land-use/cover map, derived from the National Land Cover Dataset (NLCD; Jin et al., 2013), was employed to identify land-use/cover type for each field. Based on these criteria, a total of 27,905 agricultural fields were selected for implementation of the optimization process.

To establish a baseline land-use and -management scenario, we assumed that all cultivated crop fields are maintained as corn-soybean rotations, the dominant agricultural production in the study area (USDA NASS, 2016), with no conservation practices. In addition to the baseline scenario, we modeled six conservation practices and five alternative land uses. The six conservation practices included: reduced tillage (CT), continuous no-tillage (NT), vegetative filter strips (FT), grassed waterway (GW), and winter cover modeled as cereal rye (CC), and a nutrient management option which assumes a 20% reduction in fertilizer (i.e., nutrient) application. The five land-use alternatives included: switch grass (SWCH), alfalfa hay (ALFA), managed forestry (Forest), conservation reserve program (CRP) modeled as grassland, and low-density residential land (URLD). All conservation practices were applied to the corn-soybean land use, and the corn-soybean rotation (C/S), with and without CPs applied, remained as a land-use option.

To compare efficiency of optimized spatial patterns of land-use change and CP targeting on DRP loading under future climate conditions, we identify efficient spatial plans using three spatial optimization scenarios: 1) optimization of land-use patterns, 2) optimization of targeted CPs, and 3) optimization of a combination of CP and land-use strategies. In total, there were 12 possible combinations of land use and management in the combined scenario (seven management options on corn-soybean, including no CPs, and five alternative land uses). For each spatial optimization scenario, we find the maximum watershed-level economic returns (NR) for a given DRP load limit (RT). By varying RT, we trace out the efficiency frontier. The efficiency frontier displays the combinations of outcomes such that it is not possible to improve one outcome without reducing the other outcome. A point on the model's efficiency frontier is found by identifying an efficient land-use and/or CP placement pattern by solving the following:

$$NR = Max \sum_{j=1}^{N} \sum_{k=1}^{P} R_j^k A_j(k_j) \qquad (1)$$

$$Subject\ To:$$

$$\sum_{j=1}^{N} \sum_{k=1}^{P} NP_j^k k_j \leq RT \qquad (2)$$

$$\sum_{k=1}^{P} k_j = 1 \qquad j = 1, \ldots, N \qquad (3)$$

$$k_j = \{0,1\} \qquad j = 1, \ldots, N \qquad (4)$$

where j indexes fields (j=1,…,N where N=27,905), k indexes land use or CP option (k=1,…,P where P=6 for Scenario 1 (land uses only), P=7 for Scenario 2 (CPs only) and P=12 for Scenario 3 (combination), k_j indicates the land use or CP option assigned to field j, R_j^k is the annual per-hectare net economic returns of choosing option k at field j, A_j is a field j's area in hectares, NP_j^k is edge-of-field DRP discharges at field j with option k, NR is maximized net profits and RT is some nutrient loading limit. The problem defined above was considered as a mixed-integer linear

optimization problem, and solved using the Mathematical Programming Language (AMPL) software (Fourer, 2007) and the CPLEX solver (IBM ILOG, 2012).

The spatial optimization framework was utilized to obtain efficiency frontiers and associated optimized land-use and land–management patterns under both the current (2001-2010) and the projected future (2046-2065) climates. To assess robustness of optimal solutions under a changing climate, we evaluated efficiency of optimal solutions under current climate in the context of projected future climates, and compared selections of optimal land-use/CP options for each field across climate conditions. We also compared optimal spatial patterns among five future climate projections to evaluate commonality of patterns for future optimal solutions.

2.3 Climate Projections

A series of climate projections was developed for the western Lake Erie basin (Basile et al., submitted). These projections represent relatively high greenhouse gas emission scenarios, using the Special Report on Emission Scenarios (SRES) A2 and Representative Concentration Pathway (RCP) 8.5 scenarios depending on climate simulations (Moss et al., 2010; Nakicenovic et al., 2000). Climate projections were produced using a set of five different general circulation models (GCMs) or regional climate models (RCMs) driven by a set of atmosphere-ocean GCMs. Daily precipitation and maximum/minimum air temperature data from the models at a range of spatial resolutions (Table 1) were implemented for a present-day baseline period (1977-1999) and a future period (2043-2065). Five RCM/CGM runs available for the study area were employed (Table 1).

Raw GCM/RCM data used in this study provided biased representations of present-day climate, relative to the climate record (Fig. 3a and b). For instance, models of present-day climate

overestimated precipitation in the winter and underestimated precipitation for August to October. Nearly all climate models exhibited a cold bias (Fig. 3b). We employed the "delta-change method" (IPCC-TGICA, 2007) to perform the bias correction necessary when forcing hydrological models with GCM/RCM runs (Piani et al., 2010). The ratios or differences of model-simulated mean monthly precipitations and temperatures, respectively, for baseline and future periods were calculated as delta change for each RCM/GCM projection. The delta change was then applied to observed daily precipitation and temperature data (Equations 1 and 2, respectively) on a monthly basis in the baseline period to calculate comparable futures for each GCM/RCM (Woznicki and Nejadhashemi, 2012). The precipitation delta (Eq. 1) uses a ratio to avoid negative precipitation values.

$$P_{daily,\ adj} = P_{daily,\ obs} \left(\frac{P_{monthly,model,future,}}{P_{monthly,\ model,baseline}} \right) \quad (1)$$

$$T_{daily,adj} = T_{daily,\ obs} + (T_{monthly,model,future} - T_{monthly,\ model,baseline}) \quad (2)$$

where $P_{daily,\ adj}$ and $T_{daily,adj}$ are adjusted daily precipitation and temperature for the future period (2046-2065), $P_{daily,obs}$ and $T_{daily,obs}$ are observed historical daily precipitation and temperature for the baseline period (1980-1999), $P_{monthly,\ model,future}$ and $T_{monthly,\ model,future}$ are average monthly precipitation and temperature from RCM/GCM for future period (2046-2065), and $P_{monthly,\ model,baseline}$ and $T_{monthly,\ model,baseline}$ are mean average monthly precipitation and temperature for the baseline period (1980-1999) from RCM/GCM runs. The delta calculation for monthly mean temperature (Eq. 2) was applied to both maximum and minimum historical daily air temperatures.

2.4 Robustness of Spatial Optimization under a Changing Climate

To evaluate the robustness of optimized spatial patterns of land-use and management options under projected future climate, we ran the SWAT model using climate inputs from both observed current conditions (2001 to 2010) and projected future climates (2046-2065) to estimate how yields and nutrient discharges for a given land-use or CP option change under projected climates. The 1980-1999 period was used as reference period for the bias-correction ('delta change') process only, and observed climate data for the 2001-2010 period were used to drive SWAT simulations for current climate conditions because farm management budgets were not available for the 1980-1999 period.

The SWAT model has been frequently used to evaluate impacts of climate change on hydrology an nutrient cycles in previous studies (Jha et al., 2006; Shrestha et al., 2012). Efficiency frontiers and associated spatial configurations of land uses and/or CPs were then generated using our integrated modeling framework. By analyzing the performance under projected climate scenarios of optimal spatial configurations obtained based on historical climate, we were able to evaluate the robustness of spatial patterns of land-use and/or CP targeting on nutrient reduction under projected future climate change.

2.5 SWAT Model Parameterization, Calibration, and Validation

The SWAT model (Arnold et al., 1998) is a semi-distributed, process-based watershed model that is widely used to evaluate the impacts of land use and management on hydrologic, sediment, and nutrient cycles for large river basins (Arnold et al., 2010). We ran the model using field boundaries, as mentioned above, and assumed tile drainage was present in row-crop and hay

agricultural land with soil in the poorly or very poorly drained categories. Methods for model set up, calibration, and validation have been detailed in Chapter 2.

We ran the model for 1993-2010, including three years for model warm up (1993-1995), 11 years of calibration (1996-2006) and four years for validation (2007-2010). Daily streamflow data were obtained from USGS Fremont gage station (Fig. 1a) and nutrient loading data were obtained from the National Center for Water Quality Research at Heidelberg University. Frequently used statistics for model fit, including the correlation coefficient (R^2), the Nash-Sutcliffe coefficient (NSE), and the percent bias (PBIAS), were used to evaluate the model's estimates of streamflow and nutrient loads including total phosphorous (TP), DRP, total nitrogen (TN), and sediment. Calibration and validation results showed that the calibrated SWAT model was able to accurately predict hydrology, sediment, and nutrient loads under current conditions. Overall there was only about a 3% discrepancy between observed and simulated stream flow over a 15-year period. We employed the calibrated model to assess the performance of spatial optimizations of land use and management approaches under projected future climates.

2.6 Representation of Conservation Practices and Alternative Land Uses

Conservation practices were implemented in the SWAT model according to existing guidance on parameterization (Arabi et al., 2008; Kalcic et al., 2015). For scenarios involving land-use change, input files depicting each land-use option at each field were created using existing SWAT databases associated with the calibrated model. Management parameters (e.g., crop type, planting time, fertilizer application, etc.) and biophysical variables (e.g., surface runoff coefficient) were adjusted according to parameter calibration results for the SWAT model.

2.7 Calibrating Crop Yields

Because the effects of alternative land uses on the optimization results depend on crop yields for alternative crops and plants, we compared yields under observed climate conditions with those under projected climate conditions. Ten-year average (2001-2010) yields for corn, soybean, cereal rye, and alfalfa hay for the study area were retrieved from USDA NASS (USDA NASS, 2015). Reported yields of switchgrass can range from 5 Mt/ha to 13 Mt/ha (Baskaran et al., 2010; Jager et al., 2010; Schmer et al., 2008). Expected yields for large-scale switchgrass production were estimated to be about 7-8 Mt/ha for the region (Miller, 2016, pers.comm), therefore we used a value of 7.5 Mt/ha. The BIO_E variable, which controls radiation use efficiency in SWAT, was the primary parameter used to calibrate crop yields and forest biomass, as suggested by previous studies (Khanal and Parajuli, 2014; Nair et al., 2011; Chapter 2, supplemental material). We assumed managed forests would include a mix of red maple and white oak harvested on a 30-year rotation. Average total biomass and marketable timber for these two species in northern Ohio were retrieved from Forest Inventory and Analysis (FIA) databases using the Forest Inventory Data Online (FIDO) tool (USDA Forest Serive, 2015).

After we calibrated modeled yields against observed or reported yields, we were able to analyze the impacts of climate change on crop yields by comparing changes in simulated yields based on historical and projected future climates. The SWAT model simulates crop and plant growth using daily precipitation, maximum and minimum air temperature data. Projected changes in precipitation and temperature regimes are likely to affect crop growth and yields (Lobell and Burke, 2008; Tubiello et al., 2007). For instance, moderate increases in air temperature may provide higher heat units, which may boost crop yields, but significant increases in temperature would also harm crop growth. By replacing observed climate data with projected future daily

data, we can use the SWAT model to estimate the impacts of climate change on crop growth and nutrient cycles simultaneously.

2.8 Economic Benefits and Costs

We ran the SWAT model for the period 2001 to 2010 to get 10-year average plant yields and nutrient discharge estimates. For each field, economic profits ($/ha/year) were calculated as revenue, which is the product of SWAT-simulated yield and observed market price less management and operation costs (e.g. fertilizer, labor; Equation 3). We included annualized installation and maintenance costs in net profits from CP implementations (Equation 4). Also, because implementation of structural CPs needs to take a portion of field out of production, yield losses due to CP placement were calculated as forgone income (Equation 4). Average crop prices and stumpage prices for timber were obtained from U.S.D.A. National Agricultural Statistics Service and Ohio State University Extension, respectively (USDA NASS (2015); OSU-Extension, 2016). Management costs for corn and soybean production were adapted from U.S.D.A. Economic Research Service (ERS) (USDA ERS, 2015). Management costs for plants other than trees were adapted from farm budgets generated by Ohio State University Extension (OSU Extension, 2015). Costs associated with forestry and CP were retrieved from Ohio Field Office Technical Guide (FOTG) prepared by the U.S.D.A. Natural Resources Conservation Service (NRCS) (2015b). Since corn and soybean prices have varied substantially over the last 10 years, partly due to the biofuel mandate, it is necessary to include both low and high prices to reflect price volatility. We calculated average prices and costs over the 2001-2015 period. Profits for corn-soybean rotation were estimated as the mean of corn and soybean profits averaged over the last 15 years.

$$\text{Profit}\left(\frac{\$}{\text{year}}\right) = \text{yield} * \text{price} - \text{management costs} \quad (3)$$

$$\text{Profit}\left(\frac{\$}{\text{year}}\right) = \text{yield} * \text{price} - \text{management costs} - \text{CP costs} - \text{foregone income} \quad (4)$$

Because they do not produce marketable products annually, low-density rural-residential lands and fields enrolled in CRP programs were treated slightly differently. Profits for CRP lands were calculated as county-level average CRP payments (USDA FSA, 2015), less maintenance costs. We modeled the present value per acre of land in rural-residential land use as a function of geographic (e.g., distance to urban centers and parks) and site conditions (e.g., parcel size, elevation, and slope) using a hedonic price function similar to Polasky et al. (2008). Rather than estimating our model using transaction data, we used appraisal data obtained from local county tax departments. We validated reliability of the model estimated using appraisal data by comparing it with a model estimated using sales data from local county tax departments, and the difference between these two values are less than 10% on average. All cost and revenue values were adjusted to 2008 dollars using the Consumer Price Index (CPI) published by U.S. Department of Labor Bureau of Labor Statistic.

3 Results

3.1 Impacts of Climate Change on Flow, Nutrient Discharges, and Yields

Compared to the observed baseline (1980-1999) climate conditions (Fig. 4a), all five future climate projections show increases in average temperature of up to 6°C (Fig. 4b and c). There is a noticeable increase in maximum temperature in the winter and fall seasons (Fig. 4b). The observed precipitation pattern shows rapid increases from winter season to spring season, peaks around June, and then gradual decreases after that (Fig.5 a). There is considerable variation

among climate projections in future precipitation patterns (Fig. 5b). Changes in average monthly precipitation range from +8.9% (CESM1) to -0.1% (GFDL-RCM4), and changes are not evenly distributed across seasons: more precipitation is consistently projected for winter and spring, and less in the fall, though with less agreement among models (Fig. 5b). Projected patterns for the summer season varied by model: while CGCM3-CRCM and GFDL-RCM4 projected a significant decrease in precipitation in the summer months, and the other three models suggest a substantial increase in precipitation around that time (Fig. 5b). This is consistent with analysis over other nearby watersheds, including the Maumee watershed (Basile et al., submitted). Notice that although average monthly precipitation was projected to increase moderately when compared to the baseline period, average precipitation was lower than that of the observed current period (2001-2010) for three out of five future climate projections (Table 2). Compared to the observed current (2001-2010) period, changes in average monthly precipitation ranges from +4.1% (CESM1) to -4.6% (GFDL-RCM4).

Comparison of SWAT simulation results driven by observed current (2001-2010) and projected future (2046-2065) climate data shows average monthly surface runoff will decrease substantially under all five climate change projections, from -35.7% (GFDL-RCM3) to -27.6% (GFDL-RCM4) (Table 3). In particular, there is a substantial projected decrease in surface runoff in the fall and winter season (Table 3). Reduction in surface runoff is likely caused by higher temperatures in the fall and winter season. Higher soil temperature makes water movement between soil layers easier, which leads to a greater amount of water percolation through the bottom of soil profile (Table 4). Other factors, like increased evapotranspiration and increased aboveground biomass, may also contribute to decreased surface runoff. Given a considerable reduction in surface runoff, average annual TP, DRP, TN and sediment loadings were also

projected to decrease significantly under future climate projections (Table 5). Although annual DRP load was projected to be lower, seasonal patterns for changes in simulated DRP load (Fig. 6) suggested an increase in future spring DRP load, which may be a concern because spring DRP load was suggested to be more relevant to water quality problems in Lake Erie (Daloğlu et al., 2012; Scavia et al., 2014)

Sensitivity of plant yields to climate change varied significantly across crops and plant species (Fig. 7). Compared to observed current (2001-2010) levels, average corn yields were projected to decrease slightly (-7% for the CGCM3-CRCM projection, and < -3% for all other projections), similar to values reported in Johnston et al. (2015). Soybean yields were projected to increase by 8% to 15%, which is within the range of reported potential changes in soybean yields (Southworth et al., 2002). Reduction in corn yield is likely caused by increased numbers of high temperature days (>30°C) in the summer season (Schlenker and Roberts, 2009), and increase in soybean yield is likely due to increased nutrient availability associated with reduced DRP loss. Average biomass for 30-year white oak is projected to increase up to 13%, while biomass for 30-year red maple is projected to decrease by up to 9%. Species-specific trends are consistent with results reported by Scheller and Mladenoff (2005). Alfalfa hay and switchgrass exhibited distinctive patterns of sensitivity: the combined effects of higher temperatures and droughts lead to considerable reductions in alfalfa hay yields, but yields for switchgrass, which is more drought tolerant, are projected to increase by 8% to 30%.

3.2 Robustness of Optimized Conservation Practices and/or Land Use to Future Climate Conditions

All three spatial land-use and management scenarios failed to remain efficient under future climate projections (Fig. 8). Nonetheless, CP targeting (Fig. 8a) was found to perform better than land-use change optimization (Fig. 8b). To achieve 60% DRP reductions, CP targeting would result in positive change or gains in annual profits under all but the CGCM3-CRCM model projection. In contrast, optimized land-use patterns based on current climate condition would lead to about $3 million (M) (HadGEM-RCM4) to $8M (CESM1) profit loss. Under the CGCM3-CRCM projection, both CP targeting and land-use optimization would lose around $20M to achieve the 60% DRP reduction target. Given the same DRP reduction target, the combination of both strategies (Fig. 8c) did not perform better than CP targeting, but performed moderately better than land-use optimization alone. Although comparison with simulated DRP load for the baseline land-use scenario suggested that DRP loading will be lower in the future period (Table 5), relying on CP targeting alone is still insufficient to achieve high DRP-reduction targets (i.e., no results were obtained for DRP reductions >65%; Fig. 8a). Land-use optimization, on the other land, would be able to reduce DRP by more than 80%, but at the cost of significantly lower profits (Fig. 8b). For high DRP reductions, combining both strategies is required, and relatively more efficient than relying on land-use optimization alone.

To reduce the extent of the hypoxic zone in Lake Erie by half and limit hypoxic days to 10 days a year, the International Joint Commission (IJC, 2014) recommended a 78% reduction in DRP load from the 2005-2011 average. Average edge-of-field DRP loads for 2005-2011 were 5% higher than the 2001-2011 average for the study area. We used the 78% reduction relative to average values from 2001-2011 SWAT runs as a reference. Based on current climate conditions,

such reductions based on the combined strategy would require approximately 40% of agricultural fields to install vegetative filter strips, and 25% and 18% corn-soybean fields to be converted to managed forest and alfalfa hay, respectively (Fig. 9).

For the same amount of reduction in DRP loading, the optimal composition of CP and land-use changes was substantially different when we optimized using projected future climates (Fig. 9 and Table 6). While alfalfa plays an important role in the current period, almost all alfalfa hay options need to be replaced by other options to achieve optimal outcomes under future climates (Table 6). Under future climate, switchgrass becomes a more important option, and fewer than 30% of current switchgrass fields were changed when compared to solutions optimized for the future period (Fig. 9). The nutrient-management option, which involves a 20% reduction in fertilizer application, seems to be necessary for both current and future periods (Fig. 9). Forest and vegetative filter strips are effective options only under some climate projections (Fig. 9).

Given significant changes in yield projections for alfalfa hay and switchgrass under future climates, we tested whether conversion from alfalfa hay to switchgrass would help with improving efficiency of land use optimization under a changed climate. Results indicate that, if alfalfa hay fields were converted to switchgrass in the future, differences between the performance of current and future optimal solutions are much smaller (Fig. 10). In fact, annual profits based on Scenario 1 would gain $0.1M to $15M under four out of five climate change projections (Fig. 10a). For the CGCM3-CRM projection, projected annual profit loss also reduced from $20M to $10M (Fig. 10a). Similarly, performance for the combined strategy also improved substantially after the conversion of hay to switchgrass (Fig. 10b).

We find that, although many fields would optimally receive a different land-use or CP option under different climate change projections (Fig. 11a), the optimized spatial distribution of most selected land-use and CP options exhibited spatially clustered patterns (Fig. 11b). Benefitting from improved switchgrass yields, the east-central portion of the watershed is no longer optimally targeted for CP implementations under projected future climatic conditions. Compared to other land-use and CP options, optimal locations for fertilizer reduction were most consistent across climate projections. Fields that were optimally selected for switchgrass and fertilizer reduction options were generally associated with fields with poor soil drainage capacity (Fig. 1d).

climate-change projections and (b) the most frequently selected option or combination of options at each field.

4 Discussion

Assuming all agricultural watersheds in the western and central Lake Erie basin aim for the same 78% DRP reduction target identified by the International Joint Commission (IJC 2014), aggressive DRP reduction in the Sandusky river watershed would be necessary. We evaluated the robustness relative to DRP-reduction and economic-production goals of three alternative approaches to optimizing spatial land-use and -management strategies (i.e., optimization of spatial patterns of CPs, of land use changes, and a combination of both strategies) under a changing climate. When applied under current and future climates separately, all strategies tended to contribute to cost-effective solutions. However, we found the performance of solutions optimized for current climate were degraded significantly under projected future climate conditions. Compared to efficient solutions generated based on future climate conditions, all optimal solutions based on current climate conditions would be less efficient in the future.

Among the three scenarios, CP targeting was found to be more robust to climate change than land-use change alone or together with CPs, but relying on CP alone is not sufficient to achieve high (>65%) DRP-reduction targets. A combined optimization of CP and land-use change approaches would be necessary to reduce DRP efficiently and effectively.

We found that the spatial patterns of land-use and -management actions, optimized to reduce nutrient pollution in the most economically beneficial way, can be quite sensitive to changes in climatic conditions, because changed temperature and precipitation patterns affect both plant/crop yields and nutrient discharges. In particular, crop and plant yields are quite sensitive to climate change and play a key role in determining the economic efficiency of DRP reductions strategies. Since projections of corn and soybean yields under future climates are relatively more stable than other modeled crops/plants, the performance of the CP targeting scenario, which applies only to the corn-soybean rotation, was found to be less affected by climate changes than was the land-use-change strategy. Efficiency of changed land-use patterns can be quite sensitive to climate change because profitability of alternative crops (e.g., alfalfa hay and switchgrass) may change considerably under future climate. For instance, although switchgrass is not an economically competitive option under current climatic and market conditions, it is predicted to outperform alfalfa hay under future climate, partly because switchgrass can withstand hot and dry periods (Hivrale et al., 2015), but elevated temperature and drought tend to reduce alfalfa yield (Aranjuelo et al., 2007).

Sensitivity to climate change of land-use-change strategies for dealing with nutrient pollution highlights the need for future spatial optimization studies to consider adaptive capacity of conservation actions under a changing climate. Although replacing corn-soybean rotations with alternative land-use options seems to carry greater risk of lost profits than installing CPs,

performance of land-use strategies can be improved considerably by allowing flexibility in optimized spatial configurations. Depending on the specific land use or crop suggestions for each field, some options can be more easily changed in the future. For instance, profits lost due to conversion from cropland to forest land are relatively hard to reverse because forestry requires decades to mature, but conversion among crops is much easier, given the annual nature of most field crops. We found that conversion between alfalfa hay and switchgrass can reduce profit losses significantly for the future period (Fig. 10). In addition, although crop yields were calibrated to observed yields for the current period, projections of crop responses to temperature and precipitation changes are still surrounded by large uncertainties (Lobell and Burke, 2008). These results suggest that, ideally, conservation planning should provide multiple time-frame suggestions, rather than a single solution for the future, so that spatial land-use plans can be more adaptive to changes in crop response and climate regimes.

Although field-level optimal CP and land-use options varied widely among climate change projections, there were still some common patterns. The spatial pattern of the most frequently selected options was clearly spatially clustered according to watershed characteristics. In particular, farm fields with poor drainage capacity tended to optimally receive either fertilizer reduction or switchgrass under all climate change projections. Fields with poorly drained soils typically need artificial subsurface (tile) drainage systems to support agricultural production, and traditional CPs are less effective on those fields since nutrient loss via tile flow is often not effectively treated (Lemke et al., 2011; Smith et al., 2015). Given the spatially clustered patterns, we can be more confident in the identification of the most preferable option for each sub-region.

Modeled results in this study indicate that hydrology and nutrient discharge are sensitive to forecasted future climate change, which is consistent with previous studies (Jha et al., 2006;

Shrestha et al., 2012). Although some studies have reported that nutrient discharge is likely to increase for the western Lake Erie basin under future climate (Bosch et al., 2014), our results indicate the opposite, largely due to different climate change projections used in SWAT model runs. For instance, climate-change projections employed in this study show a noticeable decrease in precipitation around October, when phosphorus fertilizer is typically applied for corn-soybean rotations. Less P losses (Fig. 6) in the fall and winter season, along with more P removal by increased crop yields, contribute partly to reduced DRP loadings under future climate conditions.

These results do not invalidate the importance of conservation actions in the future, because the reduced DRP loads we estimated are still significantly higher than what is recommended to solve water quality problems in Lake Erie. Instead, our results reconfirm the need to take aggressive conservation actions under both current and future climate, though more innovative solutions may be needed to improve cost-effectiveness of DRP reduction. Also, because climate-change projections for future decades are subject to considerable uncertainty (Hawkins and Sutton, 2009; Meehl et al., 2009), it is important to keep in mind that results of modeling studies only hold in the context of climate change projections used. While some studies predict that precipitation may increase in the future (Hayhoe et al., 2010), recent studies reported increased drought risk (Cook et al., 2015). For many regions, even the general trend in mean precipitation is uncertain (Hawkins and Sutton, 2011). In addition, studies found that assessment studies using the SWAT model is sensitive to climate change (Jha et al., 2006; Shrestha et al., 2012).

In addition to uncertainty in climate change projections, performance of alternative land-use options is also subject to changes in market prices of commodities. Optimality of alternative land-use options can be sensitive to fluctuations in agricultural returns (Johnson et al., 2012). We did not include market price scenarios in our study because it is not possible to obtain reliable

decadal price projections for field crops. Also, yield and crop changes on regional and continental scales would change the supply of certain crops, which may change market prices accordingly. In addition, we estimated the market value for switchgrass using that for grass hay, but switchgrass is not considered as a high-quality hay, and local demand for grass hay can be limited since it is closely linked to livestock production. However, demand for switchgrass may become stronger as it has been considered a potentially attractive feedstock for biofuel production (Chung et al., 2014; Schmer et al., 2008).

While we assessed the predominant land-use and –management options for reducing nutrient loadings, we did not include all possible CPs or alternative land use options in this study. For instance, Williams et al. (2015) reported that drainage water management might be a potential CP option to reduce nutrient loss via tile flow. Also, nutrient discharges are estimated at field scale, and the sum of field-level discharges is different from total watershed nutrient load, which requires a dynamic link between the SWAT model and the optimization model. Dynamic linking would require tens of thousands of simulations to trace out efficiency frontiers (Maringanti et al., 2009), but a single simulation took about three hours in this study. Insufficient computing power given the current model configuration prohibits us from employing the dynamic link strategy. The effects of CPs on nutrient reduction is expected to be lower at the watershed-scale than the field-scale, because in-stream processing may dampen the response (Bosch et al., 2014). In this case, our results provide a conservative estimate of the measures needed to reduce nutrient loads, and additional actions might be needed to achieve the same level of nutrient reduction at the watershed scale.

5 Conclusion

We assessed the performance of three alternative scenarios for spatial land-use and/or -management changes for reducing DRP load from an agricultural watershed under both current and future climate conditions using the SWAT model. We used an integrated spatial optimization model to identify optimal spatial configurations for each land-use and/or -management scenario, given field-level crop/plant yields and nutrient discharges simulated by the SWAT model, and observations of market prices and operational costs, including conservation practices, for each option. Results indicate that outcomes from the spatial optimization scenarios can be quite sensitive to projected climate changes. When optimized under current and future climate separately, optimization of either land use changes or CPs can be effective ways to achieve moderate levels of DRP reduction, and mixing of both strategies can provide noticeable additional benefits under both current and future climate. However, if performance of patterns optimized under current climate is evaluated in the context of future climate, then all three scenarios fail to remain efficient in the future. In terms of robustness of individual strategies, our results indicate that performance of optimized CPs may be more stable under future climate than optimized land-use patterns, but relying on CPs alone is not sufficient to achieve high DRP reduction targets (>60%). Land-use change, on the other hand, is capable of achieving high levels of DRP reduction, but carries greater risks of significant reduction in net profits, because yields of alternative crop/plants may change substantially under future climate conditions. Accounting for flexibility or adaptive capacity in optimized land-use patterns can improve efficiency under future climate. Future optimization studies should consider providing solutions over multiple time frames to cope with future changes more efficiently. The comparative experiments presented in this study provide input to researchers interested in choosing among

alternative spatial land-use and -management strategies to address NPS pollution from agricultural land.

Table 3.1 Characteristics of models used to generate future climate projections

Coupled Model (GCM-RCM)	General Circulation Models (GCMs)	Regional Climate Models (RCMs)	Emission Scenario	Resolution (km, lat x long)	Grids Used	Baseline Period	Future Period
CESM1-CAM5	Community Earth System Model 1.0 with CAM 5.2	NA global only	RCP 8.5	100 x 106	2	1977 – 1999	2043 – 2065
CGCM3-CRCM	Coupled Global Climate Model 3	Canadian Regional Climate Model	A2	50 x 50	5	1977 – 1999	2043 – 2065
GFDL-RCM4	Geophysical Fluid Dynamics Laboratory	Regional Climate Model V4	RCP 8.5	25 x 25	11	1977 – 1999	2043 – 2065
HADGEM-RCM4	Hadley Centre Global Environment Model 2.0 -ES	Regional Climate Model V4	RCP 8.5	25 x 25	11	1977 – 1999	2043 – 2065
GFDL-RCM3	Geophysical Fluid Dynamics Laboratory	Regional Climate Model V3	A2	50 x 50	4	1977 – 1999	2043 – 2065

Table 3.2 Comparison of average monthly precipitation in the watershed by season under the observed current (2001-2010) and the projected future (2046-2065) climate conditions.

Climate Data	Winter (mm)	Spring (mm)	Summer (mm)	Fall (mm)	Average (mm)
Observed Climate					
2001-2010	70.52	110.54	101.89	81.40	91.09
Projected Climate					
CESM1(GCM)	75.57	120.48	111.07	72.19	94.83
CGCM3-CRCM	69.10	115.04	92.34	86.39	90.72
GFDL-RCM4	72.65	126.70	80.29	68.13	86.94
HadGEM-RCM4	70.96	113.10	110.82	78.68	93.39
GFDL-RCM3	63.82	114.49	106.90	70.66	88.97

Table 3.3 Comparison of SWAT simulated average monthly surface runoff by season under the observed current (2001-2010) and the projected future (2046-2065) climate conditions.

Climate Data	Winter (mm)	Spring (mm)	Summer (mm)	Fall (mm)	Average (mm)
Observed Climate					
2001-2010	27.41	7.08	7.41	13.92	13.96
Projected Climate					
CESM1(GCM)	15.56	8.44	9.72	5.22	9.74
CGCM3-CRCM	17.30	7.36	5.05	10.58	10.07
GFDL-RCM4	19.36	11.77	3.76	5.56	10.11
HadGEM-RCM4	16.42	6.94	9.60	6.99	9.99
GFDL-RCM3	14.22	7.55	8.71	5.44	8.98

Table 3.4 Comparison of SWAT simulated average monthly water percolation past bottom of soil profile by season under the observed current (2001-2010) and the projected future (2046-2065) climate conditions.

Climate Data	Winter (mm)	Spring (mm)	Summer (mm)	Fall (mm)	Average (mm)
Observed Climate					
2001-2010	12.56	21.39	3.78	5.84	10.89
Projected Climate					
CESM1(GCM)	18.14	24.04	6.26	10.91	14.84
CGCM3-CRCM	15.01	22.11	3.72	11.79	13.16
GFDL-RCM4	11.29	25.78	3.49	4.56	11.28
HadGEM-RCM4	16.47	21.51	6.06	12.32	14.09
GFDL-RCM3	13.00	22.37	5.23	9.56	12.54

Table 3.5 Comparison of SWAT simulated average annual watershed level total phosphorus (TP), dissolved reactive phosphorus (DRP), total nitrogen (TN) and sediment load under the observed current (2001-2010) and the projected future (2046-2065) climate conditions.

Climate Data	TP(Mt/yr)	DRP (Mt/yr)	TN(Mt/yr)	Sediment(10^3Mt/yr)
Observed Climate				
2001-2010	312.55	63.46	8599.49	260.03
Projected Climate				
CESM1(GCM)	235.11	54.21	7066.38	224.15
CGCM3-CRCM	237.42	55.82	6867.26	208.57
GFDL-RCM4	251.38	56.33	7561.95	233.24
HadGEM-RCM4	231.82	53.77	6806.24	213.24
GFDL-RCM3	216.30	52.15	6844.52	201.79

Table 3.6 Robustness of CP and land-use optimizations, reported as percentage of area fields receiving a given treatment under current climate conditions that are different when optimized for future climate.

CP and land-use options	Area adopted under current climate	% of fields changed from current optimal option to a different option under optimizations based on future climate projections				
	(km2)	GDFL-RCM	CGCM3-CRCM	GFDL-RCM3	HADGEM-RCM4	CESM1
Switchgrass	157.1	7.7	24.1	31.9	1.2	1.0
Alfalfa	455.6	100.000	100.0	99.9	100.0	100.0
Residential	10.0	21.8	23.6	12.9	22.9	23.5
Forest	631.4	88.3	36.6	36.9	97.8	98.3
CRP	7.5	65.9	29.6	26.1	55.5	73.4
Filter strips	1083.8	71.7	98.6	72.6	99.9	100.0
-20% fertilizer	347.6	23.2	49.6	33.9	38.5	31.7

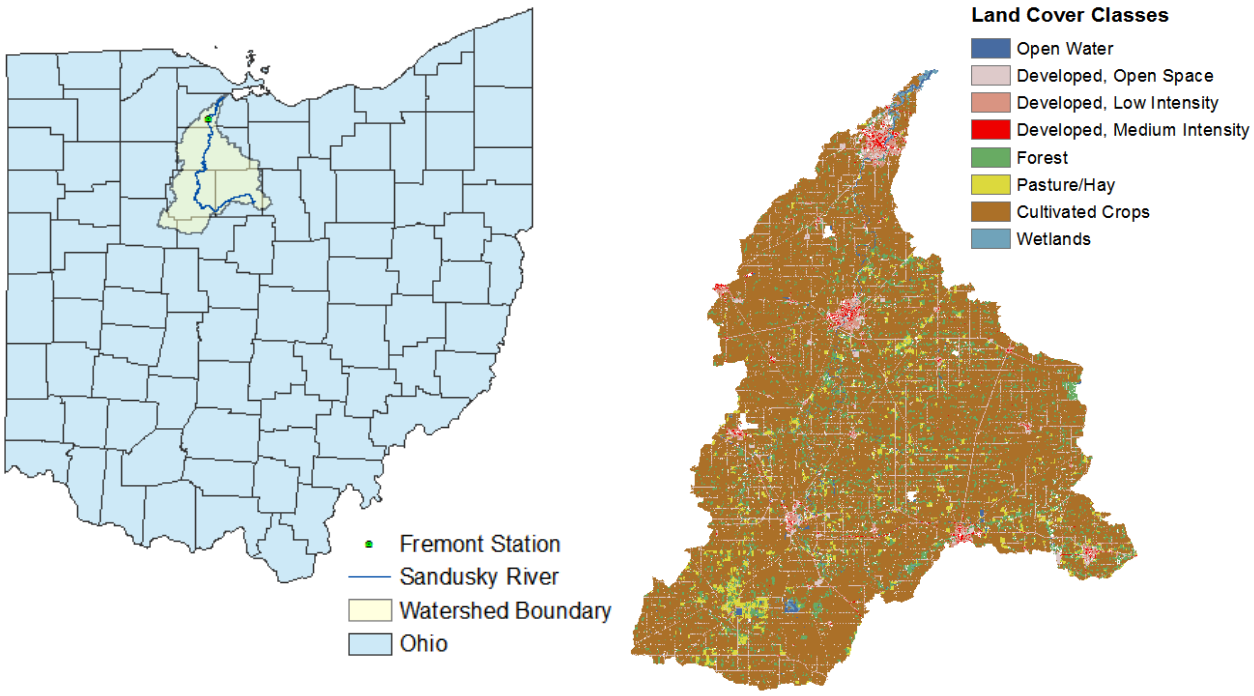

(a) (b)

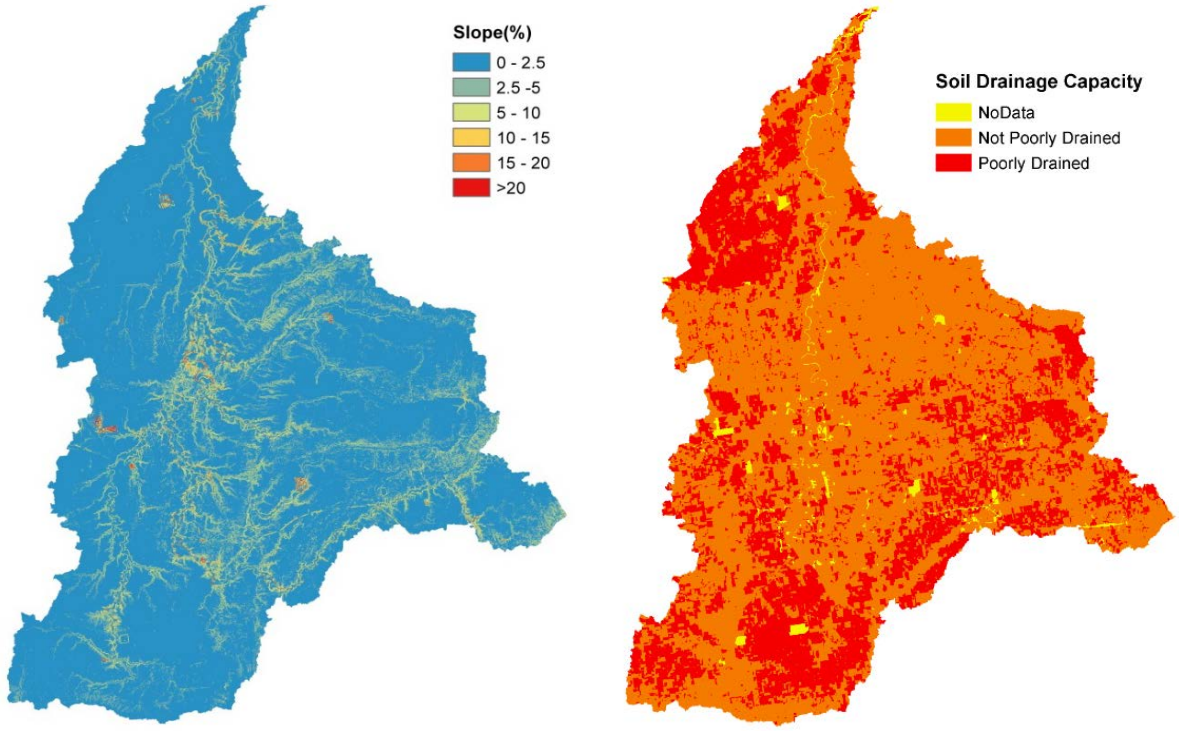

(c) (d)

Figure 3.1 Sandusky River watershed: (a) location of the watershed in Ohio; (b) land cover/use in 2006 (Jin et al., 2013b); (c) slope; and (d) soil-drainage capacity(USDA NRCS, 2015a).

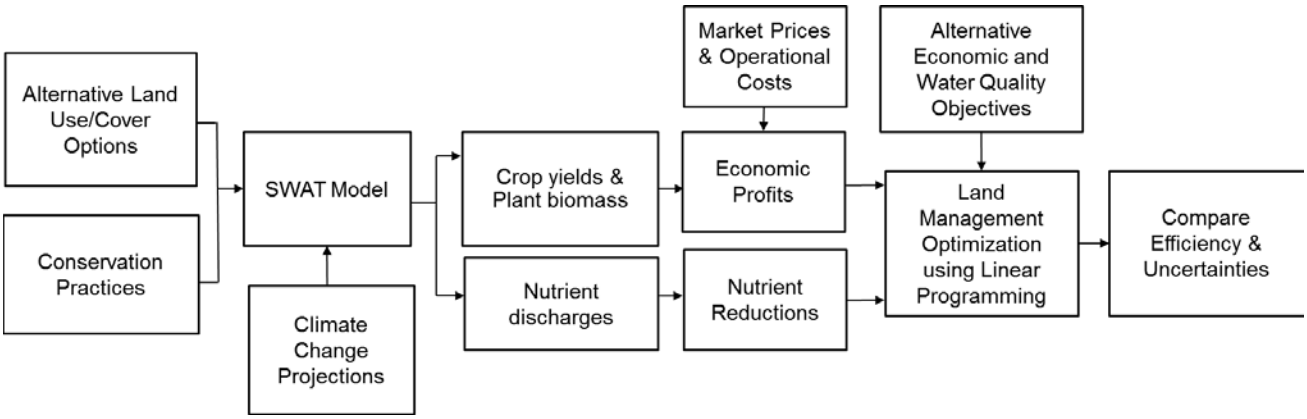

Figure 3.2 Overall Simulation Framework

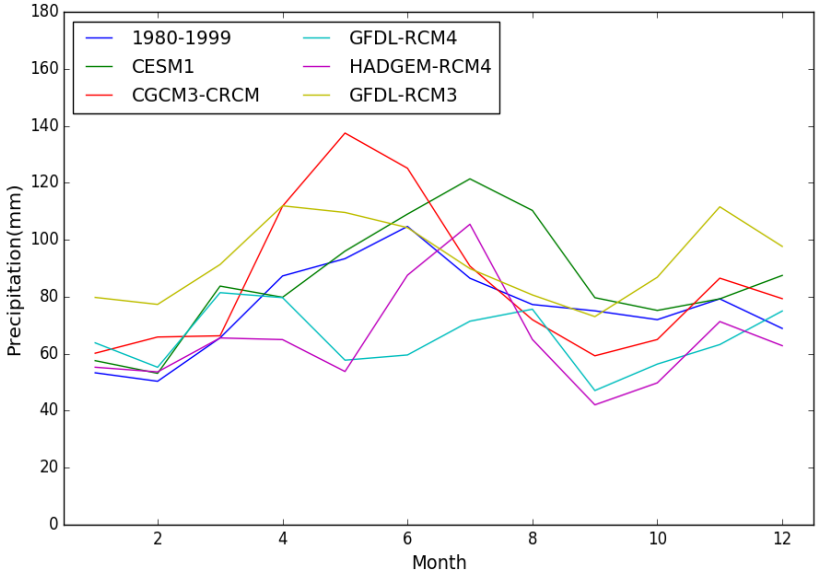

(a)

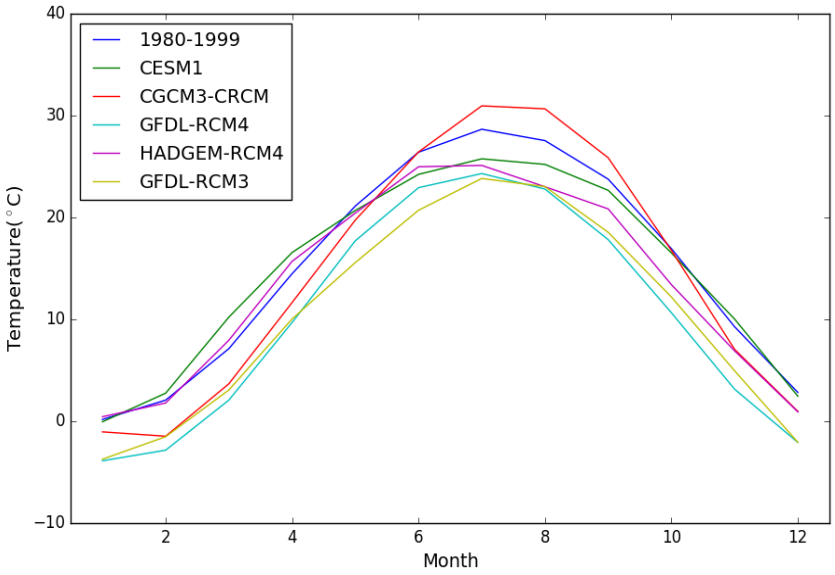

(b)

Figure 3.3 Comparison of average monthly (a) precipitation and (b) mean maximum temperature by month for both observed baseline (1980-1999) and future (2046-2065) periods. Precipitation and temperature datasets for future period were projected by five different GCM/RCM model sets (Table 1).

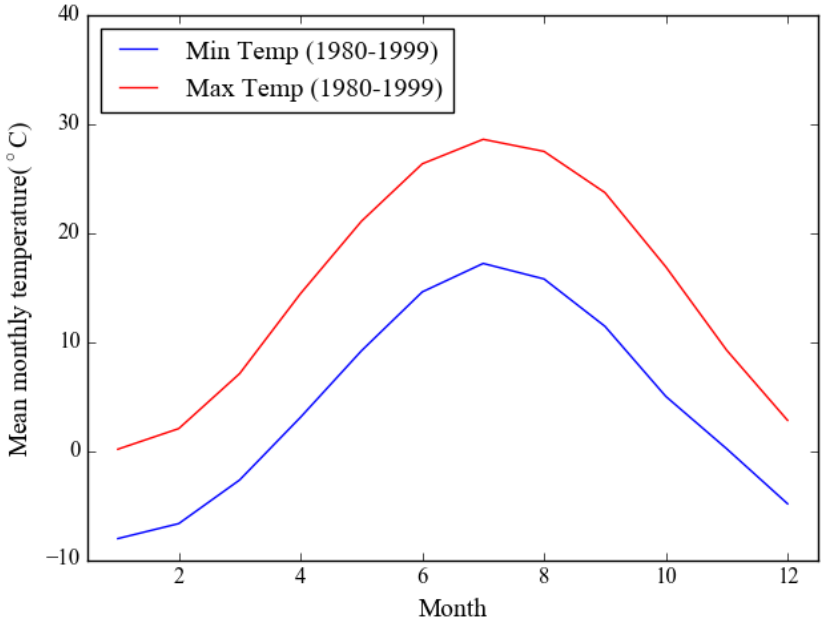
Min Temp (1980-1999)
Max Temp (1980-1999)
Mean monthly temperature(° C)
Month
40
30
20
10
0
−10
2
4
6
8
10
12

(a)

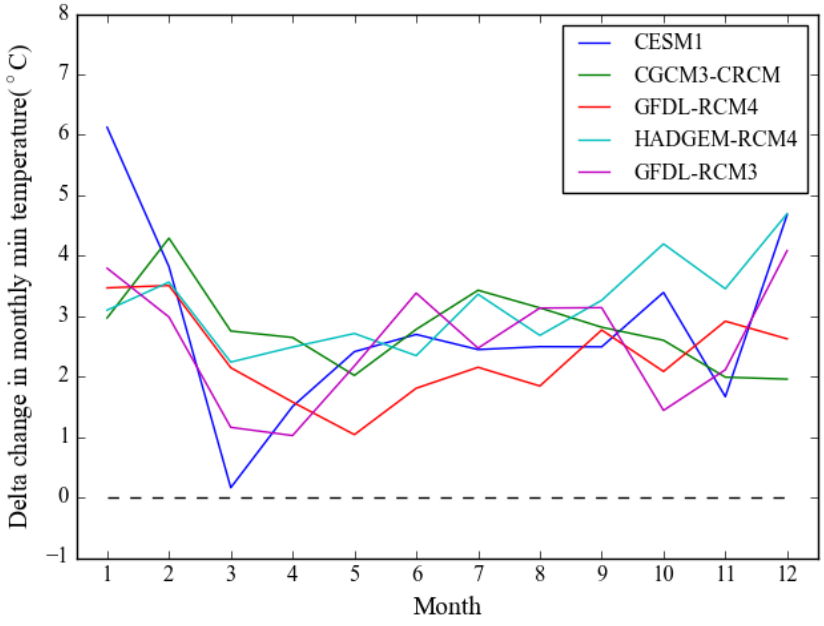
CESM1
CGCM3-CRCM
GFDL-RCM4
HADGEM-RCM4
GFDL-RCM3
Delta change in monthly min temperature(° C)
Month
8
7
6
5
4
3
2
1
0
−1
1
2
3
4
5
6
7
8
9
10
11
12

(b)

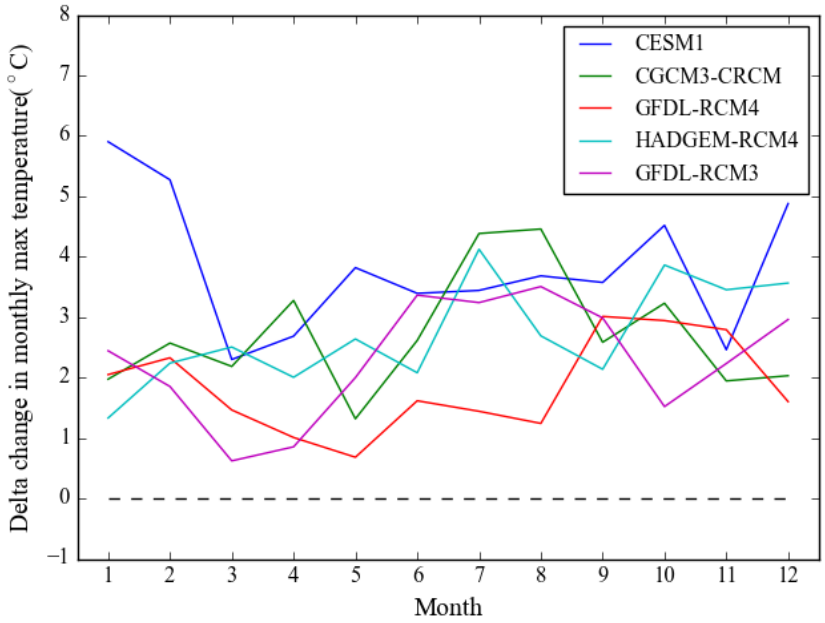

(c)

Figure 3.4 Deviations (‘delta’) between (a) the observed baseline (1980-1999) and (b) the projected future (2046-2065) mean maximum daily temperature and (c) minimum daily temperature by month for each CGM/RCM projection.

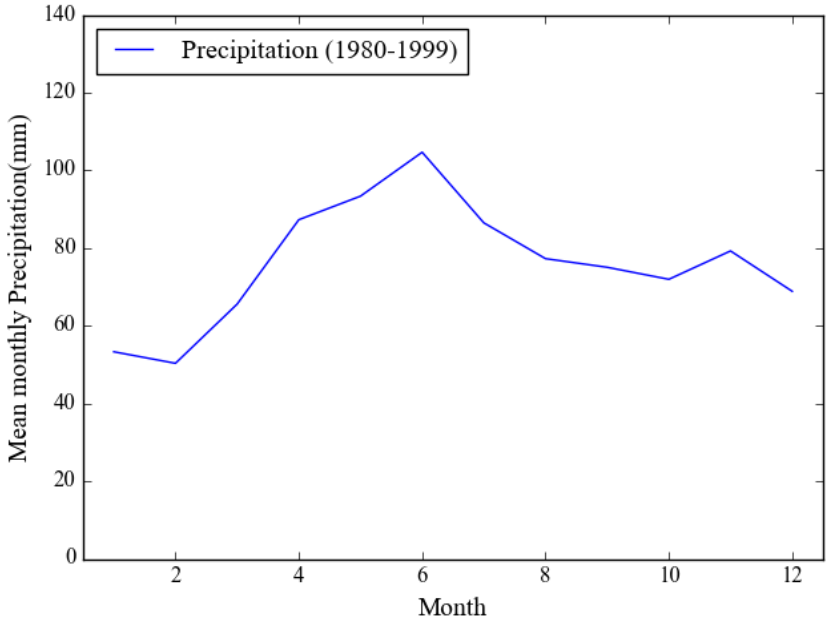

(a)

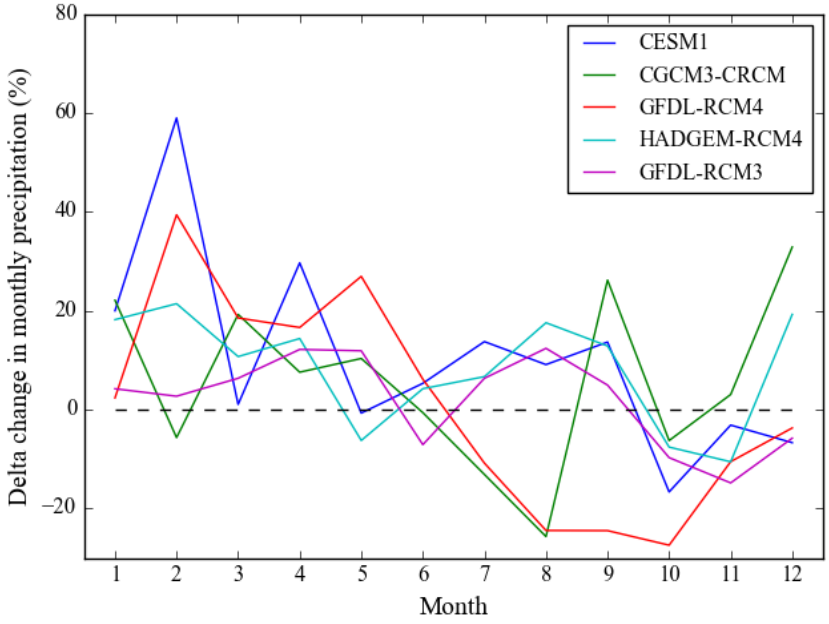

(b)

Figure 3.5 Observed mean monthly precipitation for the baseline (1980-1999) period (a) and (b) percentage of change (‘delta’) in monthly precipitation between the future and baseline periods for each bias-adjusted GCM/RCM projection.

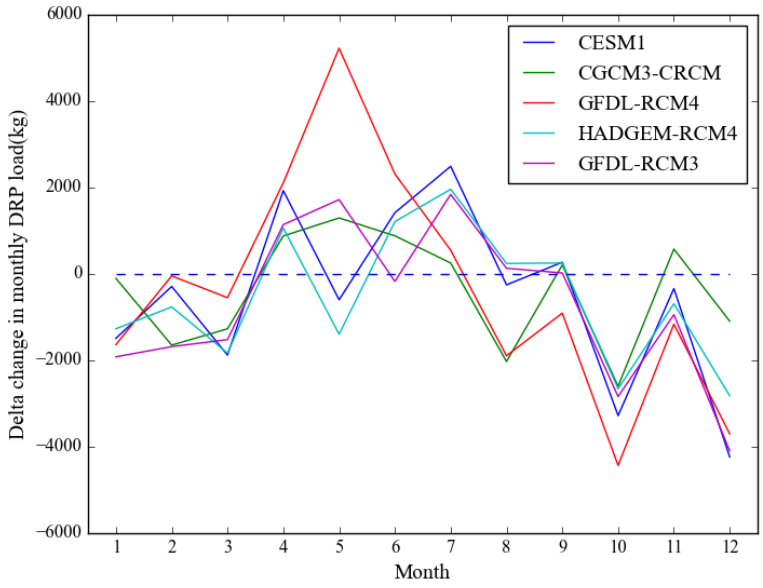

Figure 3.6 Deviations (‘delta’) of SWAT simulated monthly watershed level DRP loading between the observed current (2001-2010) and the future (2046-2065) periods by GCM/RCM projections.

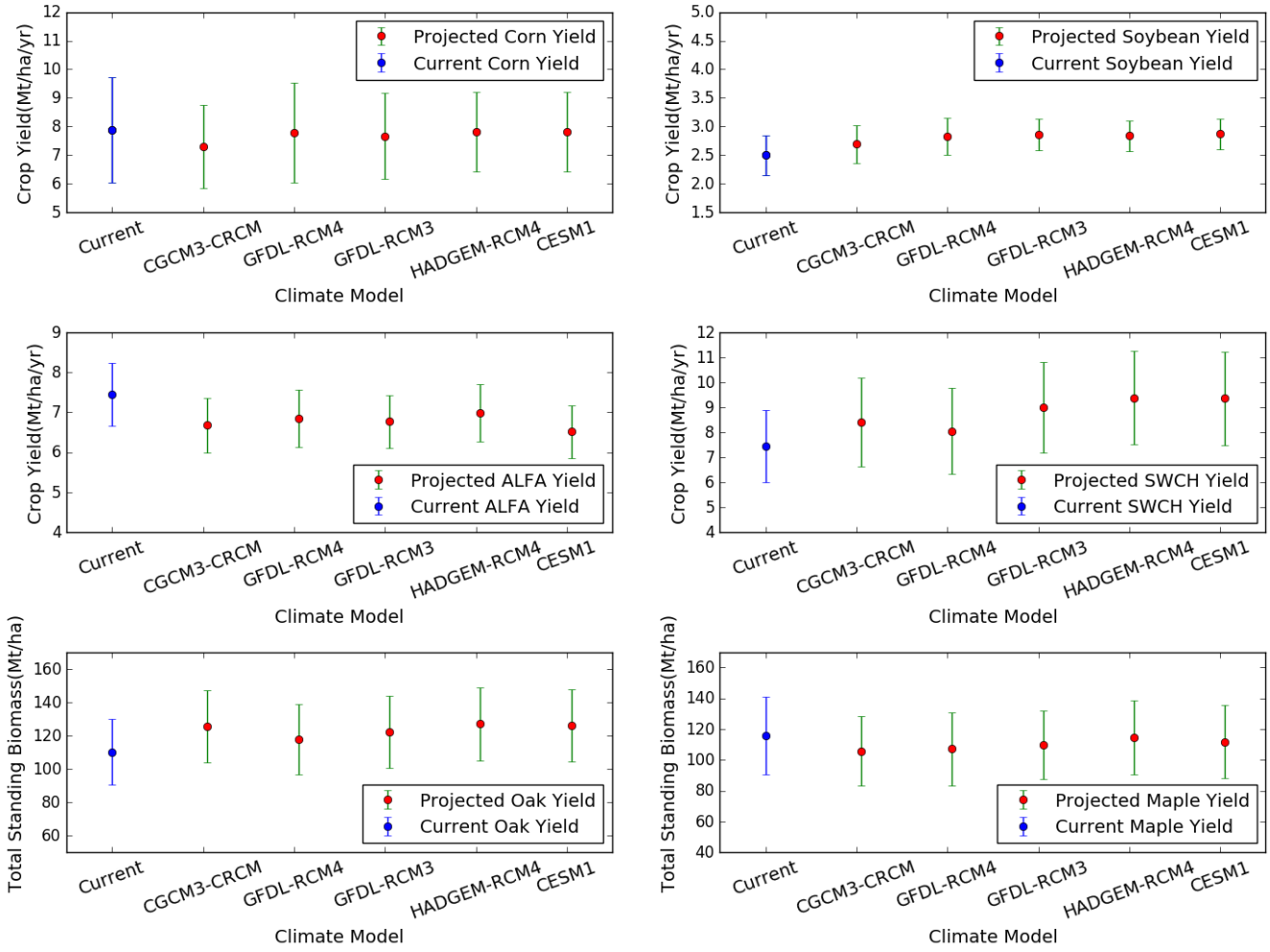

Figure 3.7 Annual crop yields and total biomass for forests with a 30-year standing age (means and standard deviations) for the observed historical (2001 to 2010) and the future (2046-2065 for field crops and 2046-2075 for forest) periods, estimated using the SWAT model.

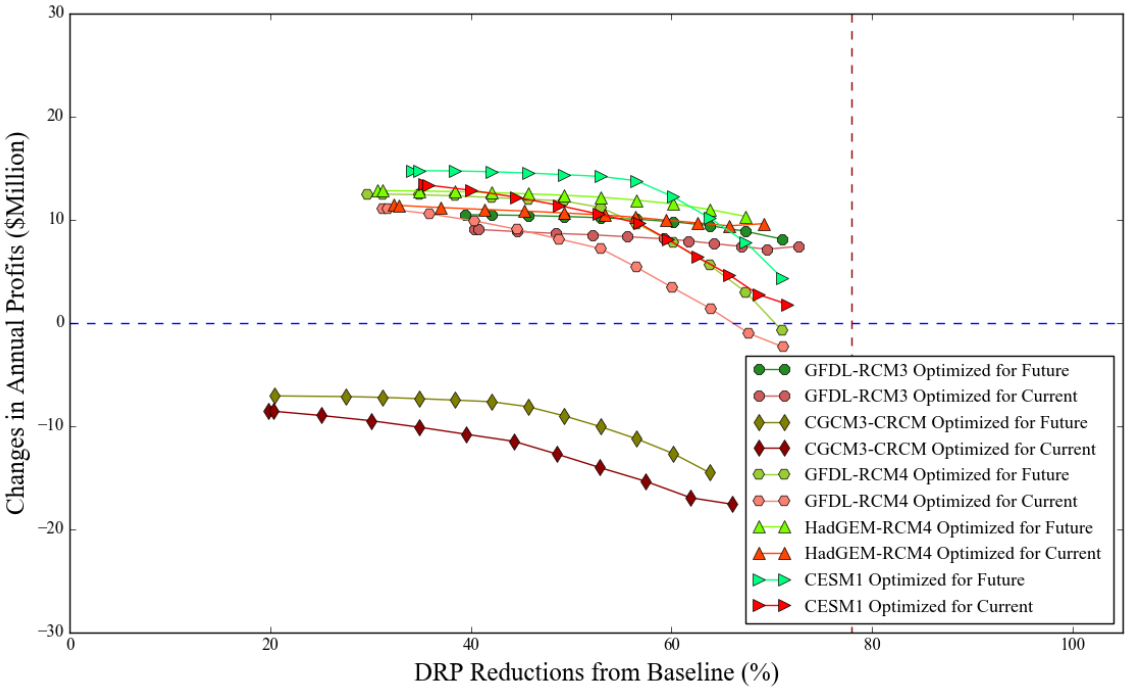
Changes in Annual Profits ($Million)
DRP Reductions from Baseline (%)
GFDL-RCM3 Optimized for Future
GFDL-RCM3 Optimized for Current
CGCM3-CRCM Optimized for Future
CGCM3-CRCM Optimized for Current
GFDL-RCM4 Optimized for Future
GFDL-RCM4 Optimized for Current
HadGEM-RCM4 Optimized for Future
HadGEM-RCM4 Optimized for Current
CESM1 Optimized for Future
CESM1 Optimized for Current

(a)

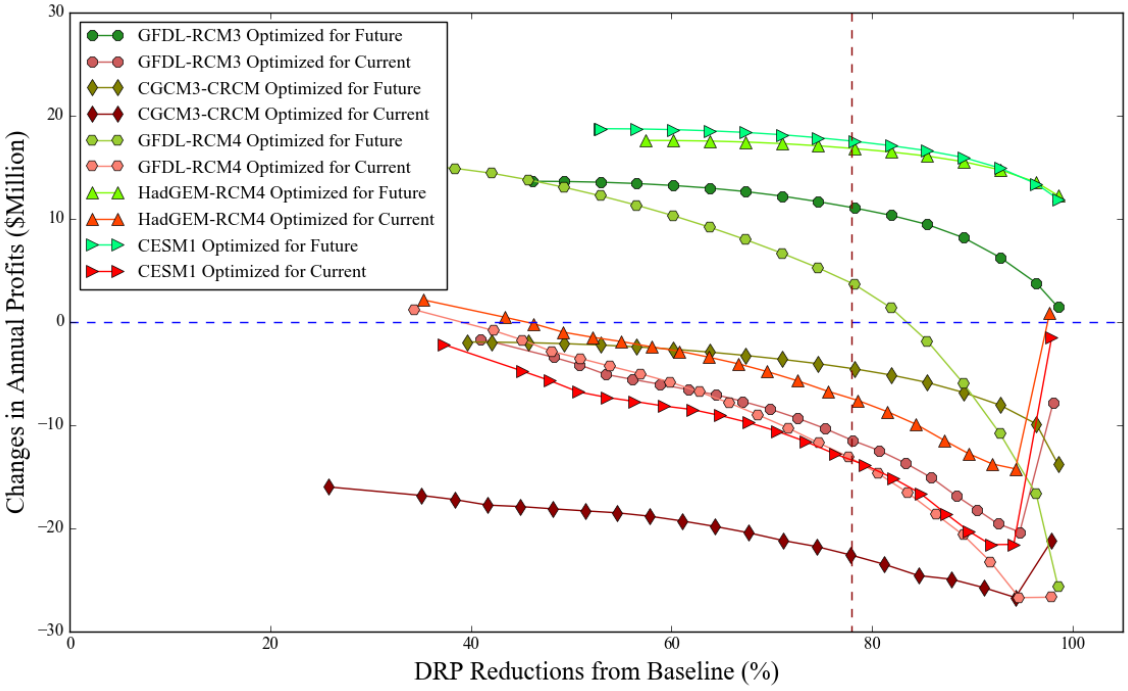
Changes in Annual Profits ($Million)
DRP Reductions from Baseline (%)
GFDL-RCM3 Optimized for Future
GFDL-RCM3 Optimized for Current
CGCM3-CRCM Optimized for Future
CGCM3-CRCM Optimized for Current
GFDL-RCM4 Optimized for Future
GFDL-RCM4 Optimized for Current
HadGEM-RCM4 Optimized for Future
HadGEM-RCM4 Optimized for Current
CESM1 Optimized for Future
CESM1 Optimized for Current

(b)

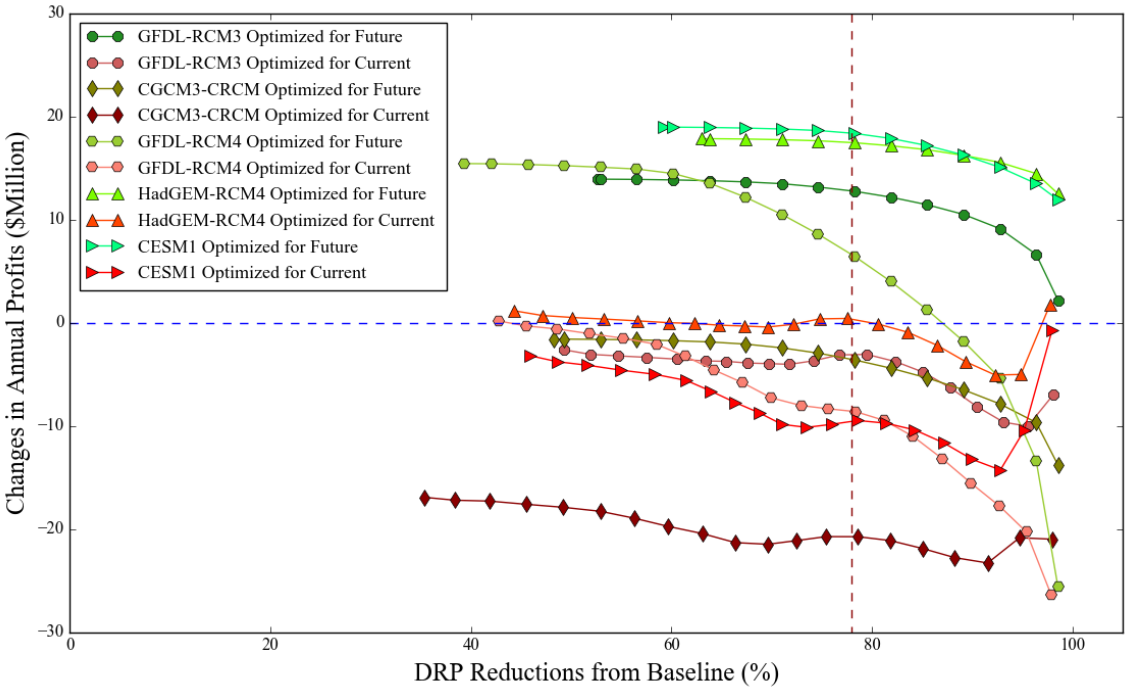

(c)

Figure 3.8 Comparison of DRP-reduction efficiency under future (2046-2065) climate for spatial land-use and -management patterns optimized under both current (2001-2010) and future (2046-2065) climate conditions, based on (a) the CP targeting, (b) the land-use-change optimization and (c) the combination of both strategies. The baseline for each optimized pattern shares the same land-use scenario, assuming corn-soybean rotations with no conservation practices on all agricultural land. The DRP target (dashed line) represents a 78% reduction in DRP from current average load level.

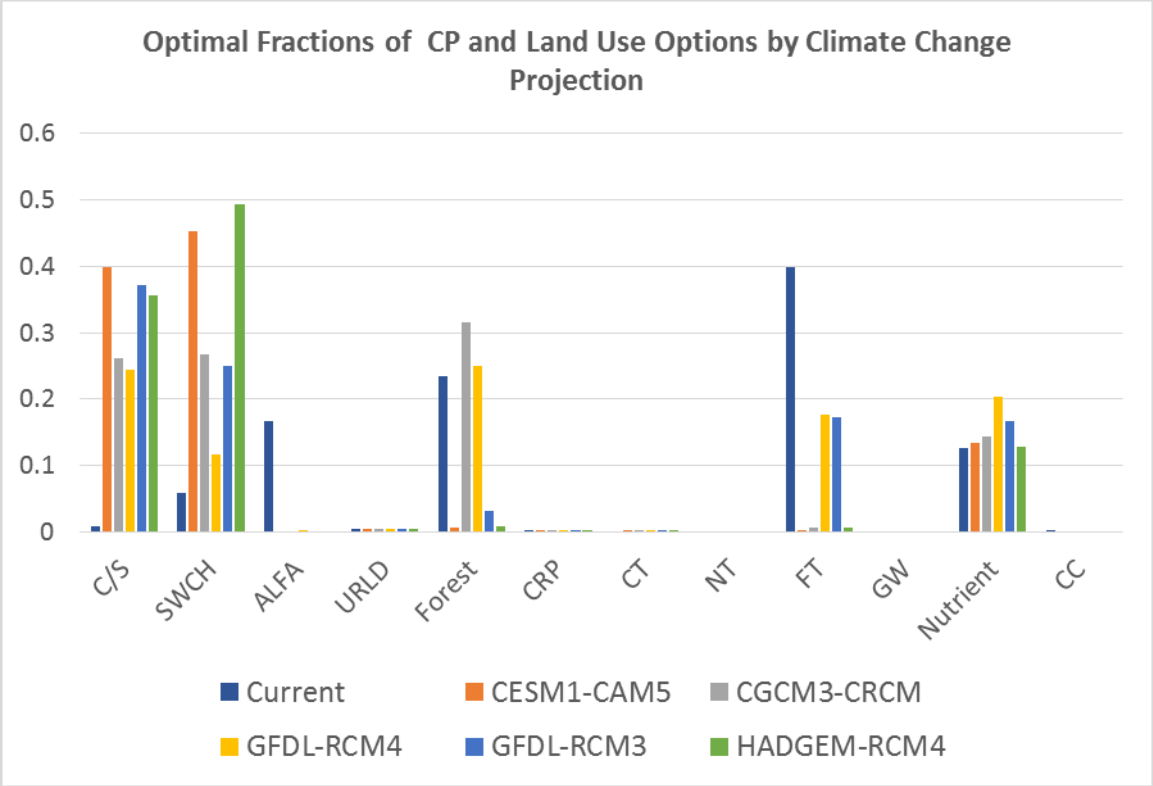

Figure 3.9 Fractions of CP and Land Use Options of Optimized Plans based on the Mixing Scenario and 78% DRP Reduction from Current Average Load for both Current (2001-2010) and Future (2046-2065) Periods.

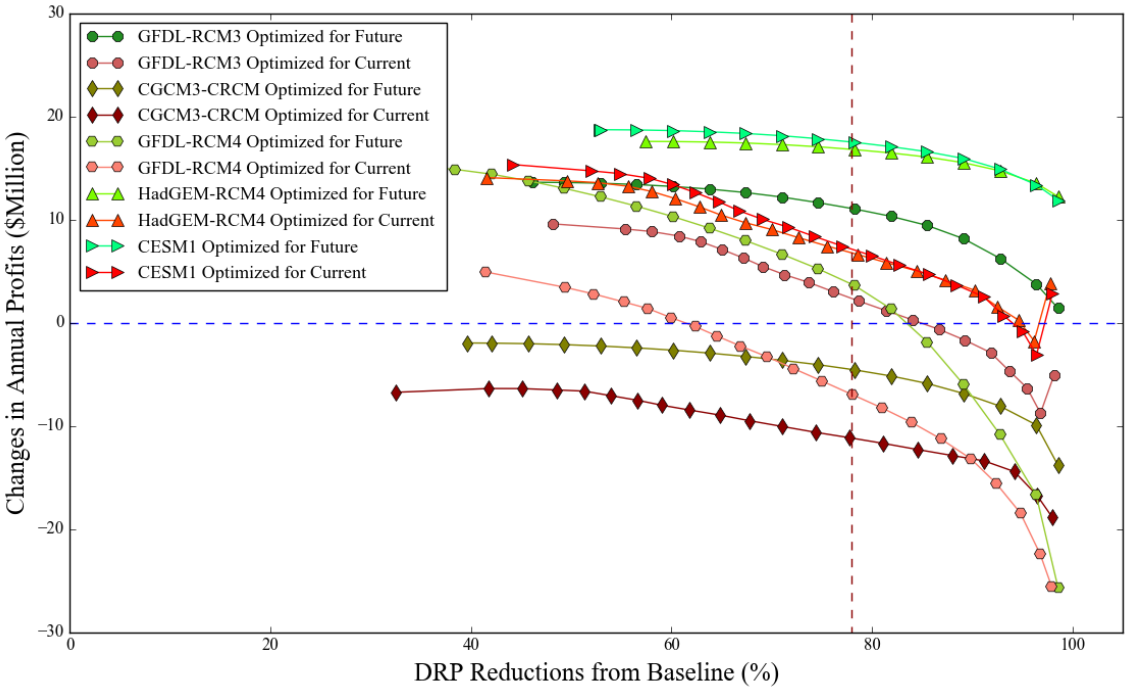

(a)

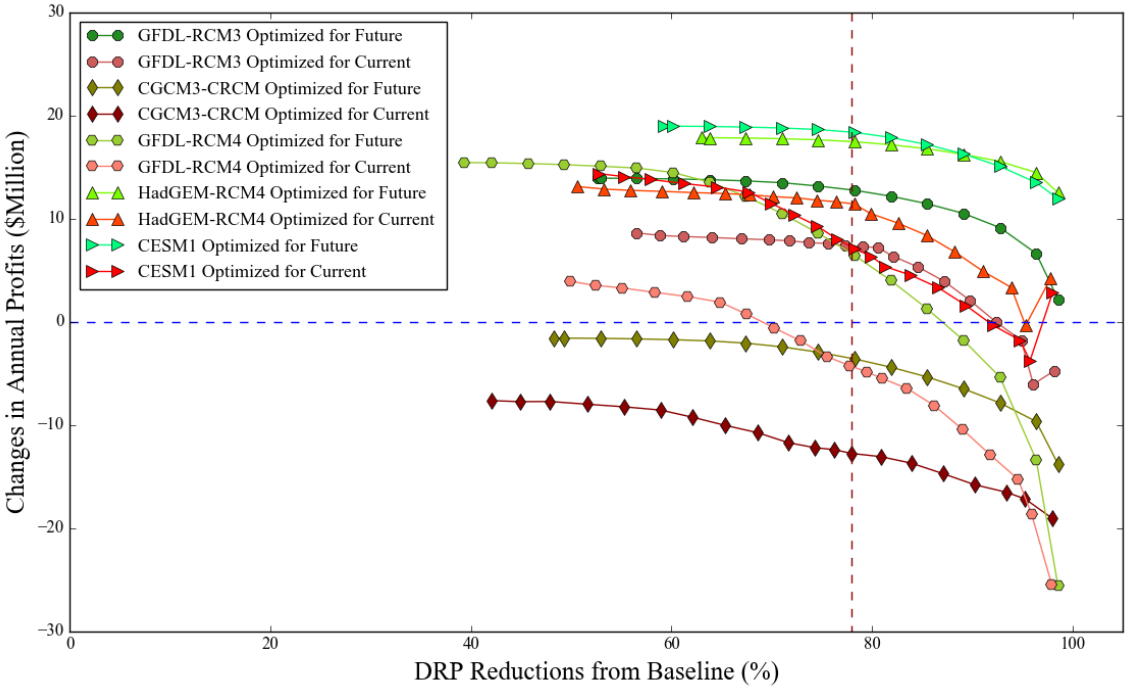

(b)

Figure 3.10 Comparison of DRP-reduction efficiencies under future (2046-2065) climate conditions for spatial patterns optimized under both current (2001-2010) and future (2046-2065)

climate conditions, based on (a) the land-use change optimization and (b) the combination of CP targeting and land-use change strategies. The analysis is the same as that for Fig. 8, except that all alfalfa hay fields in current optimal plans were converted to switchgrass for the future period. The baseline for each climate change projection shares the same land use scenario, assuming corn/soybean rotations for all agricultural land; DRP target dashed line represents a 78% reduction in DRP from current average load level.

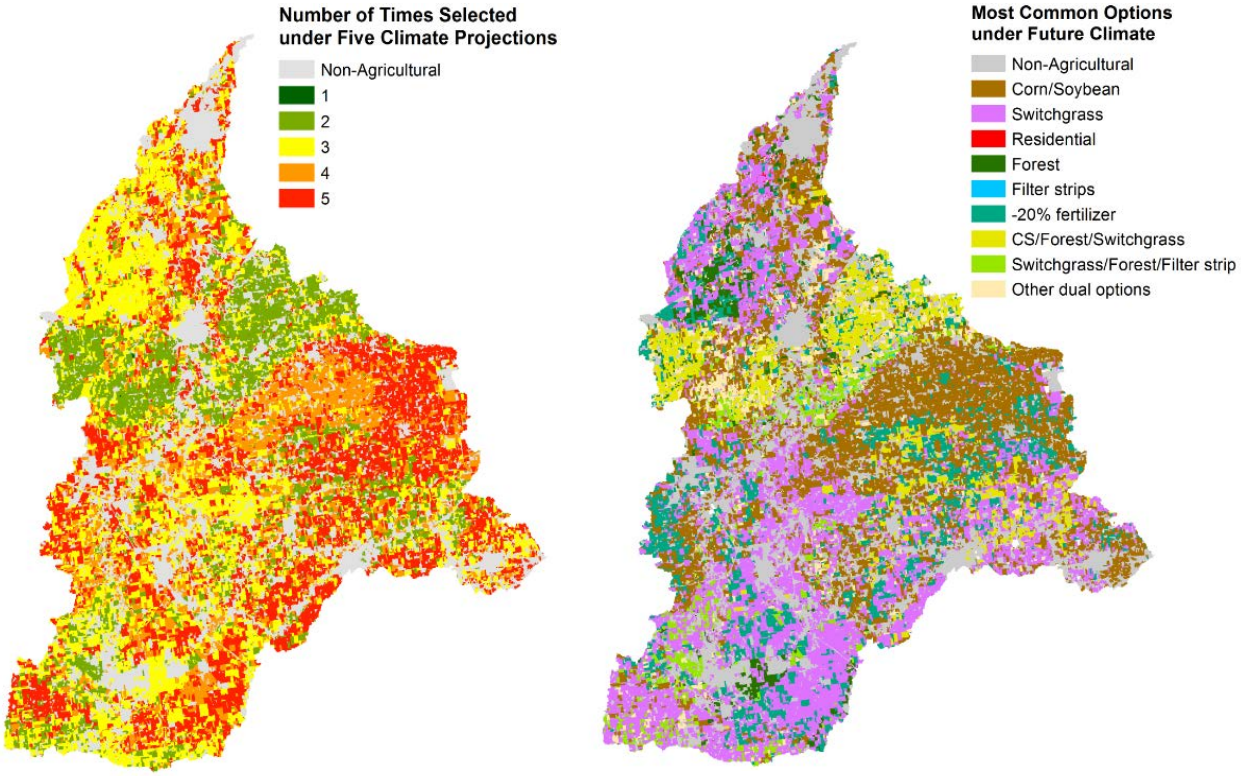

(a) (b)

Figure 3.11 Robustness of spatial patterns of land-use and -management options across climate conditions: (a) number of times the most common option at each field occurs across five future climate-change projections and (b) the most frequently selected option or combination of options at each field.

Chapter 4
Conclusions

The dissertation includes three computational studies that improve (a) the ability of land-change modelers to provide reliable future projections of land-cover change, (b) understanding of how alternative spatial land-use and -management strategies can reduce NPS pollution effectively and efficiently, and (c) robustness of spatial land optimization approaches under a changing climate.

The first chapter addressed a fundamental question for LCM modeling: how do alternative approaches to defining spatial land units affect the output from a given LCM? I developed an innovative modeling approach that can handle both pixel and polygonal land units, and the ability to include parcel subdivision scenarios so that polygonal boundaries can be updated over time. For each parcel subdivision scenario, the same parcelization schemes were applied to all parcels. The results demonstrate a clear tradeoff between the goal of accurate location of land-cover changes, which is more easily achieved with the pixel-based approach, and accurate reproduction of the spatial patterns of land-cover change, which is more easily achieved with the polygonal approach.

The analysis pointed towards opportunities for future research on the polygon-based approach to modeling. The simple parcel subdivision process we used kept the model efficient, but may have limited model performance. For instance, figure of merit (FoM) scores suggest that suitability of parcel subdivision scenario depended on the type of land-cover transition and the resolution at which the validation was performed. At the resolution of 64 pixels, the equal_2 scenario was

found to work well for modeling the transition of agriculture and forest land to developed land, but equal_6 was found to outperform other scenarios for modeling agriculture to developed land transition. For future study, the modeling approach could be improved by replacing the uniform parcel subdivision scenario with a mixing of multiple parcelization configurations and allow the LCM to select suitable configurations for each parcel, depending on local geographic characteristics and the type of land-cover transition to be modeled. Also, to make the parcel subdivision process more realistic, it would be helpful to include road networks and make sure all new parcels have road access. Furthermore, it is well known that some LCMs may be sensitive to the size of cells. It would be interesting to evaluate how trade-offs between pixel and polygonal land units might be changed when pixel-based simulations are run at multiple coarser resolutions.

In the second chapter, I developed the first integrated modeling approach that compares the relative economic efficiency of alternative spatial land-use and -management strategies for addressing NPS pollution from agricultural land. Evaluating the tradeoffs in the performance of land-use versus land-management tools for reducing nutrient pollution can provide valuable guidance for future planning because financial resources for conservation efforts are limited and prioritization is needed. Using the Sandusky watershed as an example, simulation results indicated that relying on traditional agricultural CPs is neither sufficient nor the most efficient strategy to meet policy goals on P reductions. Integrating land-use-change strategies into conservation planning can help not only overcome limitations of CPs on improving water quality, but also improve economic returns.

Estimated conservation efforts in this study tend to be optimistic, because field-of-edge estimation does not take into consideration in-stream processing of nutrients and lag time in

response to actions to change management or land use. When nutrient transport processes beyond fields are considered, it is expected that the effect of spatially optimized CPs on P reduction will be less effective (Bosch et al., 2014; Tuppad et al., 2010). Estimates of nutrient loading at the watershed outlet require a dynamic link between the watershed model and the optimization model, so that the effect of each candidate CP or land-use change can be propagated through to the watershed outlet. Obtaining the efficiency frontiers using the dynamic link would require thousands of runs, but a single simulation took about three hours because HRUs were set up at field scale. With the current model formulation and implementation, it would take decades to estimate the efficiency frontiers. However, it is possible for future research to parallelize the SWAT model for use on high performance computers, so as to improve its computational efficiency at the field scale, and significantly reduce model simulation times.

Although observed market prices and costs related to crops and forest production, including conservation practices, were used to estimate economic returns of alternative land-use and -management options, feedbacks between changes in supply and demand, and consequent market prices, were not included in the optimization framework. For the Sandusky river watershed, optimized plans involved converting approximately 17% of corn-soybean fields to alfalfa hay production in order to achieve 78% DRP reductions, but increased alfalfa hay production may result in lower hay prices in the region if demand does not increase accordingly. To more robustly evaluate the impact of spatial land management strategies, future studies aiming at larger study areas should consider interactions between land-use change and market prices. There are multiple approaches to including these interactions. For instance, it is possible to predict price changes using regression models. A likely more robust method is to link land-use change outcomes with a computable general equilibrium model (CGE), because GCE models

capture a wider set of economic interactions associated with the implementation of a spatial land-use change and -management plan.

An important factor affecting implementation of proposed optimal plans for land use and management is farmers' attitudes toward alternative conservation plans. Successfully implementing conservation plans requires not only reliable scientific information, but also farmers' active participation. Although economic incentives were calculated in this study to reflect P abatement costs, adoption of conservation practices is a multidimensional choice involving individual farmers' preferences. An important complementary study is needed to investigate differences in famers' attitudes toward alternative land-use and –management options. For instance, would land-use change options require greater economic incentives than CP targeting because land-use change options carry greater risks of lost profits? Would a program similar to ARC/PLC increase farmers' willingness to accept land-use-change options? To answer these questions would require further research that may involve interviews, econometric modeling, and perhaps agent-based modeling to reflect the effects of variations in individual preferences.

In the third chapter, I found that the effectiveness and efficiency of spatially optimized land-use and -management patterns can be quite sensitive to climate change, because changed temperature and precipitation patterns affect both plant/crop yields and nutrient discharge. In particular, the economic performance of CPs was found to be more robust than land-use changes at given levels of nutrient reduction, largely because corn-soybean yields were projected to be stable under future climate, whereas yields of alternative crops were projected to change significantly in the future. Although a strategy based on land-use change seems carry greater risk of lost profits than

installing CPs, integration of both strategies is still needed to achieve stated policy goals for DRP reductions.

Sensitivity to climate change of land-use-change strategies for dealing with nutrient pollution highlights the need for future spatial optimization studies to consider the adaptive capacity of conservation actions under a changing climate. My findings illustrate how the performance of land-use strategies can be improved considerably by allowing flexibility in optimized spatial configurations. For instance, conversion between alfalfa hay and switchgrass can reduce loss of profits significantly for the future period. These results suggest that future optimization studies should evaluate solutions over multiple time frames to cope with future changes more efficiently. Instead of providing a single solution for the next decades, it is preferable to design an adaptive conservation plan that allows land-use and -management options to be updated over time. For instance, if climate change information is available over time, then biophysical models can be used to estimate how crop yields and nutrient discharges would change over time. If conversion between two land-use or -management options cannot be completed easily, then calculation of profits needs to include conversion costs (e.g., site preparation). It is expected that optimal spatial patterns of land-use and -management options will vary over time, and the optimization model needs to consider total benefits over multiple time frames. Researchers may still need to balance short-term versus long-term benefits, and popular valuation methods like discounting future revenues can be helpful for this purpose.

In addition to climate change, uncertainties in market prices may also affect the economic performance of alternative land-use and -management options significantly. Future market price scenarios were not included in this study because it is impossible to obtain reliable decadal price projections for field crops. Still, future studies should include sensitivity analysis to price

fluctuations, along with climate change, to provide a more complete analysis of robustness of spatial land-use and -management options under future climate and market conditions.

Climate-change projections for future decades are subject to considerable uncertainty, and this uncertainty was not fully assessed in this study. For instance, in addition to high CO_2 emission scenarios (A2 and RCP 8.5), future studies should include other emission scenarios to evaluate how performance of optimization of CPs and/or land-use changes may vary under different CO_2 emission scenarios. Because outputs from climate models typically need some form of bias correction to be applied in hydrological modeling studies, I employed the 'delta-change method.' Several other methods exist, including multiple linear regression, local intensity scaling and distribution mapping. For future study, it would be interesting to investigate how alternative downscaling algorithms affect outcomes of spatial optimization studies, given the same set of climate change projections.

Finally, I did not include all possible CPs or alternative land-use options in this study. For instance, a key factor limiting the effectiveness of CPs for reducing DRP loading is the presence of tile drainage system, because traditional CPs target surface flows. Recent studies suggested that drainage water management might be an effective approach to addressing nutrient load via tile flows. Future studies should include more innovative land-use and -management options in the optimization modeling framework to better understand the potential efficiency of CPs versus land-use change for improving water quality to meet policy goals

References

Alexandridis, K., Pijanowski, B.C., 2007. Assessing multiagent parcelization performance in the MABEL simulation model using Monte Carlo replication experiments. Environment and Planning B: Planning and Design 34, 223–244. doi:10.1068/b31181

Arabi, M., Frankenberger, J.R., Engel, B.A., Arnold, J.G., 2008. Representation of agricultural conservation practices with SWAT. Hydrological processes 22, 3042–3055.

Arabi, M., Govindaraju, R.S., Hantush, M.M., 2006. Cost-effective allocation of watershed management practices using a genetic algorithm. Water Resources Research 42.

Aranjuelo, I., Irigoyen, J.J., S??nchez-D??az, M., 2007. Effect of elevated temperature and water availability on CO2 exchange and nitrogen fixation of nodulated alfalfa plants. Environmental and Experimental Botany 59, 99–108. doi:10.1016/j.envexpbot.2005.10.008

Arnold, J.G., Gassman, P.W., White, M.J., 2010. New Developments in the SWAT Ecohydrology Model, in: 21st Century Watershed Technology: Improving Water Quality and Environment. pp. 21–24.

Arnold, J.G., Srinivasan, R., Muttiah, R.S., Williams, J.R., 1998. Large area hydrologic modeling and assessment part I: model development. Journal of the American Water Resources Association 34, 73–89. doi:10.1111/j.1752-1688.1998.tb05961.x

Ballestores Jr., F., Qiu, Z.Y., 2012. An integrated parcel-based land use change model using cellular automata and decision tree. Proceedings of the International Academy of Ecology and Environmental Sciences.

Balmford, A., Fisher, B., Green, R.E., Naidoo, R., Strassburg, B., Turner, R.K., Rodrigues, A.S.L., 2011. Bringing ecosystem services into the real world: An operational framework for assessing the economic consequences of losing wild nature. Environmental and Resource Economics 48, 161–175. doi:10.1007/s10640-010-9413-2

Basile, S.., Rauscher, S.A., Steiner, A.L., n.d. Projected precipitation changes within the Great Lakes and Western Lake Erie Basin: A multi-model analysis of intensity and seasonality. International Journal of Climatology.

Baskaran, L., Jager, H., Schweizer, P., Srinivasan, R., 2010. Progress toward Evaluating the Sustainability of Switchgrass as a Bioenergy Crop using the SWAT Model. Transactions Of The ASABE 53, 1547–1556. doi:10.13031/2013.34905

Bateman, I.J., Harwood, A.R., Mace, G.M., Watson, R.T., Abson, D.J., Andrews, B., Binner, A., Crowe, A., Day, B.H., Dugdale, S., Fezzi, C., Foden, J., Hadley, D., Haines-Young, R., Hulme, M., Kontoleon, A., Lovett, A. a, Munday, P., Pascual, U., Paterson, J., Perino, G.,

Sen, A., Siriwardena, G., van Soest, D., Termansen, M., 2013. Bringing ecosystem services into economic decision-making: land use in the United Kingdom. Science (New York, N.Y.) 341, 45–50. doi:10.1126/science.1234379

Bhattarai, R., Kalita, P.K., Patel, M.K., 2009. Nutrient transport through a Vegetative Filter Strip with subsurface drainage. Journal of Environmental Management 90, 1868–1876. doi:10.1016/j.jenvman.2008.12.010

Boegman, L., Loewen, M.R., Culver, D.A., Hamblin, P.F., Charlton, M.N., 2008. Spatial-dynamic modeling of algal biomass in Lake Erie: relative impacts of dreissenid mussels and nutrient loads. Journal of Environmental Engineering 134, 456–468.

Bosch, N.S., Allan, J.D., Dolan, D.M., Han, H., Richards, R.P., 2011. Application of the Soil and Water Assessment Tool for six watersheds of Lake Erie: Model parameterization and calibration. Journal of Great Lakes Research 37, 263–271. doi:10.1016/j.jglr.2011.03.004

Bosch, N.S., Allan, J.D., Selegean, J.P., Scavia, D., 2013. Scenario-testing of agricultural best management practices in Lake Erie watersheds. Journal of Great Lakes Research 39, 429–436.

Bosch, N.S., Evans, M.A., Scavia, D., Allan, J.D., 2014. Interacting effects of climate change and agricultural BMPs on nutrient runoff entering Lake Erie. Journal of Great Lakes Research 40, 581–589. doi:10.1016/j.jglr.2014.04.011

Briner, S., Elkin, C., Huber, R., Grêt-Regamey, A., 2012. Assessing the impacts of economic and climate changes on land-use in mountain regions: A spatial dynamic modeling approach. Agriculture, Ecosystems and Environment 149, 50–63. doi:10.1016/j.agee.2011.12.011

Brown, D.G., Goovaerts, P., Burnicki, A., Li, M.-Y., 2002. Stochastic Simulation of Land-Cover Change Using Geostatistics and Generalized Additive Models. Photogrammetric Engineering & Remote Sensing 1051.

Brown, D.G., Verburg, P.H., Pontius Jr, R.G., Lange, M.D., 2013. Opportunities to improve impact, integration, and evaluation of land change models. Current Opinion in Environmental Sustainability 5, 452–457. doi:http://dx.doi.org/10.1016/j.cosust.2013.07.012

Burnicki, A.C., Brown, D.G., Goovaerts, P., 2007. Simulating error propagation in land-cover change analysis: the implications of temporal dependence. Computers, Environment and Urban Systems 31, 282–302.

Carpenter, S.R., Stanley, E.H., Vander Zanden, M.J., 2011. State of the World's Freshwater Ecosystems: Physical, Chemical, and Biological Changes. Annual Review of Environment and Resources 36, 75–99. doi:10.1146/annurev-environ-021810-094524

Chaubey, I., Chiang, L., Gitau, M.W., Mohamed, S., 2010. Effectiveness of best management practices in improving water quality in a pasture-dominated watershed. Journal of Soil and Water Conservation 65, 424–437. doi:10.2489/jswc.65.6.424

Chen, Y., Li, X., Liu, X., Ai, B., 2014. Modeling urban land-use dynamics in a fast developing

city using the modified logistic cellular automaton with a patch-based simulation strategy. International Journal of Geographical Information Science 28, 234–255. doi:10.1080/13658816.2013.831868

Chung, D., Cha, M., Guss, A.M., Westpheling, J., 2014. Direct conversion of plant biomass to ethanol by engineered Caldicellulosiruptor bescii 111, 8931–8936. doi:10.1073/pnas.1402210111

Cook, B.I., Ault, T.R., Smerdon, J.E., 2015. Unprecedented 21st century drought risk in the American Southwest and Central Plains. Science Advances 1, 1–7. doi:10.1126/sciadv.1400082

Courbaud, B., Goreaud, F., Dreyfus, P., Bonnet, F.R., 2001. Evaluating thinning strategies using a tree distance dependent growth model: Some examples based on the CAPSIS software "uneven-aged spruce forests" module. Forest Ecology and Management 145, 15–28. doi:10.1016/S0378-1127(00)00571-5

Crooks, A., 2010. Constructing and Implementing an Agent-Based Model of Residential Segregation through Vector GIS. International Journal of Geographical Information Science 24, 661–675. doi:10.1080/13658810903569572

Dahal, K.R., Chow, T.E., 2014. A GIS toolset for automated partitioning of urban lands. Environmental Modelling & Software 55, 222–234. doi:10.1016/j.envsoft.2014.01.024

Daloğlu, I., Cho, K.H., Scavia, D., 2012. Evaluating causes of trends in long-term dissolved reactive phosphorus loads to Lake Erie. Environmental science & technology 46, 10660–10666.

de Groot, R.S.S., Alkemade, R., Braat, L., Hein, L., Willemen, L., 2010. Challenges in integrating the concept of ecosystem services and values in landscape planning, management and decision making. Ecological Complexity 7, 260–272. doi:10.1016/j.ecocom.2009.10.006

Donnelly, S., Evans, T.P., 2008. Characterizing spatial patterns of land ownership at the parcel level in south-central Indiana, 1928–1997. Landscape and Urban Planning 84, 230–240. doi:10.1016/j.landurbplan.2007.08.004

Duh, J.-D., Brown, D.G., 2007. Knowledge-informed Pareto simulated annealing for multi-objective spatial allocation. Computers, Environment and Urban Systems 31, 253–281. doi:10.1016/j.compenvurbsys.2006.08.002

Duriancik, L.F., Bucks, D., Dobrowolski, J.P., Drewes, T., Eckles, S.D., Jolley, L., Kellogg, R.L., Lund, D., Makuch, J.R., O'Neill, M.P., Rewa, C. a., Walbridge, M.R., Parry, R., Weltz, M. a., 2008. The first five years of the Conservation Effects Assessment Project. Journal of Soil and Water Conservation 63, 185A–197A. doi:10.2489/jswc.63.6.185A

Ellis, E.C., Wang, H., Xiao, H.S., Peng, K., Liu, X.P., Li, S.C., Ouyang, H., Cheng, X., Yang, L.Z., 2006. Measuring long-term ecological changes in densely populated landscapes using current and historical high resolution imagery. Remote Sensing of Environment 100, 457–

473. doi:10.1016/j.rse.2005.11.002

Foley, J.A., DeFries, R., Asner, G.P., Barford, C., Bonan, G., Carpenter, S.R., Chapin, F.S., Coe, M.T., Daily, G.C., Gibbs, H.K., 2005. Global consequences of land use. science 309, 570–574.

Fourer, D.G., 2007. Modeling Language for Mathematical Programming.

Fourer, R., Gay, D.M., Hill, M., Kernighan, B.W., Laboratories, T.B., 1990. AMPL : A Mathematical Programming Language. Management Science 36, 519–554. doi:10.1007/BF01783416

Frate, L., Saura, S., Minotti, M., Di Martino, P., Giancola, C., Carranza, M., 2014. Quantifying Forest Spatial Pattern Trends at Multiple Extents: An Approach to Detect Significant Changes at Different Scales. Remote Sensing 6, 9298–9315. doi:10.3390/rs6109298

Fry, J.A., Coan, M.J., Homer, C.G., Meyer, D.K., Wickham, J.D., 2008. Completion of the national land cover database (NLCD) 1992-2001 land cover change retrofit product. US Geological Survey open-file report 1379, 18.

García, A.M., Santé, I., Boullón, M., Crecente, R., 2012. A comparative analysis of cellular automata models for simulation of small urban areas in Galicia, NW Spain. Computers, Environment and Urban Systems 36, 291–301. doi:10.1016/j.compenvurbsys.2012.01.001

Garrity, D.P., Akinnifesi, F.K., Ajayi, O.C., Weldesemayat, S.G., Mowo, J.G., Kalinganire, A., Larwanou, M., Bayala, J., 2010. Evergreen Agriculture: A robust approach to sustainable food security in Africa. Food Security 2, 197–214. doi:10.1007/s12571-010-0070-7

Gassman, P.W., Reyes, M.R., Green, C.H., Arnold, J.G., 2007. The soil and water assessment tool: Historical development, applications, and future research directions. Transactions of the Asabe 50, 1211–1250. doi:10.1.1.88.6554

Gaucherel, C., Fleury, D., Auclair, D., Baudry, J., Dreyfus, P., Smithers, R., others, 2004. Forest modelling based on landscape ecology concepts., in: Landscape Ecology of Trees and Forests. Proceedings of the Twelfth Annual IALE (UK) Conference, Cirencester, UK, 21-24 June 2004. pp. 309–312.

Gaucherel, C., Fleury, D., Auclair, D., Dreyfus, P., 2006. Neutral models for patchy landscapes. Ecological Modelling 197, 159–170. doi:10.1016/j.ecolmodel.2006.02.044

Gaucherel, C., Giboire, N., Viaud, V., Houet, T., Baudry, J., Burel, F., 2006. A domain-specific language for patchy landscape modelling: The Brittany agricultural mosaic as a case study. Ecological Modelling 194, 233–243. doi:10.1016/j.ecolmodel.2005.10.026

Gelfand, I., Snapp, S.S., Robertson, G.P., 2010. Energy Efficiency of Conventional, Organic, and Alternative Cropping Systems for Food and Fuel at a Site in the U.S. Midwest. Environmental Science & Technology 44, 4006–4011. doi:10.1021/es903385g

Gesch, D., Oimoen, M., Greenlee, S., Nelson, C., Steuck, M., Tyler, D., 2002. The National Elevation Dataset. Photogrammetric Engineering and Remote Sensing 68, 5–11.

Gillenwater, D., Granata, T., Zika, U., 2006. GIS-based modeling of spawning habitat suitability for walleye in the Sandusky River, Ohio, and implications for dam removal and river restoration. Ecological Engineering 28, 311–323.

Goldstein, J.H., Caldarone, G., Duarte, T.K., Ennaanay, D., Hannahs, N., Mendoza, G., Polasky, S., Wolny, S., Daily, G.C., 2012. Integrating ecosystem-service tradeoffs into land-use decisions. Proceedings of the National Academy of Sciences of the United States of America 109, 7565–70. doi:10.1073/pnas.1201040109

Grunwald, S., Qi, C., 2006. GIS-based water quality modeling in the Sandusky Watershed, Ohio, USA. Journal of the American Water Resources Association 42, 957–973. doi:10.1111/j.1752-1688.2006.tb04507.x

Guerry, A.D., Polasky, S., Lubchenco, J., Chaplin-Kramer, R., Daily, G.C., Griffin, R., Ruckelshaus, M., Bateman, I.J., Duraiappah, A., Elmqvist, T., Feldman, M.W., Folke, C., Hoekstra, J., Kareiva, P.M., Keeler, B.L., Li, S., McKenzie, E., Ouyang, Z., Reyers, B., Ricketts, T.H., Rockström, J., Tallis, H., Vira, B., 2015. Natural capital and ecosystem services informing decisions: From promise to practice. Proceedings of the National Academy of Sciences 112, 201503751. doi:10.1073/pnas.1503751112

Hastie, T., Tibshirani, R., 2005. Generalized Additive Model. Encyclopedia of Biostatistics.

Hawkins, E., Sutton, R., 2011. The potential to narrow uncertainty in projections of regional precipitation change. Climate Dynamics 37, 407–418. doi:10.1007/s00382-010-0810-6

Hawkins, E., Sutton, R., 2009. The potential to narrow uncertainty in regional climate predictions. Bulletin of the American Meteorological Society 90, 1095–1107. doi:10.1175/2009BAMS2607.1

Hayhoe, K., VanDorn, J., Croley, T., Schlegal, N., Wuebbles, D., 2010. Regional climate change projections for Chicago and the US Great Lakes. Journal of Great Lakes Research 36, 7–21. doi:10.1016/j.jglr.2010.03.012

Heidelberg University, N.C. for W.Q.R., 2015. Tributary Loading Website [WWW Document]. URL http://www.heidelberg.edu/academiclife/distinctive/ncwqr/data (accessed 1.3.14).

Herold, M., Scepan, J., Clarke, K.C., 2002. The use of remote sensing and landscape metrics to describe structures and changes in urban land uses. Environment and Planning A 34, 1443–1458. doi:10.1068/a3496

Hivrale, V., Zheng, Y., Puli, C.O.R., Jagadeeswaran, G., Gowdu, K., Kakani, V.G., Barakat, A., Sunkar, R., 2015. Characterization of drought- and heat-responsive microRNAs in switchgrass. Plant Science 242, 214–223. doi:10.1016/j.plantsci.2015.07.018

Homer, C., Dewitz, J., Yang, L., Jin, S., Danielson, P., Xian, G., Coulston, J., Herold, N., Wickham, J., Megown, K., 2015. Completion of the 2011 national land cover database for the conterminous United States – Representing a decade of land cover change information. Photogrammetric Engineering and Remote Sensing 81, 346–354.

Hoornbeek, J., Hansen, E., Ringquist, E., Carlson, R., 2013. Implementing Water Pollution

Policy in the United States: Total Maximum Daily Loads and Collaborative Watershed Management. Society & Natural Resources 26, 420–436. doi:10.1080/08941920.2012.700761

Houck, O.A., 2002. The Clean Water Act TMDL Program: Law, Policy, and Implementation. Environmental Law Institute, 2000 L Street, N.W. Suite 620 Washington DC 20036 USA.

Houet, T., Loveland, T.R., Hubert-Moy, L., Gaucherel, C., Napton, D., Barnes, C. a., Sayler, K., 2010. Exploring subtle land use and land cover changes: A framework for future landscape studies. Landscape Ecology 25, 249–266. doi:10.1007/s10980-009-9362-8

IBM ILOG, 2012. CPLEX 12.5.1 Rerference Manual and Software.

International Joint Commission, 2014. A Balanced Diet for Lake Erie: Reducing Phosphorus Loadings and Harmful Algal Blooms. Report of the Lake Erie Ecosystem Priority [WWW Document]. URL http://www.ijc.org/files/publications/2014 IJC LEEP REPORT.pdf (accessed 5.10.10).

IPCC-TGICA, 2007. General Guidelines on the Use of Scenario Data for climate impact and adaptation assessment. Finnish Environment Institute 312, 66. doi:10.1144/SP312.4

Jager, H.I., Baskaran, L.M., Brandt, C.C., Davis, E.B., Gunderson, C.A., Wullschleger, S.D., 2010. Empirical geographic modeling of switchgrass yields in the United States. GCB Bioenergy 2, 248–257. doi:10.1111/j.1757-1707.2010.01059.x

Jeppesen, E., Kronvang, B., Meerhoff, M., Søndergaard, M., Hansen, K.M., Andersen, H.E., Lauridsen, T.L., Liboriussen, L., Beklioglu, M., Ozen, A., Olesen, J.E., 2009. Climate change effects on runoff, catchment phosphorus loading and lake ecological state, and potential adaptations. Journal of Environmental Quality 38, 1930–1941. doi:10.2134/jeq2008.0113

Jha, M., Arnold, J.G., Gassman, P.W., Giorgi, F., Gu, R.R., 2006. Climate change sensitivity assessment on Upper Mississippi River Basin streamflows using SWAT. Journal of the American Water Resources Association 42, 997–1016. doi:10.1111/j.1752-1688.2006.tb04510.x

Jin, S., Yang, L., Danielson, P., Homer, C., Fry, J., Xian, G., 2013a. A comprehensive change detection method for updating the national land cover database to circa 2011. Remote Sensing of Environment 132, 159–175.

Jin, S., Yang, L., Danielson, P., Homer, C., Fry, J., Xian, G., 2013b. A comprehensive change detection method for updating the National Land Cover Database to circa 2011. Remote Sensing of Environment 132, 159–175. doi:10.1016/j.rse.2013.01.012

Johnson, K. a., Polasky, S., Nelson, E., Pennington, D., 2012. Uncertainty in ecosystem services valuation and implications for assessing land use tradeoffs: An agricultural case study in the Minnesota River Basin. Ecological Economics 79, 71–79. doi:10.1016/j.ecolecon.2012.04.020

Johnston, R.Z., Sandefur, H.N., Bandekar, P., Matlock, M.D., Haggard, B.E., Thoma, G., 2015.

Predicting changes in yield and water use in the production of corn in the United States under climate change scenarios. Ecological Engineering 82, 555–565. doi:10.1016/j.ecoleng.2015.05.021

Kalcic, M.M., Chaubey, I., Frankenberger, J., 2015. Defining Soil and Water Assessment Tool (SWAT) hydrologic response units (HRUs) by field boundaries. International Journal of Agricultural and Biological Engineering 8, 1–12. doi:10.3965/j.ijabe.20150803.951

Kalcic, M.M., Frankenberger, J., Chaubey, I., 2015. Spatial Optimization of Six Conservation Practices Using Swat in Tile-Drained Agricultural Watersheds. JAWRA Journal of the American Water Resources Association 51, 956–972. doi:10.1111/1752-1688.12338

Khanal, S., Parajuli, P.B., 2014. Sensitivity Analysis and Evaluation of Forest Biomass Production Potential Using SWAT Model. Journal of Sustainable Bioenergy Systems 04, 136–147. doi:10.4236/jsbs.2014.42013

Kirilenko, A.P., Sedjo, R.A., 2007. Climate change impacts on forestry. Proceedings of the National Academy of Sciences of the United States of America 104, 19697–702. doi:10.1073/pnas.0701424104

Kleinman, P.J.A., Sharpley, A.N., McDowell, R.W., Flaten, D.N., Buda, A.R., Tao, L., Bergstrom, L., Zhu, Q., 2011. Managing agricultural phosphorus for water quality protection: Principles for progress. Plant and Soil 349, 169–182. doi:10.1007/s11104-011-0832-9

Le Ber, F., Lavigne, C., Adamczyk, K., Angevin, F., Colbach, N., Mari, J.F., Monod, H., 2009. Neutral modelling of agricultural landscapes by tessellation methods-Application for gene flow simulation. Ecological Modelling 220, 3536–3545. doi:10.1016/j.ecolmodel.2009.06.019

Lemke, a M., Kirkham, K.G., Lindenbaum, T.T., Herbert, M.E., Tear, T.H., Perry, W.L., Herkert, J.R., 2011. Evaluating agricultural best management practices in tile-drained subwatersheds of the Mackinaw River, Illinois. Journal of environmental quality 40, 1215–1228. doi:10.2134/jeq2010.0119

Li, X., Lin, J., Chen, Y., Liu, X., Ai, B., 2013. Calibrating cellular automata based on landscape metrics by using genetic algorithms. International Journal of Geographical Information Science 27, 594–613. doi:10.1080/13658816.2012.698391

Lobell, D.B., Burke, M.B., 2008. Why are agricultural impacts of climate change so uncertain? The importance of temperature relative to precipitation. Environmental Research Letters 3, 34007. doi:10.1088/1748-9326/3/3/034007

Lobell, D.B., Cassman, K.G., Field, C.B., 2009. Crop Yield Gaps: Their Importance, Magnitudes, and Causes. Annual Review of Environment and Resources 34, 179–204. doi:10.1146/annurev.environ.041008.093740

Löf, M., Brunet, J., Filyushkina, A., Lindbladh, M., Skovsgaard, J.P., Felton, A., 2015. Management of oak forests: striking a balance between timber production, biodiversity and

cultural services. International Journal of Biodiversity Science, Ecosystem Services & Management 3732, 1–15. doi:10.1080/21513732.2015.1120780

Lowrance, R., Altier, L.S., Newbold, J.D., Schnabel, R.R., Groffman, P.M., Denver, J.M., Correll, D.L., Gilliam, J.W., Robinson, J.L., Brinsfield, R.B., 1997. Water quality functions of riparian forest buffers in Chesapeake Bay watersheds. Environmental Management 21, 687–712.

Lubowski, R.N., Plantinga, A.J., Stavins, R.N., 2008. What Drives Land-Use Change in the United States ? A National Analysis of Landowner Decisions 84, 529–550.

Mani, S., Tabil, L.G., Sokhansanj, S., 2004. Grinding performance and physical properties of wheat and barley straws, corn stover and switchgrass. Biomass and Bioenergy 27, 339–352. doi:10.1016/j.biombioe.2004.03.007

Maringanti, C., Chaubey, I., Popp, J., 2009. Development of a multiobjective optimization tool for the selection and placement of best management practices for nonpoint source pollution control. Water Resources Research 45.

Mas, J.-F., Kolb, M., Paegelow, M., Camacho Olmedo, M.T., Houet, T., 2014. Inductive pattern-based land use/cover change models: A comparison of four software packages. Environmental Modelling & Software 51, 94–111. doi:10.1016/j.envsoft.2013.09.010

Mas, J.-F., Pérez-Vega, A., Clarke, K.C., 2012. Assessing simulated land use/cover maps using similarity and fragmentation indices. Ecological Complexity 11, 38–45.

Mbow, C., Smith, P., Skole, D., Duguma, L., Bustamante, M., 2014. Achieving mitigation and adaptation to climate change through sustainable agroforestry practices in africa. Current Opinion in Environmental Sustainability. doi:10.1016/j.cosust.2013.09.002

McCarty, G.W., McConnell, L.L., Hapeman, C.J., Sadeghi, A., Graff, C., Hively, W.D., Lang, M.W., Fisher, T.R., Jordan, T., Rice, C.P., Codling, E.E., Whitall, D., Lynn, A., Keppler, J., Fogel, M.L., 2008. Water quality and conservation practice effects in the Choptank River watershed. Journal of Soil and Water Conservation 63, 461–474. doi:10.2489/jswc.63.6.461

McGarigal, K., Cushman, S.A., Neel, M.C., Ene, E., 2012. FRAGSTATS v4: Spatial Pattern Analysis Program for Categorical and Continuous Maps. University of Massachusettes, Amherst, MA. URL http://www.umass.edu/landeco/research/fragstats/fragstats.html. doi:citeulike-article-id:287784

Meehl, G.A., Goddard, L., Murphy, J., Stouffer, R.J., Boer, G., Danabasoglu, G., Dixon, K., Giorgetta, M.A., Greene, A.M., Hawkins, E.D., Hegerl, G., Karoly, D., Keenlyside, N., Kimoto, M., Kirtman, B., Navarra, A., Pulwarty, R., Smith, D., Stammer, D., Stockdale, T., 2009. Decadal prediction: Can it be skillful? Bulletin of the American Meteorological Society 90, 1467–1485. doi:10.1175/2009BAMS2778.1

Meentemeyer, R.K., Tang, W., Dorning, M. a., Vogler, J.B., Cunniffe, N.J., Shoemaker, D. a., 2013. FUTURES: Multilevel Simulations of Emerging Urban–Rural Landscape Structure Using a Stochastic Patch-Growing Algorithm. Annals of the Association of American

Geographers 121004082925004. doi:10.1080/00045608.2012.707591

Mehaffey, M., Smith, E., Van Remortel, R., 2012. Midwest U.S. landscape change to 2020 driven by biofuel mandates, in: Ecological Applications. pp. 8–19. doi:10.1890/10-1573.1

Mehmood, S., Zhang, D., 2001. Forest parcelization in the United States: a study of contributing factors. Journal of Forestry 99, 30–34.

Menne, M.J., Durre, I., Korzeniewski, B., McNeal, S., Thomas, K., Yin, X., Anthony, S., Ray, R., Vose, R.S., E.Gleason, B., Houston, T.G., 2012. Global Historical Climatology Network - Daily (GHCN-Daily), Version 3. [WWW Document]. NOAA National Climatic Data Center. doi:10.7289/V5D21VHZ

Menne, M.J., Durre, I., Vose, R.S., Gleason, B.E., Houston, T.G., 2012. An Overview of the Global Historical Climatology Network-Daily Database. Journal of Atmospheric and Oceanic Technology 29, 897–910. doi:10.1175/JTECH-D-11-00103.1

Merriman, K.R., Gitau, M.W., Chaubey, I., 2009. A tool for estimating best management practice effectiveness in Arkansas. Applied Engineering in Agriculture 25, 199–213.

Michalak, A.M., Anderson, E.J., Beletsky, D., Boland, S., Bosch, N.S., Bridgeman, T.B., Chaffin, J.D., Cho, K., Confesor, R., Daloğlu, I., DePinto, J. V, Evans, M.A., Fahnenstiel, G.L., He, L., Ho, J.C., Jenkins, L., Johengen, T.H., Kuo, K.C., LaPorte, E., Liu, X., McWilliams, M.R., Moore, M.R., Posselt, D.J., Richards, R.P., Scavia, D., Steiner, A.L., Verhamme, E., Wright, D.M., Zagorski, M.A., 2013. Record-setting algal bloom in Lake Erie caused by agricultural and meteorological trends consistent with expected future conditions. Proceedings of the National Academy of Sciences 110, 6448–6452. doi:10.1073/pnas.1216006110

Millie, D.F., Fahnenstiel, G.L., Bressie, J.D., Pigg, R.J., Rediske, R.R., Klarer, D.M., Tester, P.A., Litaker, R.W., 2009. Late-summer phytoplankton in western Lake Erie (Laurentian Great Lakes): bloom distributions, toxicity, and environmental influences. Aquatic Ecology 43, 915–934.

Moreno, N., Ménard, A., Marceau, D.J., 2008. VecGCA: A vector-based geographic cellular automata model allowing geometric transformations of objects. Environment and Planning B: Planning and Design 35, 647–665. doi:10.1068/b33093

Moriasi, D., 2015. Hydrologic and Water Quality Models: Performance Measures and Evaluation Criteria. doi:10.13031/trans.58.10715

Moss, R.H., Edmonds, J.A., Hibbard, K.A., Manning, M.R., Rose, S.K., van Vuuren, D.P., Carter, T.R., Emori, S., Kainuma, M., Kram, T., 2010. The next generation of scenarios for climate change research and assessment. Nature 463, 747–756.

Moulds, S., Buytaert, W., Mijic, A., 2015. An open and extensible framework for spatially explicit land use change modelling in R: the lulccR package (0.1.0). Geoscientific Model Development Discussions 8, 3359–3402. doi:10.5194/gmdd-8-3359-2015

Nair, S.S., King, K.W., Witter, J.D., Sohngen, B.L., Fausey, N.R., 2011. Importance of crop

yield in calibrating watershed water quality simulation tools. Journal of the American Water Resources Association 47, 1285–1297. doi:10.1111/j.1752-1688.2011.00570.x

Nakicenovic, N., Swart, R., Nakiceenovic, N., Alcamo, J., Davis, G., de Vries, B., Fenhann, J., Gaffin, S., Gregory, K., Grubler, A., Yong, J.T., Kram, T., La Rovere, E.L., Michaelis, L., Mori, S., Morita, T., Pepper, W., Pitcher, H., Price, L., Riahi, K., Roehrl, A., Rogner, H.-H., Sankovski, A., Schlesinger, M.E., Shukla, P., Smith, S., Swart, R., van Rooijen, S., Victor, N., Dadi, Z., 2000. Special Report on Emissions Scenarios, Working Group III of the Intergovernmental Panel on Climate Change IPCC.

Neitsch, S.., Arnold, J.., Kiniry, J.., Williams, J.., 2011. Soil & Water Assessment Tool Theoretical Documentation Version 2009. Texas Water Resources Institute, TR-406 1–647. doi:10.1016/j.scitotenv.2015.11.063

Nelson, E., Polasky, S., Lewis, D.J., Plantinga, A.J., Lonsdorf, E., White, D., Bael, D., Lawler, J.J., 2008. Efficiency of incentives to jointly increase carbon sequestration and species conservation on a landscape. Proceedings of the National Academy of Sciences of the United States of America 105, 9471–6. doi:10.1073/pnas.0706178105

NRC, 2013. Advancing Land Change Modeling: Opportunities and Research Requirements. The National Academies Press.

NRC (National Research Council), 2009. Nutrient Control Actions for Improving Water Quality in the Mississippi River Basin and Northern Gulf of Mexico. National Academies Press, Washington, D.C. doi:10.17226/12544

Ohio State University(OSU)-Extension, 2016. Ohio Timber Price Reports 2003 - 2016 [WWW Document]. URL http://woodlandstewards.osu.edu/ohio-timber-price-report (accessed 4.1.16).

Ohio State University(OSU)-Extension, 2015. Ohio Farm Management Enterprise Budgets [WWW Document]. Enterprise Budgets 2001-2015. URL http://aede.osu.edu/research/osu-farm-management/enterprise-budgets (accessed 5.27.16).

Olschewski, R., Benítez, P.C., 2010. Optimizing joint production of timber and carbon sequestration of afforestation projects. Journal of Forest Economics 16, 1–10. doi:10.1016/j.jfe.2009.03.002

Osmond, D., Meals, D., Hoag, D., Arabi, M., Luloff, A., Jennings, G., McFarland, M., Spooner, J., Sharpley, A., Line, D., 2012. Improving conservation practices programming to protect water quality in agricultural watersheds: Lessons learned from the National Institute of Food and Agriculture-Conservation Effects Assessment Project. Journal of Soil and Water Conservation 67, 122A–127A. doi:10.2489/jswc.67.5.122A

Paegelow, M., Olmedo, M.T.C., Mas, J.-F., Houet, T., Pontius Jr., R.G., 2013. Land change modelling: moving beyond projections. International Journal of Geographical Information Science. doi:10.1080/13658816.2013.819104

Paerl, H.W., Paul, V.J., 2012. Climate change: Links to global expansion of harmful

cyanobacteria. Water Research 46, 1349–1363. doi:10.1016/j.watres.2011.08.002

Paeth, H., Born, K., Girmes, R., Podzun, R., Jacob, D., 2009. Regional Climate Change in Tropical and Northern Africa due to Greenhouse Forcing and Land Use Changes. Journal of Climate 22, 114–132. doi:10.1175/2008JCLI2390.1

Parker, D.C., Manson, S.M., Janssen, M. a., Hoffmann, M.J., Deadman, P., 2003. Multi-agent systems for the simulation of land-use and land-cover change: A review. Annals of the Association of American Geographers 93, 314–337. doi:10.1111/1467-8306.9302004

Patzek, T.W., 2004. Thermodynamics of the Corn-Ethanol Biofuel Cycle. Critical Reviews in Plant Sciences 23, 519–567. doi:10.1080/07352680490886905

Perrin, R., Vogel, K., Schmer, M., Mitchell, R., 2008. Farm-Scale Production Cost of Switchgrass for Biomass. BioEnergy Research 1, 91–97. doi:10.1007/s12155-008-9005-y

Pijut, P.M., 2003. Planting Hardwood Seedlings in the Central Hardwood Region [WWW Document]. URL http://www.extension.purdue.edu/extmedia/FNR/FNR-210.pdf

Polasky, S., Lewis, D.J., Plantinga, A.J., Nelson, E., 2014. Implementing the optimal provision of ecosystem services. Proceedings of the National Academy of Sciences of the United States of America 111, 6248–53. doi:10.1073/pnas.1404484111

Polasky, S., Nelson, E., Camm, J., Csuti, B., Fackler, P., Lonsdorf, E., Montgomery, C., White, D., Arthur, J., Garber-Yonts, B., Haight, R., Kagan, J., Starfield, A., Tobalske, C., 2008. Where to put things? Spatial land management to sustain biodiversity and economic returns. Biological Conservation 141, 1505–1524. doi:10.1016/j.biocon.2008.03.022

Pontius, R.G., Boersma, W., Castella, J.-C., Clarke, K., de Nijs, T., Dietzel, C., Duan, Z., Fotsing, E., Goldstein, N., Kok, K., 2008. Comparing the input, output, and validation maps for several models of land change. The Annals of Regional Science 42, 11–37.

Pontius, R.G., Peethambaram, S., Castella, J.-C., 2011. Comparison of Three Maps at Multiple Resolutions: A Case Study of Land Change Simulation in Cho Don District, Vietnam. Annals of the Association of American Geographers 101, 45–62. doi:10.1080/00045608.2010.517742

Pordesimo, L.O., Hames, B.R., Sokhansanj, S., Edens, W.C., 2005. Variation in corn stover composition and energy content with crop maturity. Biomass and Bioenergy 28, 366–374. doi:10.1016/j.biombioe.2004.09.003

R Development Core Team, 2014. R: A Language and Environment for Statistical Computing [WWW Document]. R Foundation for Statistical Computing. doi:10.1007/978-3-540-74686-7

Rabotyagov, S.S., Campbell, T.D., White, M., Arnold, J.G., Atwood, J., Norfleet, M.L., Kling, C.L., Gassman, P.W., Valcu, A., Richardson, J., Turner, R.E., Rabalais, N.N., 2014. Cost-effective targeting of conservation investments to reduce the northern Gulf of Mexico hypoxic zone. Proceedings of the National Academy of Sciences 111, 18530–18535. doi:10.1073/pnas.1405837111

Rabotyagov, S.S., Jha, M., Campbell, T.D., 2010. Nonpoint-Source Pollution Reduction for an Iowa Watershed: An Application of Evolutionary Algorithms. Canadian Journal of Agricultural Economics/Revue canadienne d'agroeconomie 58, 411–431.

Rockström, J., Steffen, W., Noone, K., Persson, A., Chapin, F.S., Lambin, E.F., Lenton, T.M., Scheffer, M., Folke, C., Schellnhuber, H.J., Nykvist, B., de Wit, C.A., Hughes, T., van der Leeuw, S., Rodhe, H., Sörlin, S., Snyder, P.K., Costanza, R., Svedin, U., Falkenmark, M., Karlberg, L., Corell, R.W., Fabry, V.J., Hansen, J., Walker, B., Liverman, D., Richardson, K., Crutzen, P., Foley, J.A., 2009. A safe operating space for humanity. Nature 461, 472–5. doi:10.1038/461472a

Ruijs, A., Kortelainen, M., Wossink, A., Schulp, C.J.E., Alkemade, R., 2015. Opportunity Cost Estimation of Ecosystem Services. Environmental and Resource Economics. doi:10.1007/s10640-015-9970-5

Sadeghi, S.H.R., Jalili, K., Nikkami, D., 2009. Land use optimization in watershed scale. Land Use Policy 26, 186–193. doi:10.1016/j.landusepol.2008.02.007

Santhi, C., Srinivasan, R., Arnold, J.G., Williams, J.R., 2006. A modeling approach to evaluate the impacts of water quality management plans implemented in a watershed in Texas. Environmental Modelling & Software 21, 1141–1157. doi:10.1016/j.envsoft.2005.05.013

Sayer, J., 2009. Reconciling Conservation and Development: Are Landscapes the Answer? Biotropica. doi:10.1111/j.1744-7429.2009.00575.x

Sayer, J., Sunderland, T., Ghazoul, J., Pfund, J.-L., Sheil, D., Meijaard, E., Venter, M., Boedhihartono, A.K., Day, M., Garcia, C., van Oosten, C., Buck, L.E., 2013. Ten principles for a landscape approach to reconciling agriculture, conservation, and other competing land uses. Proceedings of the National Academy of Sciences 110, 8349–8356. doi:10.1073/pnas.1210595110

Scavia, D., David Allan, J., Arend, K.K., Bartell, S., Beletsky, D., Bosch, N.S., Brandt, S.B., Briland, R.D., Daloğlu, I., DePinto, J. V., Dolan, D.M., Evans, M.A., Farmer, T.M., Goto, D., Han, H., Höök, T.O., Knight, R., Ludsin, S.A., Mason, D., Michalak, A.M., Peter Richards, R., Roberts, J.J., Rucinski, D.K., Rutherford, E., Schwab, D.J., Sesterhenn, T.M., Zhang, H., Zhou, Y., 2014. Assessing and addressing the re-eutrophication of Lake Erie: Central basin hypoxia. Journal of Great Lakes Research. doi:10.1016/j.jglr.2014.02.004

Scheller, R.M., Mladenoff, D.J., 2005. A spatially interactive simulation of climate change,harvesting, wind, and tree species migration andprojected changes to forest composition and biomass innorthern Wisconsin, USA. Global change biology 11, 307–321. doi:10.1111/j.1365-2486.2005.00906.x

Schilling, K.E., Chan, K.-S., Liu, H., Zhang, Y.-K., 2010. Quantifying the effect of land use land cover change on increasing discharge in the Upper Mississippi River. Journal of Hydrology 387, 343–345. doi:10.1016/j.jhydrol.2010.04.019

Schlenker, W., Roberts, M.J., 2009. Nonlinear temperature effects indicate severe damages to U.S. crop yields under climate change. Proceedings of the National Academy of Sciences

106, 15594–15598. doi:10.1073/pnas.0906865106

Schmer, M.R., Vogel, K.P., Mitchell, R.B., Perrin, R.K., 2008. Net energy of cellulosic ethanol from switchgrass 2007, 21–26.

Seppelt, R., Voinov, a, 2002. Optimization methodology for land use patterns using spatially explicit landscape models. Ecological Modelling 151, 125–142. doi:Pii S0304-3800(01)00455-0\rDoi 10.1016/S0304-3800(01)00455-0

Seto, K.C., Fragkias, M., 2005. Quantifying spatiotemporal patterns of urban land-use change in four cities of China with time series landscape metrics. Landscape Ecology 20, 871–888. doi:10.1007/s10980-005-5238-8

Shrestha, R.R., Dibike, Y.B., Prowse, T.D., 2012. Modeling Climate Change Impacts on Hydrology and Nutrient Loading in the Upper Assiniboine Catchment. JAWRA Journal of the American Water Resources Association 48, 74–89. doi:10.1111/j.1752-1688.2011.00592.x

Smith, D.R., King, K.W., Johnson, L., Francesconi, W., Richards, P., Baker, D., Sharpley, A.N., 2015. Surface Runoff and Tile Drainage Transport of Phosphorus in the Midwestern United States. Journal of Environment Quality 44, 495. doi:10.2134/jeq2014.04.0176

Smith, V.H., Joye, S.B., Howarth, R.W., 2006. Eutrophication of Freshwater and Marine Ecosystems. Limnology and Oceanography 51, 351–355. doi:10.2307/4499594

Sohl, T.L., Sayler, K.L., Drummond, M. a., Loveland, T.R., 2007. The FORE-SCE model: a practical approach for projecting land cover change using scenario-based modeling. Journal of Land Use Science 2, 103–126. doi:10.1080/17474230701218202

Southworth, J., Pfeifer, R.A., Habeck, M., Randolph, J.C., Doering, O.C., Johnston, J.J., Rao, D.G., 2002. Changes in soybean yields in the Midwestern United States as a result of future changes in climate, climate variability, and CO2 fertilization. Climatic Change 53, 447–475. doi:10.1023/A:1015266425630

Stevens, D., Dragicevic, S., 2007. A GIS-based irregular cellular automata model of land-use change. Environment and Planning B: Planning and Design 34, 708–724. doi:10.1068/b32098

Sumner, D.A., Rosen-Molina, J.T., 2011. Alfalfa in the context of global crop price prospects, in: 41st Western Alfalfa & Forage Symposium. University of California Cooperative Extension, Department of Plant Sciences, University of California, Davis, CA 95616, Las Vegas, NV, p. 419.

Tejeda, H.A., Kim, M.-K., Feuz, D.M., 2015. Dynamic Relationships and Price Discovery of Western Alfalfa Markets, in: 2015 AAEA & WAEA Joint Annual Meeting, July 26-28, San Francisco, California. San Francisco, California.

Teshager, A.D., Gassman, P.W., Secchi, S., Schoof, J.T., Misgna, G., 2016. Modeling Agricultural Watersheds with the Soil and Water Assessment Tool (SWAT): Calibration and Validation with a Novel Procedure for Spatially Explicit HRUs. Environmental

Management 57, 894–911. doi:10.1007/s00267-015-0636-4

Tiessen, K.H.D., Elliott, J. a., Yarotski, J., Lobb, D. a., Flaten, D.N., Glozier, N.E., 2010. Conventional and Conservation Tillage: Influence on Seasonal Runoff, Sediment, and Nutrient Losses in the Canadian Prairies. Journal of Environmental Quality 39, 964–980. doi:10.2134/jeq2009.0219

Tomer, M.D., Locke, M.A., 2011. The challenge of documenting water quality benefits of conservation practices: A review of USDA-ARS's conservation effects assessment project watershed studies. Water Science and Technology. doi:10.2166/wst.2011.555

Tomer, M.D., Porter, S.A., James, D.E., Boomer, K.M.B., Kostel, J.A., McLellan, E., 2013. Combining precision conservation technologies into a flexible framework to facilitate agricultural watershed planning. Journal of Soil and Water Conservation 68, 113A–120A. doi:10.2489/jswc.68.5.113A

Tong, S.T.Y., Chen, W., 2002. Modeling the relationship between land use and surface water quality. Journal of Environmental Management 66, 377–393.

Tubiello, F.N., Soussana, J.-F., Howden, S.M., 2007. Crop and pasture response to climate change. Proceedings of the National Academy of Sciences of the United States of America 104, 19686–90. doi:10.1073/pnas.0701728104

Tuppad, P., Kannan, N., Srinivasan, R., Rossi, C.G., Arnold, J.G., 2010. Simulation of Agricultural Management Alternatives for Watershed Protection. Water Resources Management 24, 3115–3144. doi:10.1007/s11269-010-9598-8

Turner, R.E., Rabalais, N.N., 2003. Linking landscape and water quality in the Mississippi river basin for 200 years. Bioscience 53, 563–572. doi:10.1641/0006-3568(2003)053[0563:llawqi]2.0.co;2

US Census Bureau, 2010. Census 2010 [WWW Document]. US Census Bureau. URL http://quickfacts.census.gov/qfd/states/13/13135.html

USDA, 2013. What is a Common Land Unit ? [WWW Document]. URL http://www.fsa.usda.gov/FSA/apfoapp?area=home&subject=prod&topic=clu

USDA ERS, 2016. USDA Agricultural Projections to 2025 [WWW Document]. URL http://www.ers.usda.gov/publications/oce-usda-agricultural-projections/oce-2016-1.aspx (accessed 5.19.16).

USDA ERS, 2015. Commodity Costs and Returns [WWW Document]. Costs and Returns for Corn and Soybean, 2001-2015. URL http://www.ers.usda.gov/data-products/commodity-costs-and-returns.aspx

USDA Forest Serive, 2015. Forest Inventory Data Online(FIDO) [WWW Document]. Forest Inventory and Analysis Databases. URL http://apps.fs.fed.us/fia/fido/index.html (accessed 10.10.15).

USDA FSA, 2016. ARC-County Yields, Revenue, and Payment Rates [WWW Document]. URL

http://www.fsa.usda.gov/Assets/USDA-FSA-Public/usdafiles/arc-plc/excel/ARC_CO_2015_data.xlsx (accessed 5.18.16).

USDA FSA, 2015. Average Conservation Reserve Program Rental Payments by County [WWW Document]. URL http://www.fsa.usda.gov/Internet/FSA_File/corentalpymnts0310.xls (accessed 5.10.16).

USDA NASS, 2016. USDA National Agricultural Statistics Service Cropland Data Layer [WWW Document]. Published crop-specific data layer. URL https://nassgeodata.gmu.edu/CropScape/ (accessed 5.18.16).

USDA NASS, 2015. Quick Stats [WWW Document]. US Department of Agriculture (USDA) National Agricultural Statistics Service (NASS).

USDA NRCS, 2015a. Soil Survey Geographic (SSURGO) Database for [U.S.] [WWW Document]. United States Department of Agriculture accessed [11/20/2015]. URL http://soildatamart.nrcs.usda.gov

USDA NRCS, 2015b. Ohio Field Office Technical Guide(FOTG) [WWW Document]. Field Office Technical Guide(FOTG), Section IV. URL https://efotg.sc.egov.usda.gov/treemenuFS.aspx (accessed 5.27.16).

USDA NRCS, 2010. Key Findings from the CEAP-Cropland Assessment of the Effects of Conservation Practices on Cultivated Cropland in the Upper Mississippi River Basin. Resources Inventory and Assessment Division.

USDA NRCS, 2009. Planting and Managing Switchgrass as a Biomass Energy Crop [WWW Document]. URL http://www.nrcs.usda.gov/Internet/FSE_DOCUMENTS/stelprdb1042293.pdf

USDA-ERS, 2013. Fertilizer Use and Price [WWW Document]. URL http://www.ers.usda.gov/data-products/fertilizer-use-and-price.aspx (accessed 5.27.16).

Vanegas, C. a., Kelly, T., Weber, B., Halatsch, J., Aliaga, D.G., Müller, P., 2012. Procedural Generation of Parcels in Urban Modeling. Computer Graphics Forum 31, 681–690. doi:10.1111/j.1467-8659.2012.03047.x

Verbree, D.A., Duiker, S.W., Kleinman, P.J.A., 2010. Runoff Losses of Sediment and Phosphorus from No-Till and Cultivated Soils Receiving Dairy Manure . J. Environ. Qual. 39, 1762–1770. doi:10.2134/jeq2010.0032

Verburg, P.H., Overmars, K.P., 2007. Dynamic simulation of land-use change trajectories with the CLUE-s model, in: Modelling Land-Use Change. Springer, pp. 321–337.

Verburg, P.H., Schot, P.P., Dijst, M.J., Veldkamp, A., 2004. Land use change modelling: current practice and research priorities. GeoJournal 61, 309–324.

White, M.J., Storm, D.E., Mittelstet, A., Busteed, P.R., Haggard, B.E., Rossi, C., 2014. Development and Testing of an In-Stream Phosphorus Cycling Model for the Soil and Water Assessment Tool. Journal of Environment Quality 43, 215.

doi:10.2134/jeq2011.0348

White, R., 2006. Pattern based map comparisons. Journal of Geographical Systems 8, 145–164.

White, R., Engelen, G., Uljee, I., 1997. Cellular automata as the basis of integrated dynamic regional modelling. Environment and Planning B: Planning and Design 24, 235–246. doi:10.1068/b240235

Williams, M.R., King, K.W., Fausey, N.R., 2015. Drainage water management effects on tile discharge and water quality. Agricultural Water Management 148, 43–51. doi:10.1016/j.agwat.2014.09.017

Wilson, G.L., Dalzell, B.J., Mulla, D.J., Dogwiler, T., Porter, P.M., 2014. Estimating water quality effects of conservation practices and grazing land use scenarios. Journal of Soil and Water Conservation 69, 330–342. doi:10.2489/jswc.69.4.330

Wood, S.N., 2006. Generalized additive models : an introduction with R. Texts in statistical science xvii, 392 p. doi:10.1111/j.1541-0420.2007.00905_3.x

Wood, S.N., 2001. mgcv: GAMs and generalized ridge regression for R. R news 1, 20–25.

Woznicki, S.A., Nejadhashemi, A.P., 2012. Sensitivity Analysis of Best Management Practices Under Climate Change Scenarios1. JAWRA Journal of the American Water Resources Association 48, 90–112. doi:10.1111/j.1752-1688.2011.00598.x

Wright, L., Turhollow, A., 2010. Switchgrass selection as a “ model” bioenergy crop: A history of the process. Biomass and Bioenergy 34, 851–868. doi:10.1016/j.biombioe.2010.01.030